Assessment of Management Strategies for a Lowland Straightened Agricultural Stream

Yannick Rousseau

A Thesis

in

The Department of

Geography, Planning and Environment

Presented in Partial Fulfilment of the Requirements
for the Degree of Master of Science (Geography, Urban and Environmental Studies) at
Concordia University,
Montreal, Québec, Canada

September, 2010

CONCORDIA UNIVERSITY

School of Graduate Studies

This is to certify that the thesis prepared

By: Yannick Rousseau

Entitled: Assessment of Management Strategies for a Lowland Straightened Agricultural Stream

and submitted in partial fulfillment of the requirements for the degree of

Master of Science (Geography, Urban and Environmental Studies)

complies with the regulations of the University and meets the accepted standards with respect to originality and quality.

Signed by the final examining committee:

Pierre Gauthier Chair

Samuel Li Examiner

Stéphane Campeau Examiner

Pascale Biron Supervisor

Approved by _____
Chair of Department of Graduate Program Director

_____20___ _____
Dean of Faculty

ABSTRACT

Assessment of Management Strategies

for a Lowland Straightened Agricultural Stream

Yannick Rousseau

Channel straightening and dredging were extensively used in the 20th century to enhance agricultural drainage and facilitate crop maintenance and harvest. Although the adverse geomorphological and ecological effects of channelization are widely acknowledged, the use of alternative management strategies remains marginal in Southwestern Québec. Bank stabilisation projects are often carried out to mitigate local erosion problems with little assessment of their effects at the reach and watershed scales and with insufficient guidance on suitable designs. The objective of this research is to assess the impacts of various management strategies by studying a case of straightened agricultural stream.

Field measurements in the Richer stream, which drains a small agricultural watershed in the St. Lawrence Lowlands, were used to parameterise a hydro-morphological model at the watershed scale and a 3D computational fluid dynamics model at the reach scale. The increase in stream power associated with the loss in sinuosity since the 1930s has resulted in noteworthy erosion problems in the studied watershed, in particular near residential development where there is limited space available to establish riparian strips. The tested management strategies at the watershed scale are the recreation of meanders and the installation of backwater

ponds whereas, at the reach scale, stream barbs and bed weirs are tested. These management strategies are also assessed through a cost-benefit analysis which also takes into account environmental and practical implementation aspects.

Results indicate that both the addition of ponds and re-meandering can markedly reduce unit stream power, thus the potential for erosion. Hydraulic structures such as stream barbs and V-shaped bed weirs re-align the flow towards channel centre, thus reducing near-bank velocities. The re-meandering approach involving natural vegetation regeneration has the highest overall effectiveness at the watershed scale whilst V-shaped weirs are found to be moderately effective at the reach scale. The diversification of flow conditions and channel morphologies associated with these approaches were important factors contributing to their higher suitability compared to other potential solutions. The modelling methodology used in this study can help limit the uncertainty surrounding restoration activities by better predicting the efficiency of proposed stabilisation techniques prior to their implementation while considering specific stream and watershed characteristics as well as ecological factors.

ACKNOWLEDGEMENTS

Many persons contributed to this project by providing data, experience and knowledge on river restoration. A special thank to Sébastien Rioux and Stéphane Lamoureux from the *Club Conseilsol Vert Cher* for initiating this project, sharing spatial data, and for guiding me in acquiring the data required by this study. I thank the *R.M.C. of La Vallée-du-Richelieu* for sharing historical documentation, and *The Natural Gault Reserve* and *Environment Canada* for providing high-resolution precipitation data. Data acquisition on the field was greatly facilitated by the help provided by several student colleagues.

Funding provided by the *Natural Sciences and Engineering Research Council of Canada, Agriculture and Agri-Food Canada* (CDAQ Défi-Solution project) and a scholarship obtained from the Faculty of Arts and Science at Concordia University supported data collection and analysis, and contributed to my subsistence.

I am particularly grateful for two organisations involved in river restoration activities in taking part in this research. Thanks to Parish Geomorphic Ltd for completing a cost-benefit analysis on the modelled stabilisation approaches. Their restoration philosophy and principles resulted in taking account of their environmental and economic effects rather than reporting solely on their technical effectiveness. *Geomorphic Solutions* provided information on river restoration processes and laws in Ontario, technical documentation on channel stabilisation techniques and guided me through a visit of restored sites near Toronto.

Finally, I thank Dr. Pascale Biron for supporting me throughout this project.

Table of contents

List of Figures

Chapter 1 – Literature Review

Chapter 2 – Methodology

Chapter 3 – Watershed Scale Management

List of Tables

Chapter 3 – Watershed Scale Management

Chapter 5 – Cost-benefit analysis

Introduction

Throughout the last century, many streams in Europe and in North America were straightened to drain agricultural fields more rapidly in the spring. These actions resulted in increased food productivity and facilitated crop maintenance following the removal of meander belts (Campbell et al., 1972; Hupp, 1992; Rhoads & Herricks, 1996; Scheumann & Freisem, 2002; Simon & Rinaldi, 2006; Beaulieu, 2007).

Channelization reduced the frequency and magnitude of overbank flow events that affected both individual land owners and infrastructure (Hupp, 1992). In the St. Lawrence Lowlands in Québec, because of the financial benefits for the farming industry, channel straightening and widening were supported and encouraged by governmental authorities from 1917 to 1986 (Ministry of Agriculture, Food and Fisheries [MAFF], 2001). It is estimated that 30,000 km of meandering rivers were straightened in the St. Lawrence Valley between 1944 and 1976, and an additional 14,000 km of straight ditches were created, draining approximately 1.5 million hectares of land (Boutin et al., 2003; Beaulieu, 2007). Since then, dredging has been used regularly to re-establish the modified channel dimensions (Beaulieu, 2007). Because straightened rivers have a tendency to return to a meandering layout, bank instability is commonly encountered in channelized streams.

From both ecological and geomorphological perspectives, many of the straightening projects involve unsustainable practices (Brookes & Sear, 1996; Frothingham et al., 2002). However, there is a general paucity of available information about past restoration projects (Bernhardt et al. 2005; Brooks & Lake, 2007). Overall, these interventions are perceived as ineffective in achieving channel stability or habitat enhancement goals (Thompson & Stull, 2002; Shields et al., 2003; Thompson, 2006).

Different strategies and methods are employed worldwide to mitigate erosion problems in straightened agricultural rivers and streams. However, some countries appear to be moving forward more rapidly than others in the implementation of sustainable practices. This may be due in part to cultural differences and legislative restrictions. An adequate understanding of the contextual limitations is therefore essential for the implementation of socially acceptable restoration projects. Here, the Richer Stream, located in south-western Québec, is used as a case study to identify some of the bank stabilisation methods and management strategies that could be used to remedy instability problems in a straightened agricultural channel. Numerical modelling is employed to assess the effectiveness of four approaches that may be beneficial to bank stability: (1) the installation of backwater ponds, (2) the re-creation of meanders, and the installation of (3) stream barbs or (4) bed weirs. In addition, the technical feasibility, social acceptability and economic costs of these methods are investigated through a cost-benefit analysis. Finally, the short- and long-term benefits and consequences that these transformations may have on biodiversity and habitat quality are discussed.

1.1. Channelization

1.1.1. Geomorphologocial and hydrological effects

Meandering rivers represent a stable channel planform on shallow slopes with fine grain size and limited sediment supply (Church, 1992). Bed topography of meandering rivers generally consists in a sequence of alternating riffle and pool features, the former being shallower and wider than the latter and covered with coarser materials (Trenhaile, 2007). Straightening involves the cutting of river bends and the removal of bedforms that contribute to the geomorphological heterogeneity of a channel; dredging is the occasional removal of shoals which may accumulate as point bars (Brookes, 1988). The purpose of this strategy is to reduce flood level in a reach by increasing flow velocity, and to widen and deepen the channel to constrain the flow in the channel and lower the water table to improve agricultural efficiency (Brookes, 1988; Rhoads & Herricks, 1996).

These interventions also lead to the simplification and homogenisation of cross-sectional geometries (usually trapezoidal) and dimensions, stream planform, substrate type and flow patterns, and in the smoothing of bed topography (Brookes & Sear, 1996; Frothingham et al., 2002). The increase in channel slope at the watershed scale was reported to be 23% in Illinois (Rhoads & Herricks, 1996), 33% in Indiana (Brookes, 1988) with local increases up to 63% in the Richer Stream, Québec (Rousseau & Biron, 2009). The shorter channel path increases flow velocity, bed shear stress and the volume of sediment transported downstream, causing vertical incision, bank collapse within the straightened reach and downstream deposition (Brookes, 1988; Simon, 1989; Surian & Rinaldi, 2003; Simon & Rinaldi, 2006). Vertical incision or degradation progresses

upstream as a knickpoint, although it may be weakened by an armoured layer or stopped by bedrock outcrops (Brookes, 1988; Simon & Rinaldi, 2006; Zawiejska & Wyzga, 2010). However, the current practice in Québec is to dredge channels to maintain their conveying capacity which destroys bed armouring and gravel streambed internal structure in the case of gravel-bed rivers, contributing to particle entrainment and channel instability (Wyzga, 2001).

Straightening also increases peak discharge, eliminates flooding, and reduces flood-wave travel time (Campbell et al., 1972; Rhoads and Herricks, 1996). The increased discharge created by the elimination of floodplain storage and the increased hydraulic efficiency in straightened channels may cause downstream flooding (Campbell et al., 1972; Brookes, 1988; Lau et al., 2006).

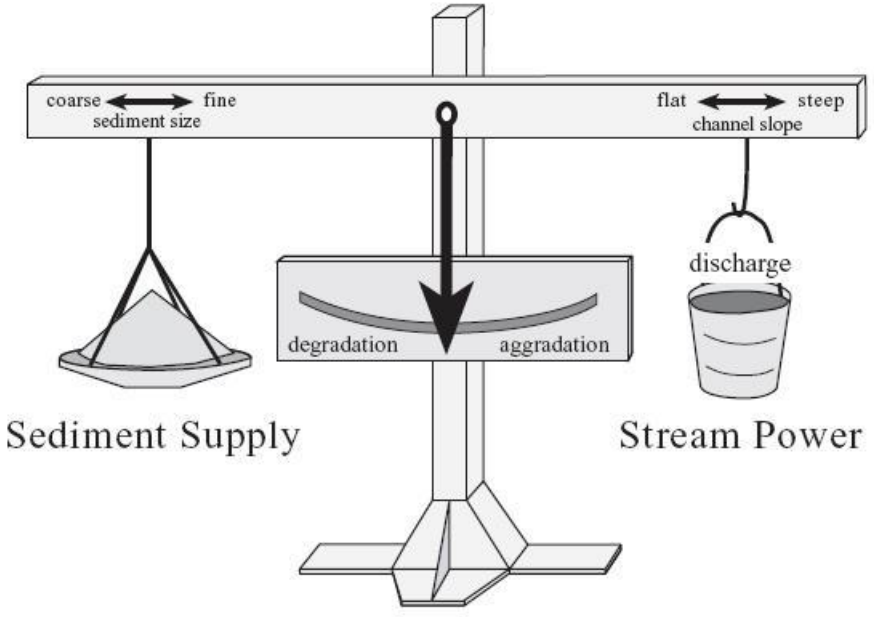

Figure 1.1. Balance model for aggradation and degradation of channels, emphasizing changes in the relationship between discharge and sediment supply. Redrawn from a widely circulated diagram that originated as an unpublished drawing by W. Borland of the USA Bureau of Reclamation, and was based on an equation by Lane (1955). From Blum and Törnqvist (2000)

By increasing the channel slope, straightening disrupts the so-called equilibrium between stream power and sediment supply in streams (Lane, 1955; Figure 1.1). Stream power is the rate of energy expenditure that is available to trigger stream bank erosion and sediment transport (Stefanovic & Bryan, 2009). The anticipated sequence of adjustments of a channel following straightening includes bed degradation, bank slumping, armouring, development of a sinuous thalweg, sinuosity recovery, and development of a sinuous course by deposition (Brookes, 1998; Surian et al., 2003). When considering ecologic in addition of geomorphic attributes the evolution is described with a 6-stage model (Hupp, 1992). This model assumes an initial aggrading meandering channel with low, convex-upward banks subject to limited mass wasting due to mature and diverse riparian community. The channel then gets channelized with a complete removal of in-stream and riparian vegetation and eventually recovers from disturbance with regards to geomorphic and ecologic attributes on average 65 years after channelization (Simon, 1989; Hupp, 1992). During the recovery process, the channel will evolve from a degradation stage to an aggradation stage with an intermediate stage also called the threshold stage.

A straightened channel adjusts locally to the new dynamics associated with the construction works. Deepening is expected to be maximal near the upstream limit of a modified reach and trigger headward erosion from that point (Simon & Rinaldi, 2006). The disruption of channel bed and banks then contributes to releasing sediments to downstream reaches (Brookes, 1985; Sear, 1996, Simon & Rinaldi, 2006). However, low energy streams generally undergo aggradation and stabilisation phases (Simon & Rinaldi, 2006). In the absence of maintenance, lateral bars can develop at the bottom of a drainage

ditch, leading to a two-stage channel that provides environmental benefits compared to a dredged channel (Landwehr & Rhoads, 2003). In the years following channel alteration, other transformations can occur to adjust to the new frequency and magnitude of discharges (Schumm, 1977). Also, downstream plants may be unable to adapt their rooting system to the substrate rising due to sedimentation (Brookes, 1988). The importance of these transformations can be predicted using a series of equations referred to as the stepwise regression technique (Brookes, 1985).

1.1.2. Ecological impacts of channelization

In many countries, the decision about whether or not a stream should be channelized is determined using cost-benefit analyses (Brookes, 1988). A solution is considered optimal if the costs are minimized while the desired benefits are maximized. The costs are those related to study, design, engineering, supervision, and compensation while the benefits relate to urban and agricultural aspects, traffic, public services, and human health and security. Potential adverse environmental effects are thus often not part of the equation (Brookes, 1988) and erosion processes are viewed as mainly negative due to potential loss of land and resource, damage to property and infrastructure, and alteration of downstream channel morphology and flood carrying capacity (Piégay et al., 2005a). However, erosion is part of the natural dynamics of rivers and it increasingly being recognized as playing a key role in ecosystem services and other benefits such as self-restoration and preservation of riparian diversity (Piégay et al., 2005a; Florsheim et al., 2008). Erosion helps increasing riparian diversity in many ways (Florsheim et al., 2008). Firstly, it provides a sediment source that creates riparian habitat. Secondly, it creates and maintains diverse natural structure and habitat functions including food

source, cover and extreme temperature attenuation (Frothingham et al., 2002). Finally, erosion modulates changes in channel morphological characteristics including bank angle, substrate heterogeneity and habitat patterns (e.g. vegetation succession, sunlight intensity) (Florsheim et al., 2008).

Suppression of vegetation

The distribution of in-stream and riparian vegetation is controlled by variation in fluvial geomorphical processes in response to the channel bed slope increase resulting from straightening (Hupp & Osterkamp, 1996). Vegetation is also affected by dredging activities either because of direct plant removal or environmental changes such as substrate alteration, channel re-sectioning, soil moisture and morphologic variability in channel bed and banks (Brookes, 1988). These changes in vegetation composition affect species composition and macroinvertebrate, fish, avian and mammal productivity (Brookes, 1988). For instance, riparian vegetation contributes large woody debris due to natural, biological, mass wasting, or anthropogenic land use changes (Simon et al., 2004). These debris control hydraulic conditions such as flow velocity and discharge and morphologic aspects such as the frequency of pools and bars, channel roughness, shear stress, bedload transport rate and reach average grain size (Montgomery & Piégay, 2003). Benthic and riparian organisms can use the debris as stable substrate (Florsheim et al., 2008). The removal of such features considerably reduces the availability and diversity of aquatic habitats (Montgomery & Piégay, 2003).

Water quality

The disturbance caused by channelization can trigger incision processes which contribute to increasing sediment concentration, turbidity and phosphorus content

(Shields et al., 2010). Water and bio-physical qualities of a stream are also affected by the increase in sediment transport capacity resulting from the densification of the hydrological network (Beaulieu, 2007; Licursi & Gómez, 2009). These impacts are often combined with those occurring as a result of the installation of artificial drainage systems and by changes in cultural practices, fertilisation method, crop type, climate and land use, and may increase peak runoff rates, sediment and nutrient loads (Skaggs et al., 1994). The intensification of subsurface land drainage lowers water tables, increases infiltration capacity, thus reducing peak flow and sediment loss, and altering pollutants outflow; losses in phosphorus and organic nitrogen are generally reduced while losses in nitrate-nitrogen and soluble salts are increased (Skaggs et al., 1994).

Effects on fish population

Straightening severely impacts fish population density, size and diversity by altering their capacity to feed, migrate, breed and shelter (Brookes, 1988; Rhoads et al., 2003; Shields and Rigby, 2005). For instance, the increased flow velocity created by channelization affects centrarchid species which need stable currents and depths to create spawning nests (Lau et al., 2006). Dredging disturbs substrate and affects feeding and reproductive activities by degrading spawning grounds, and altering egg and larval growth (Brookes, 1988; Lau et al., 2006). Channel incision caused by unstable channel can severely degrade aquatic physical habitat and reduce fish species richness (Shields et al., 2010). Silt deposits also reduce the food available for fish by killing bottom-dwelling organisms (Brookes, 1988). While straightening reduces the overall habitat area, dredging removes fish cover such as undercut banks, overhanging shoreline vegetation, deep pools, logs and boulders (Brookes, 1988; Licursi & Gómez, 2009). In natural rivers,

the accumulation of fallen logs and leaf-litter debris creates damming or temporary pools which reduce current intensity; removing these features increases flow velocity further and eliminates drought relief mechanism they offer (Lau et al., 2006). The removal of riparian vegetation and associated shade heats surface waters and results in algal blooms and oxygen-robbing effects from decomposition (Lau et al., 2006). Finally, channelization removes pool and riffle features, altering fish habitat and eliminating intolerant species (Lau et al., 2006).

1.2. River management

River management is the process of designing and operating management programs to achieve specific ecological, economical and social river-related objectives. Despite the growing number of solutions proposed to stabilise straightened lowland agricultural streams or streams whose natural development is subject to space limitations, current river management strategies in some countries such as Canada still incorporate a recurrent dredging procedure (Brookes, 1988; MAFF, 2001; Piégay et al., 2005a). This section lists and explores some of the alternative management schemes. It also includes a summary of the nature, purpose and effectiveness of some of the documented hydraulic structures and bioengineering techniques that are expected to help achieving these objectives. However, these structures and techniques are generally used to enhance bank protection by increasing erosional resistance rather than treating the causes of erosion (Hey, 1996; Brookes & Sear, 1996; Florsheim et al., 2008).

1.2.1. Perspectives on management

Three degrees of interventions are distinguished, depending on the extent to which the structural and functional characteristics of a channel are to be re-established with

respect to the pre-disturbance state. Restoration consists of the complete recovery of former characteristics and rehabilitation in the partial recovery whereas enhancement corresponds to any improvement (National Research Council, 1992; Rhoads & Herricks, 1996; Shields et al. 2003). For instance, some of the adverse environmental impacts of channel realignment and dredging could be greatly reduced by minimizing the extent of the modifications undertaken in terms of channel dimension, sinuosity, roughness, geometry, and vegetation cover and composition (Brookes, 1988). This can be achieved by limiting excavation and fill works, and performing selective modifications (e.g. modify a single bank when widening is envisaged) in order to preserve biological richness, improve aesthetics and avoid sensitive habitats. Replanting vegetation consisting of native species and installing original substrate will stabilise the channel before the next flood in addition of setting conditions similar to those of the original configuration (Brookes and Shields, 1996). Although the resulting channel is far from its initial conditions, improving the maintenance procedure favours a faster recovery of river functions.

The selected strategy may integrate both ecological and financial aspects (Rhoads & Herricks, 1996; Frothingham et al., 2002; Piégay et al., 2005a). For instance, an erodible corridor allows a river to self-regulate (i.e. migrate freely) within a defined zone to minimize channel maintenance and protect public infrastructure and dwellings outside the corridor (Piégay et al., 2005a). The ecological benefits of this strategy are to enhance the diversity of geomorphic features, which can be beneficial to aquatic and riparian species (Florsheim et al, 2008). The acquisition of property rights within the corridor can be obtained by negotiation with owners or by the outright buying of property (Piégay et al., 2005a). A river corridor approach is now widely promoted in the state of Vermont not

only to reduce flood hazards but also because the implemented easements are expected to reduce channel management costs by 70% in unstable reaches (Vermont DEC, 2009; Kline and Cahoon, 2010). This approach also allows sediments and nutrients to be captured, enhancing the health of lakes and rivers.

Stream restoration programs must consider the causes, direction, and speed of morphological change (Shields et al., 2003). The incorporation of geomorphological principles into river engineering practices then facilitates the establishment of sustainable long-term management strategies by "reactivating geomorphic processes at both the watershed and at the reach scale" (Rhoads & Herricks, 1996, p. 297). These principles can be achieved with the modification of discharge regulation, bed load input from watershed, corridor management, and channel maintenance and structure. Assuming a good understanding of the river's behaviour and a regular follow-up, these subtle adjustments allow riparian habitats to be maintained. Naturalisation, the implementation of a socially-acceptable management strategy that is expected to increase the geomorphological heterogeneous in shape and planform of a specific channel (Frothingham et al., 2002; Schwartz & Herricks, 2007) can be implemented with de-channelization, i.e. the relocation of a river inside its initial channel. Geomorphic features such as bars, riffles and pools, diversity and functions are expected to redevelop quickly with such a strategy. The habitat value is enhanced by providing a wider range of geomorphic features, a higher concentration and better vertical distribution of dissolved oxygen, and refuges with cooler temperatures for warmer months (Toth, 1996). However, fluvial features and vegetation are expected to develop rapidly in a freshly cut sinuous reach without having to create bed forms or to seed the banks (Gurnell et al., 2006).

1.2.2. Hydraulic structures

Hydraulic structures are often referred to as hard-engineering methods because their underlying river management approach relies on the installation of unnatural in-stream physical components such as dams, energy dissipators and deflectors to alter river flow, or as revetments for bank protection. The use of these structures was widespread during the last decades as a way to prevent or mitigate erosion problems, improve fish habitat quality, or both.

Dams and weirs

Dams allow water impoundment and are divided into three groups, depending on the type of material used: loose rock or boulder dams, log dams and check dams (assemblages of man-made materials). They may also take different shapes to serve specific in-stream functions. Log weirs can be used to mitigate stream incision and bank instability as illustrated in an experience of rehabilitation conducted in a steep colluvial valley channel near Lake Oswego, Oregon, where nine consecutive channel-spanning log weirs (each one tied to a stepped log cribwall bank structure) were manually installed (Morris & Moses, 1998). Natural features such as beaver dams can help reversing channel incision whilst providing environmental benefits (Zawiejska & Wyzga, 2010). The presence of a dam leads to bed aggradation which can provide support for the development of riparian vegetation that will eventually reconnect the floodplain to the channel. The resulting rise in water table ensures a more important base flow and provides cooler water temperatures in the summer months.

Grade control structures

The challenges facing the rehabilitation of steep channels include the re-

establishment of grade control, the dissipation of excess energy and the shoring-up of oversteepened stream banks (Morris & Moses, 1998). Although straightening is usually associated with lowland regions, it is reasonable to assume that a straightened river may also be considered steep due to the planform changes (i.e. meanders removal) that results in increased bed slope compared to historical conditions. Grade control structures can take various forms, depending on the type of structure used and whether they are constructed using natural or artificial material. In all cases, they are designed to dissipate energy in a flow that runs through a steeper and shorter armoured channel section (Pagliara & Chiavaccini, 2006). In addition, grade control structures prevent excessive sediment in the bed from being eroded and deposited in a downstream reach while stabilising upstream banks and beds due to reduced bank heights (Mendrop & Little, 1997). Environmental benefits associated with the installation of such structures consist of pools upstream of the weir, higher channel bed substrate stability and fast natural rejuvenation of vegetation cover on formally eroded banks (Mendrop & Little, 1997). When a block ramp is used to provide grade control, the amount of dissipated energy is a function of the concentration, layout and roughness of the boulders (Pagliara & Chiavaccini, 2006). Four types of structure are primarily used by the U.S. Corps of Engineers. Low drop grade control structures are employed to intercept head-cuts migrating upstream if vertical drop is less than 2-m high. High drop grade control structures are used in deeply incised channels to intercept head-cuts for vertical drop up to 4.3 m; this results in raising the bed upstream of the structure. Box culvert grade control structures are used instead of bridges and culverts to establish a vertical grade up to 2.7 m. Finally, riser pipe grade control structures are employed to reduce lateral gully erosion by transporting the water from the floodplain to

the channel through underground pipes (Mendrop & Little, 1997).

Thorough examination of such structures in western Iowa suggests that the movement of riprap is the leading cause of the decrease in performance and durability of these structures in streams with large flow discharges (Gu et al., 1999). Other problems include downstream erosion of stilling basin, downstream and upstream side-slope instability (which sometimes induces mass movement of riprap), displacement of engineering fabric, erosion around ends of weirs, seepage under concrete blocks and through grouted riprap, settlement of concrete blocks, and the disruption of downstream sediment transmission (Gu et al., 1999; Simon & Darby, 2002). However, many of the structural deterioration problems are caused by poor maintenance (Litvan et al., 2008). Since these structures trap sediment, they cause the stream to be more abrasive downstream which can produce bed lowering (Mendrop & Little, 1997).

Grade control structures may be used instead of drop structures to cope with ecological concerns (Pagliara & Chiavaccini, 2006). However, these structures can hinder or obstruct fish migration (Thompson & Stull, 2002). Those designed with steep gradient or damaged structures are especially likely to act as a barrier for fish during periods of low or high flows or when the resulting flow velocities and depths are incompatible with fish migration capabilities (Litvan et al., 2008). Non-migratory fish species may also be affected by the installation of these structures if they move within their resident stream. Therefore, it is recommended to use a 1:20 (or gentler) slope and to plan a water depth varying between 0.3 and 0.4 m in order to facilitate fish passage under a wide range of flow conditions (Litvan et al., 2008). However, a balance must be reached between economic costs and stream rehabilitation goals as the cost of these structures increases as

slope decreases (Litvan et al., 2008).

The installation of a grade control structure results in the formation of a downstream hydraulic jump as the supercritical flow (produced by flow acceleration on the falling limb of the structure) becomes subcritical due to a sudden increase in flow depth, causing an abrupt decrease in flow velocity and dissipating energy. A supercritical flow has a Froude number ($F = V/\sqrt{g \cdot Y}$ where V is flow velocity, g is the acceleration due to gravity, and Y is flow depth) that is greater than 1 whereas a subcritical flow as a Froude number that is less than 1 (Dingman, 1984; Knighton, 1998). Such natural process can be mimicked by installing various materials or structures in a section where flow energy needs to be reduced.

Screens

Vertically-placed screens are effective in dissipating energy downstream of small hydraulic structures, and protecting these structures against scouring (Bozkus et al., 2007). The parameters affecting the screens efficiency include porosity, thickness, and location. A porosity of 40% was found to be the most effective (Rajaratnam & Hurtig, 2000; Bozkus et al., 2007). Double screens were found to be slightly more effective in dissipating energy but also stronger than single screens (Rajaratnam & Hurtig, 2000). These results were obtained from experiments performed in laboratory setting and their implementation may not be possible in all rivers due to the accumulation of debris that may occur or due to the damage they may induce.

Deflectors

Deflectors are hydraulic structures of various shapes and building materials that are

used both in bank protection and in fish habitat development. Various terms are used to refer to these hydraulic structures. Barbs, groins, spurs and dykes refer to these unsubmerged structures whereas vanes refer to submerged deflectors (Haltigin et al., 2007; Practical Action Nepal, 2007). Submerged vanes are small profiled deflectors that can be used in a channel bend bed to reduce flow velocity and concentrate the flow in the center of the stream without constraining fish movement (Paice & Hay, 1989). Barbs are dike-like stone structures that can be used to protect stream banks against undermining and local erosion in the outer-bank region of a sharp bend and promote sediment deposition. The system performance depends on parameters such as barbs alignment and location, and the channel bend curvature (Matsuura & Townsend, 2004; Minor et al., 2007). Groins consist of piles (often woody) laid out in rows, anchored to the bed, and overtopping the water surface to protect specific banks from erosion; the key variables affecting the efficiency of the system are the depth of the pile embedment, flow velocity and discharge and cohesion (Abam, 1995). Spurs protrude in the river and redirect the course of a river away from a vulnerable bank (Practical Action Nepal, 1997). Finally, dykes are structures made of individual rocks that protrude in the river from the sides to protect its banks from high flow velocities (Practical Action Nepal, 1997). Gabions, wire cages filled with rocks, can be used to decrease construction cost and provide good stability of spurs and dykes.

Bank infrastructure

Some other structures provide bank protection without significantly redirecting the course of water. Channel bank infrastructure such as riprap or lining is often used to limit land loss and associated hazards and damages (Florsheim et al., 2008). Riprap stabilises

banks by reducing the effect of erosional processes using rocks that resist hydraulic forces; variables affecting the performance of this type of revetment include the size, shape, gradation, quality and thickness of the layer of rock, discharge or velocity and slope (Gu et al., 1999). However, bank infrastructure does generally not address bed incision and may be ineffective over multidecadal timescales if a flood exceeds the magnitude for which the infrastructure is designed (Florsheim et al., 2008). For instance, the repetitive failure of the bank infrastructure installed between 1975 and 1979 in the Little Choconut Creek, near Binghamton, New York is explained by the use of bed sediment to form protection structures, the lack of adequate foundations to avoid basal scour, and the placement of structures near strong secondary currents (Brookes, 1988). Hard structures may also encourage more damaging erosion events since they do not allow geomorphic adjustments except incision (Florsheim et al., 2008). As mentioned above, bank infrastructure prevents the ecological benefits associated with bank erosion (Florsheim et al., 2008).

A protection apron may however be effective in preventing erosion when installed on the concave bank of an acute bend (Jueyi et al., 2006). The side effects of using such a structure include scour along the outside wall of the downstream section and the accumulation of sediments along the inside wall. Those impacts are attenuated by the inclination and smaller dimensions of the protection apron. Since scour depth is related to flow obstruction, upstream-oriented embankments result in maximum scour depth as opposed to those oriented toward the bank at a certain angle (Chang, 1988). Local scour decreases with increasing protection apron, and transversal and longitudinal scours decrease with decreasing protection apron slope (Jueyi et al., 2006). The results obtained

from flume experiments suggest that scour volume increases with spur dike volume and that an increase in overtopping flow ratios (i.e. flow depth divided by dike height) moves the location of the scour zone downstream of the dike towards the bank (Kuhnle et al., 1999). Some other parameters affecting scour include the grain size of the channel bed material, the incoming velocity, and water depth (Jueyi et al., 2006). Scour along instream structures can also provide pool habitat which can be beneficial for fish species. Spurs of various lengths and inclination were found to increase fish biomass by 1.2 to 15 times when compared to continuous stone toe protection running parallel to bank (Kuhnle et al., 1999).

Limitations

Three limitations are recognized in the use of hydraulic structures. Firstly, there is no common agreement on their effectiveness, on the type of building materials and on the most appropriate design to use (Biron et al., 2004). Secondly, "basic watershed processes remain misunderstood" (Thompson & Stull, 2002, p. 14). For instance, many projects involving paired deflectors to maintain deep pools were unsuccessful due to the lack of knowledge about the complex three-dimensional flow dynamics created by this type of hydraulic structure (Haltigin et al., 2007). The lack of knowledge about physical processes will be more acute for structures that are less frequently used. Lastly, bank protection might not be beneficial in a case where erosion is already taking place (Shields et al., 2003). Also, most of the documented assessment reports involving hydraulic structures suggest that many of the installed hydraulic structures failed either because they were destroyed by floods or because they reduced aquatic species diversity and disrupted invertebrate populations (Thompson & Stull, 2002; Kondolf & Yang, 2008).

1.2.3. Flow retention facilities

It is also possible to inhibit stream hydrology by retarding water input in the channel in order to reduce peak flow discharges. Without altering land use, this can be achieved with the installation of backwater ponds or retention basins. In the former case, water is free to move from the stream to an accumulation pond as the flow discharge increases over a certain value. Brent River Park regeneration Project used such structures (Brent Council, 2010). Retention basins can serve different purposes: hydraulic purposes, sustainable drainage, environmental protection, recreational activities and landscape aesthetics (Scholz, 2007). Based on 34 classification variables, Sholtz (2007) defines the following basin categories: hydraulic flood retention basin, traditional sustainable flood retention basin, sustainable flood retention wetland, aesthetic flood treatment wetland, integrated flood retention wetland and natural flood retention wetland. When the primary concern to be addressed is channel stability, hydraulic flood retention basins can be built to retain water coming from the fields in addition to promoting sedimentation (MAPAQ, 2009). Two types of hydraulic retention basins are distinguished: dry and moist. The dry basin is covered with grass and will evacuate water whenever water is available in the basin. A humid basin will evacuate water only when a certain depth is reached within the basin, thus it always contains water (except if it does not rain for a while and all the water body evaporates completely) and requires water-tolerant vegetation species. Although the latter type would certainly enhance biodiversity by extending the humid zone, the former is probably more realistic in an agricultural context which requires the soil to be dry to a certain depth for better crop growth. Although the size of retention basins is strongly linked with climate conditions, the capacity of the retention basin should lie between 60 to

200 m^3/ha (MAPAQ, 2009).

1.2.4. Vegetation for ecological management

The use of vegetation to enhance river stability is recognized as a soft-engineering approach because it uses natural river constituents (e.g. shrubs, trees) to enhance bank cohesion and limit sediment input by overland and instream flow. If used appropriately, vegetation can help the river self-sustain and can markedly enhance channel habitat quality and diversity. The temporary installation of unnatural structures may be employed to facilitate the establishment or re-colonisation by vegetation.

Vegetation

The importance of vegetation is often highlighted in the geomorphology and ecology literature (Abernethy & Rutherfurd, 1998; Beechie et al., 2010). For instance, simulations performed with the two-dimensional depth-averaged model mRIPA suggest that high density riparian stripes constituted from trees having deep and extensive root network can enhance bank stability and reduce floodplain area loss, and therefore influence channel planform evolution and bed topography (De Wiel & Darby, 2004). Using field measurements, Micheli et al. (2004) found agricultural floodplains to be 80 to 150 percent more susceptible to erosion than riparian forest floodplains. Soil strength could be increased compared to bare soil by maintaining a riparian vegetated strip consisting of woody and grass species. However, the net effect of this approach on channel bank stability varies with plant species assemblage and moisture content (Simon & Collison, 2002; Simon et al., 2006). Nevertheless, a riparian strip consisting of a combination of shrubs and trees is expected to enhance vegetation colonisation and channel narrowing due to improved channel stability (Malkinson & Wittenberg, 2007). In addition, riparian zones

increase the overall catchment's response times to precipitation events, decrease peak discharges, and reduce associated erosion processes (Anderson et al., 2006).

Plant roots interact with the soil matrix by providing mechanical reinforcement. The resulting increase in bank strength prevents mass failure in lower reaches (Abernethy & Rutherfurd, 1998; Millar, 2000; Rey et al., 2004). Plants are most efficient in improving stability over a range of bank geometries when used along failure planes under worst-case hydrological scenarios (Abernethy & Rutherfurd, 2000). In addition of varying spatially and temporally in magnitude, the effect of root reinforcement decreases as soil moisture increases and shear strength decreases (Pollen, 2007). Variability in the distribution of living roots from different species is more significant for root reinforcement than the variability in the strength of individual roots (Abernethy & Rutherfurd, 2001). However, there is threshold diameter above which any root will break when subject to a certain stress, and below which it may either break or be pulled out (Pollen, 2007).

In addition to mechanically altering bank cohesion, vegetation affects sediment transport processes. In-stream vegetation decreases near-bank flow velocity and associated particle entrainment in mid-basin reaches by protecting soil particles against raindrops, trapping and retaining sediment, increasing infiltration rate, and decreasing erosion potential by runoff (Abernethy & Rutherfurd, 1998; Millar, 2000; Rey et al., 2004; Lau et al., 2006). Vegetation density is a key factor controlling velocity reduction and flow diversion (Bennett et al., 2002). Carline and Walsh (2007) reported 47-87% and 75-83% reductions in total suspended load five years after the installation of a three-meter buffer strip, respectively for base and storm flows. Foliage significantly inhibits the sub-aerial processes causing erosion in the upper reaches of a stream by minimizing soil surface

weathering and by reducing sediment transfer rate from the banks to the flow (Abernethy & Rutherfurd, 1998).

When comparing the functions of plant types, individual trees act more locally than shrubs since the latter contribute both to the reduction in near-bank flow velocity and to soil cohesion (Malkinson & Wittenberg, 2007). Similarly, in order to maximize the effectiveness of a steep slope stabilisation project, the choice of plant species should rely on factors such as soil type and use, plant capacity to hold soil particles by its root system, physical structure, leaf area coverage, and tolerance/requirements in terms of local temperature, moisture, and sunniness (Morris & Moses, 1998; Rey et al., 2004).

Well-developed riparian vegetated strips also prevent fertilizers and pesticides from polluting the stream (Lau et al., 2006). A greater diversity enhances productivity in plant communities which leads to greater nutrient retention (Tilman, 2000). For instance, a monitoring study conducted in Iowa reported an important reduction in nitrate-nitrogen levels (from 12 mg/L to less than 2 mg/L) four seasons after the implementation of a riparian multispecies vegetated strip (Schultz et al., 1995). Such a strip also provides habitat to wildlife, produces biomass for on-farm use and high-quality hardwood for the future, and enhance the aesthetics of the agroecosystem (Schultz et al., 1995).

Bioengineering

Bioengineering bank stabilisation projects involve the installation of vegetation on surfaces affected by erosive processes in order to reduce the speed at which a bank erodes (Sudduth & Meyer, 2006). Such strategies can be implemented as a flexible treatment at the edge of built and natural environments to allow self-adjustment of the stream dimensions and profile and thus protect engineered structures (e.g. bridge abutments) that

may otherwise be damaged by scour (Li, 2006). The degree of erosion caused by rainfall, runoff and wind, and the amount of suspended sediments both decrease significantly with the use of geosynthetical mulching mats; theses membranes facilitate the establishment and growth of seeds and vegetation on steep slopes by holding seeds and fertilizers and preventing them from being washed away (Ahn et al., 2002). Mats, also referred to as rolled erosion control products (RECPs), are biodegradable to reduce long-term environmental impacts, light weight and portable for ease of installation, and capable of holding high water content while remaining substantially unaffected (Ahn et al., 2002; Rey et al., 2004). Other methods used include wattles (straw rolled in natural geotextile fibres, placed in trenches and staked down), coir roll (cylindrical structures to anchor plant roots), live fascine (cuttings tied together in linear cylindrical bundles), live brush mattress (branch cuttings placed on the bank face), brush layering (live cuttings installed into stream banks between layers of soil), and live willow stakes (live and rootable willows planted into the soil) (Frothingham, 2007). Contrasting permissible and actual values of velocity and shear stress for different types of bank stabilisation materials can be obtained from a stability threshold analysis, which provides a range of stabilisation approaches for eroding banks (Frothingham, 2007).

The Québec provincial laws require a riparian zone at least three meters wide in agricultural areas; this measure would be sufficient to capture fertilizers, pesticides and eroded soil particles, but insufficient for most plant and animal species requirements; plant species require a buffer zone 10 to 30 m above high water mark, and birds 75 to 175 m (Spackman & Hugues, 1995; Boutin et al., 2003). In addition to stabilising banks, bioengineering has a small positive ecological effect on bank habitat and macro-

invertebrate communities in urban streams; an increase in biodiversity and biomass was noted and associated with increased root and wood habitat (Sudduth & Meyer, 2006). Higher plant diversity reduces nutrient losses which benefits water quality (Tilman, 2000).

1.2.5. Channel layout and morphological alterations

Environmental alternatives to traditional engineering methods such as straightening include relief channels, partial dredging, distant flood banks, two-stage channel beds and river corridors (Hey, 1996, Piégay et al., 2005a). A relief channel is used to divert the flow above a given stage away from the main channel. Partial dredging limits dredging to the central section of a channel to increase its cross-sectional area. Distant flood banks are built at the edge of meander belts to restrict overbank flows flooding to a strip of floodplain whereas two-stage channels consist in the excavation of the upper section of the floodplain adjacent to the river. These methods allow increasing flow capacity while avoiding a complete destruction of habitats and flora, as is the case with straightening (Hey, 1996).

Another alternative consists in the creation of a new irregular sinuous channel having specific bankfull depth, slope and velocity (Hey, 1987; 1996). Several scenarios should be envisaged in the design process, each of them accounting for parameters such as channel-forming discharge, bed material size distribution, natural bed slope and meander geometry (Shields et al., 2003). A channel can be designed using a reference reach from the same hydrophysiographic region with a similar basin area and valley type to ensure similar flow and sediment transport regimes. Valley parameters include width, slope, materials, landform and vegetation density (Hey, 2006). The extent and magnitude of the applied modifications should be minimal to restrict habitat disturbance. Stability checks

may be performed to test stability and sediment transport for specific bed and bank stabilisation solutions (Shields et al., 2003). In particular, bank gradient must take account soil texture and the bank stabilisation method to be used (D'Auteuil & Dubois, 1994).

In cases where channel remeandering is unachievable due to space limitation or agricultural drainage restrictions, the installation of pool-riffle units in stable straight channels (not undergoing significant active erosion) can enhance aquatic habitat by providing some of the benefits associated with natural river morphology (Rhoads et al., in press). Although pool-riffle sequences are usually found in meandering or sinuous-thalweg channels, numerous case studies suggest that the pool-riffle sequence can be preserved in low-gradient (< 0.01) channels with limited amounts of mobile bed material (Rhoads et al., in press). Channel maintenance is provided by flow convergence which requires the use of immovable material to perpetuate convergence, which is known to be very important in pool formation (MacWilliams et al., 2006; Sawyer et al., 2010), and to protect bank toes.

1.3. Restoration projects and public perception

As pointed out by Hassett et al. (2007), interviews with practitioners provide information that is not necessarily available elsewhere and that should be captured in some written form before the knowledge gets lost. Useful information includes the goals and degree of success achieved in river-related projects, and the observations made during their implementation and monitoring processes. The most common goals include aesthetics/recreation/education, bank stabilisation, channel reconfiguration, fish passage, floodplain reconnection, flow modification, in-stream habitat improvement and species management, riparian management, stormwater management, and water quality

management. However, the significance of these goals depends upon the perception of river services.

Public perception of river functions is an important aspect to consider when elaborating management strategies. For instance, woody debris in streams and rivers are beneficial to aquatic and riverine ecology, as evidenced by the existence of strong linkages between large woody debris and fish abundance and diversity (Montgomery & Piégay, 2003). However, there are clear cultural differences in public perception among countries and among disciplinary groups, notably in terms of aesthetics, naturalness, danger, and need for improvements (Piégay et al., 2005b). According to a study aiming at assessing the intuitive perception of the German population in respect to the use of woody debris in streams and rivers for ecological benefits, the conditions influencing the population perception included (1) personal experiences, knowledge and appreciation of the wilderness appearance of natural forests and (2) the degree of environmental education provided by mass media about the implementation of various projects aiming at intervening in rivers while minimizing damages to the environment (e.g. forestation, increasing water retention in natural upstream reaches) (Mutz et al., 2006). The elaboration of a socially acceptable solution is therefore influenced by stakeholders' education and communication among them (Piégay et al., 2005b) and is thus site-specific. In some cases, public pressure results in restoration efforts, as was the case for the river Gelså, Denmark which was improved both in terms of aesthetics and recreational opportunities (Nielsen, 1996). This example clearly demonstrates the influence of public perception and power on decision making processes (Nielsen, 1996).

Contrasting perceptions also exist among disciplinary groups in the field of stream

restoration (Piégay et al., 2005b; Mutz et al., 2006), notably in the definition and assessment of success criteria. This argument is evident when comparing the perspective of engineers versus that of geomorphologists or biologists. For instance, Mendrop & Little (1997) suggests that grade control structures provide the stability required to accelerate the rejuvenation of habitat diversity and enhance environmental aspects of the total watershed system. Also, although Gu et al. (1999) identified nine common technical structural problems associated with grade control-structures, no mention is made of the potential adverse ecological effects that these structures may have. On the other hand, Litvan et al. (2008) expressed concerns about fish passage criteria within grade control structures, as well as identifying durability-related structural problems. In that study, fish migration was found to be altered for four fish species in failed structures or in structures having a slope between 1:13 and 1:18. Even the concept of erosion does not make unanimity: although erosion was traditionally mainly recognized as damaging and costly (Piégay et al., 2005), a growing number of scientists are now recognizing some of its benefits (Bravard et al., 1999; Piégay et al., 2005b; Florsheim et al., 2008).

The integration and cooperation of experts from different disciplines including geomorphology, engineering and biology therefore appears to be a crucial element in reducing the uncertainty associated with restoration efforts (Thompson & Stull, 2002). Public perception can also restrict the choice of socially acceptable restoration options, thus it must be considered in any management program.

1.4. Fluvial processes modelling

Modelling is increasingly being employed in fluvial geomorphology to understand landscape evolution and predict flow hydraulics and sediment transport in natural settings

or in response to anthropogenic land cover and channel modifications (Lane & Ferguson, 2005). Several models can also be combined into a single model, as performed by Yeh (2006) who calculated erosion, sediment yield, runoff, nutrient pollution and the economic costs associated with land use in Keelung River, Taiwan.

Darby and Van de Wiel (2003) proposed a framework for applying modelling tools in practical applications. Its major steps are problem identification and formulation, reconnaissance and data collection, model selection and application, calibration and validation, comparison of predictions, and results interpretation. The selected model must be compatible with the scale of the phenomenon to be investigated. The following four categories of models are recognized, each one generally applying at a specific scale: conceptual (scale of a reach up to that of an entire landscape), statistical and empirical (scale of individual cross-sections), analytical (usually at the scale of the river cross-section), and numerical (no specific scale) (Darby & van de Wiel, 2003). A conceptual model provides a qualitative description and some predictions regarding landform and landscape evolution. In statistical models, functional relationships are implemented between dependent morphological variables and independent variables such as sediment load and discharge. An analytical model is based on the physical processes responsible for the evolution of channel morphology. Lastly, a numerical model spatially represents physical characteristics of a terrain in a grid of discrete values. Geomorphological models can also be divided in two categories based upon their spatial application extent. A watershed scale model is usually employed to study a phenomenon using one or two spatial dimensions whereas a greater level of details may be required to thoroughly study a phenomenon at a more local scale. In small-scale modelling (i.e. large area covered),

the computation of details may be impossible due to technological limitations (i.e. memory, duration) but may also be irrelevant for the selected scale.

The role of vegetation on channel morphology is known to be important, and numerical modelling has been used to analyse the contribution of plants to soil strength, by emphasising on the distribution and variation among species and types (Simon & Collison, 2002). Furthermore, the transformation of a straight, degraded stream channel into a meandering, ecologically functional river corridor following the planting of emergent, rigid vegetation has been confirmed by the simulations of Bennett et al. (2008) using the two-dimensional (2D) model developed by Wu et al. (2005). The results suggest that morphological changes such as channel expansion and widening, thalweg meandering and riffle and pool development are expected to occur in response to the planting of rigid emergent vegetation and that the magnitude of these changes depends upon the shape and density of instream vegetated. Channel meandering processes such as downstream translation and lateral extension in non-cohesive banks can also be simulated using a 2D hydrodynamic model (Duan & Julien, 2005). Furthermore, an integrated modelling approach such as the GIBSI model can be used to predict the effects of various timber harvest scenarios on runoff or to investigate the effects of management programs aiming at improving water quality (Rousseau et al., 2000).

Many studies have focussed on modelling sediment transport and erosion processes. For instance, Simon et al. (2003) studied bank-toe erosion caused by hydraulic shear using a bank-stability model and a two-dimensional hydrological model that simulates pore-water pressures (Simon et al., 2000). In this model, pore-water pressure distributions, layering, confining pressures, reinforcement effects of riparian vegetation,

complex bank geometries, and hydraulic effects are considered. Similarly, Chu-Agor et al. (2008) investigated the changes in bank stability produced by seepage undercutting using a general limit equilibrium bank stability model (SLOPE/W) and the output of a second model that simulates pore-water pressures (SEEP/W). The CAESAR model was developed to simultaneously simulate meandering and braiding processes in an attempt to model channel migration (Coulthard & Van De Wiel, 2006). An improved version of the model was developed to provide higher-resolution computations of flow routing, sediment transport, sediment suspension and lateral erosion (Van De Wiel et al., 2007). The model allows simulating morphological processes such as bar formation, floodplain deposition, river bank erosion, channel migration, and terrace formation.

Rodriguez et al. (2004) proposed that flow velocity properties can be accurately predicted in a sinuous channel using STREMR, a depth-averaged two-dimensional model or FLOW-3D, a fully three-dimensional model. Jia and Wang (1999) reached the same conclusion with CCHE2D, a two-dimensional hydraulic model after validating flow hydraulics in a meandering irregular channel and around spur dykes. Since flow hydraulics is directly related to channel morphology, a growing number of hydraulic structures and management strategies can be tested before implementation, ideally with a three-dimensional model. For instance, Jia et al. (2005) analysed flow characteristics using the model CCHE3D around submerged weirs and concluded that these structures are efficient in realigning the flow and thus facilitating navigation in channel bendways. Three-dimensional modeling performed with the model SSIIM reproduced flow conditions and the patterns of erosion and deposition in a series of seven stream barbs (Jamieson et al., 2009). The same model was also used to predict flow changes following

the installation of different layout of U-, V- and W-shaped weirs (Bhuiyan & Hey, 2007).

1.5. Summary and research objectives

The channelization of the hydrological network undertaken in agricultural watersheds in the 20th century was beneficial for crop productivity, farmers' wealth and social security. However, there is a growing consensus that the unsustainable management approaches that are currently used should be reviewed and improved to better integrate environmental and economical aspects. Despite ongoing research in fluvial geomorphology and river engineering to improve our understanding of flow hydraulics and channel dynamics, failures in river enhancement projects are common.

Numerical modelling can help identify the most effective management strategies for channelized streams at relatively low cost since many variants of each alternative strategy can be tested until the benefits are maximised. Since instability problems exist at the watershed and local scales, different models are needed to understand and predict responses at each scale. The objective of this research is to assess the hydrological and geomorphological impacts of different management strategies to improve the stability of an agricultural straightened channel using numerical modelling. At the watershed scale, the management strategies are the installation of backwater ponds and the re-creation of meanders. They are assessed using a numerical model based on that developed by Rousseau (2008). At the reach scale, the tested strategies are bed weirs and stream barbs. Their impact on flow hydraulics is analysed using a 3D computational fluid dynamics model (Phoenics) in straight and meandering reaches, respectively. The technical feasibility, installation ease, financial costs and environmental benefits that the four management strategies are expected to bring are considered in their overall assessment.

2.1. Study site

The Richer Stream is located in southwestern Québec near the municipality of Saint-Marc-sur-Richelieu, approximately 25 km east of Montréal (73.20ºW, 45.68ºN). This second order stream is a tributary of the Richelieu River, which drains into the St. Lawrence River. The Richer drainage basin covers 17 km² and includes a 6.9 km long stream and nine tributaries totalling 13.5 km in length (Figure 2.1). Its channel was extensively modified between 1943 and 1986, resulting in a 32% average increase in channel slope and a 9.9% increase in the cross-sectional area (Rousseau & Biron, 2009). Only a few downstream reaches kept their initial natural planform since at least 1932, date at which the oldest available aerial photograph was taken (Figure 2.1b).

Due to the instability of a straight channel in the geomorphological context of the St. Lawrence Lowlands and the deficiency in bank protection, dredging is performed regularly on the Richer Stream to re-establish the channel's trapezoidal cross-sections and linear planform. This expensive maintenance systematically removes any obstacle that hinders stream flow, including vegetation, boulders and branches. As is the case in many agricultural watersheds in the province of Québec, the vegetated riparian strip is very narrow and sometimes non-existent. Land loss due to bank erosion is a source of concern for riparian residential land owners and farmers. For this reason, dredging is seen by many residents and decision makers as the sole realistic solution capable of solving this erosion problem. Furthermore, the regional municipality of the county (RMC) of *La Vallée-du-Richelieu* has a legal obligation to intervene quickly by dredging the Richer channel following a complaint from land owners regarding bank instability. As the channel quickly

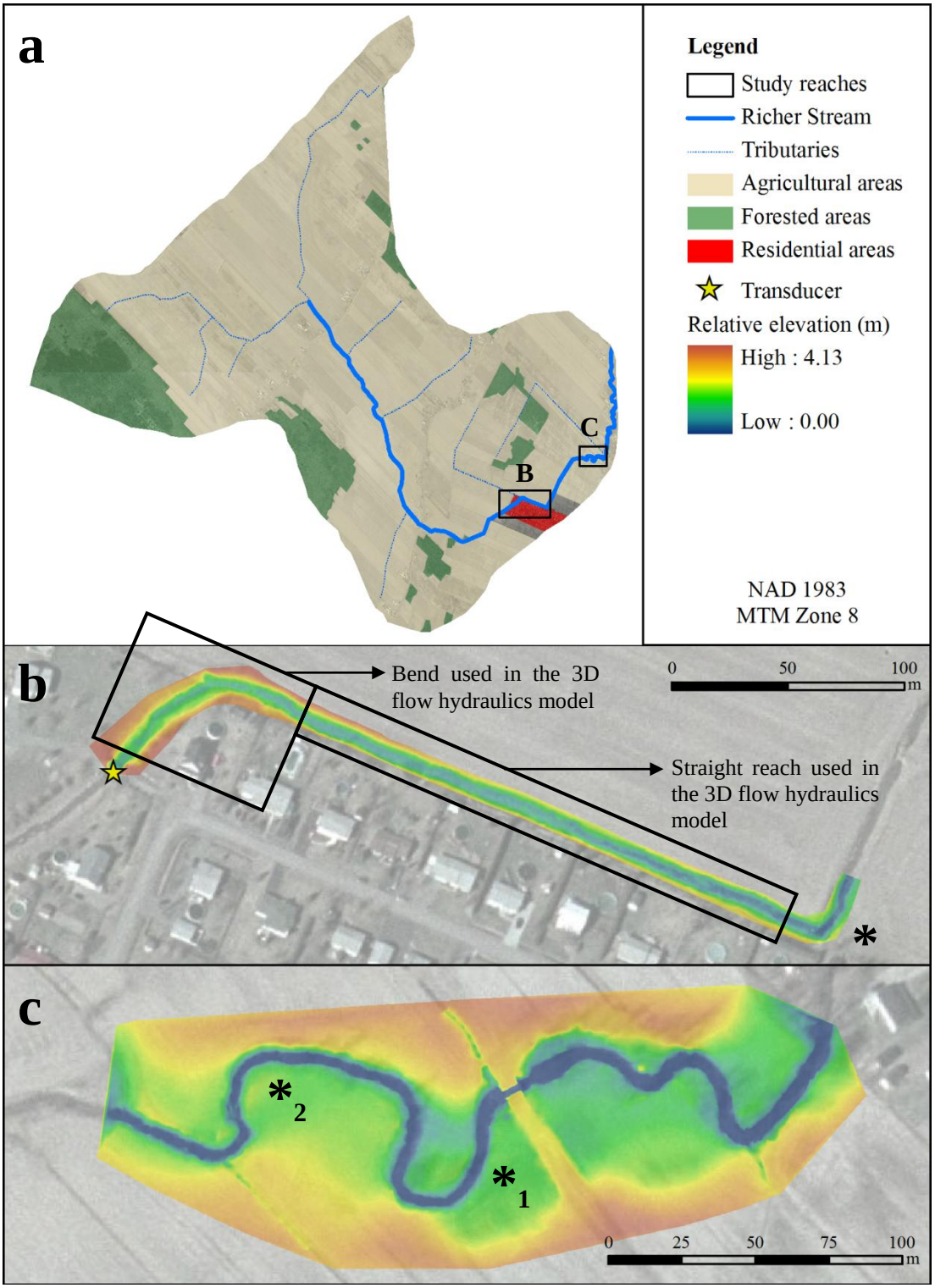

Figure 2.1. (a) The Richer watershed and stream. The (b) straight and (c) meandering study reaches. The points (*) correspond to the viewing locations in (b) Figure 2.2a and in (c) Figure 2.3.

erodes again soon after the completion of dredging works, it typically leads to further channel maintenance requirements.

This research involves investigating processes occurring at the watershed and reach scales. The first study reach has been extensively straightened, and is located near the municipality of Saint-Marc-sur-Richelieu (Figure 2.1a). It includes two unnatural sharp bends where bank erosion is recurrent and flooding hazards are important (Figure 2.2). In this reach, crops are found within the legally required 3-meter zone above high water mark (Figure 2.2b). Sheds, fences and other private goods are sometimes located in this zone on the urbanised side of the channel. The effects of bank erosion are significantly less dramatic in the second study reach which is meandering (Figure 2.1b) and which is completely surrounded by agricultural fields (Figure 2.3). In this reach, a pilot project is currently testing biotechnical methods to strengthen stream banks that are already partially naturally protected with mature riparian trees and shrubs.

Since straightening and dredging were widely used in industrialised countries in the twentieth century, this case is representative of many agricultural watersheds in Québec and elsewhere in Canada, United States and Europe. The results of the current study may

Figure 2.2. The straight study reach (a) at high flow in March 2009 and at (b) low flow in September 2007. The view is looking upstream from the point (*) indicated on Figure 2.1b.

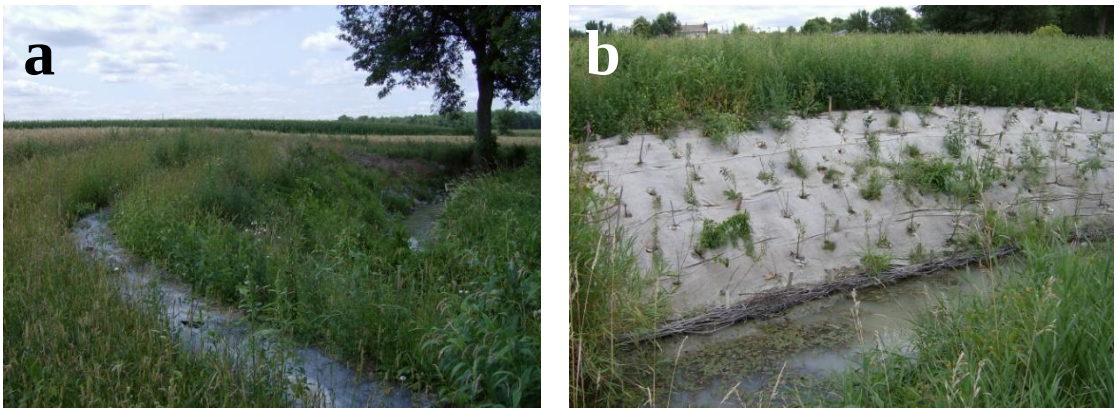

Figure 2.3. The meandering study reach (Figure 2.1c) showing (a) mature tree and rows of juvenile native trees (looking upstream from point *1) and (b) bank stabilisation with coco jute, trellised branches, and shrubs (looking towards the opposite bank from point *2).

therefore apply to other drainage basins facing similar problems.

2.2. Data collection and processing

2.2.1. Available data

Documentation spanning 1943 to 2006 and covering legal and technical aspects of the Richer watershed was provided by Julie Thibodeau, stream coordinator for the regional municipality of the county (R.M.C.) of *La Vallée-du-Richelieu*. Personal communications with stakeholders (e.g. riparian residents, farmers and local authorities) also helped understanding and quantifying some of the historical aspects of the management process.

The Club Conseilsol Vert Cher, an agro-environmental group involved in promoting ecological farming, gave us access to their GIS database on the Richer watershed for this project. The database included a digital elevation model (DEM) of the watershed, geo-referenced aerial photographs dating from 1932, 1964, 2000, 2004 and 2006, and land use, vegetation cover, water runoff and land erosion maps. The DEM was built from a total of 3928 unevenly distributed elevation points (with significantly more points close to the

stream). A high-resolution DEM (cell size of 6 x 6 m), relying on manual photogrammetry, was also provided by the non-profit organisation Géomont. Because the latter only detects the elevation of vegetation top rather than ground surface, both elevation models were combined using the inverse distance weighting (IDW) interpolation method in the GIS software ArcGIS (version 9.2) to maximize their respective strengths. This DEM is subsequently employed to calculate the area of the drainage basin contributing to the flow discharge at certain cross-sections.

Geomont also provided a database containing agricultural drainage plans for the Montérégie region. The plans associated with the studied watershed were extracted and georeferenced using ArcGIS. Since they were not updated since 1986, all drainage pipe ends associated with the main stem of the Richer stream were identified on the field in late autumn 2009. Their geographical coordinates were taken using a Garmin GPS (eTrex Vista HCx). The objectives were to (1) determine if the pipe ends identified on the plans were still in operation and to (2) verify if other drainage systems were added since the the last update.

Although technical reports about the outcome of individual stream restoration projects are sometimes available from the literature, few discuss the effectiveness of the strategies employed in the province of Québec to stabilise channels. Following Hassett et al. (2007), semi-structured interviews were conducted with a few managers and practitioners involved in stream restoration. The objectives were to determine the methods currently being employed in the field and the degree of success generally achieved in each case. Mikael Guillou from *The Ministry of Agriculture, Food and Fisheries of Québec* (MAFFQ) provided some useful information about the methods used in Québec. The staff

from Geomorphic Solutions (Mississauga, Ontario) accepted to share their information and to guide us in a field trip on various restoration projects they have conducted in southern Ontario. Finally, Joanna Eyquem, a senior fluvial geomorphologist currently working at Parish Geomorphic Ltd also contributed to this project. As she has also extensive experience in river restoration in the UK, she provided useful information and links about the restoration philosophy, methods and projects in that country.

2.2.2. Supplemental data requirements

This study required further field data to complement those already available from previous studies. We have sent an information letter along with an access request form to the owners of lands located next to the main stem of the Richer stream. Some of the farmers were met in person to provide them with further details about the research project. This process also provided useful information on their farming experience and on undocumented historical aspects of the Richer Stream.

Watershed and channel topography

Bed channel topography measurements in the two studied reaches (Figures 2.1b,c) were taken with a Leica total station model TC805L during the automn 2007 and summer 2008. The acquisition of topographic points is essential in the parameterisation of both the 3D flow hydraulics computational model, and the hydro-morphological model. Approximately 1800 topographic points were collected over a distance of 350 m in the straight reach (density of 0.39/m²) (Figure 2.1b). Nearly 2600 points were taken in a 390-m downstream meandering reach (density of 0.18/m²) (Figure 2.1c). Points were usually acquired by cross-sections, with 4 points taken on the bed and 4 on each bank, with a distance of 3 to 5 meters separating the cross-sections. Intermediate points were also taken

to capture in-channel irregularities such as collapsed banks and islands, and additional points were collected in bends. The DEMs of in-channel topography (for both study reaches) were produced using the Natural Neighbours method in ArcGIS. This method was chosen after comparing it to other interpolation methods (IDW, kriging, spline). The chosen algorithm is more appropriate for the Richer Stream which exhibits rapid changes between shallow and deep sections.

Discharge and velocity measurements

Flow velocity and discharge data are needed to calibrate both the 3D flow dynamics and the hydro-morphological models. A pressure transducer (Solinst Junior 3001) was mounted on a privately-owned bridge crossing the Richer Stream in the residential area and recorded flow depth every 15 minutes between 6 June 2008 and 3 December 2009 (Figure 2.4). This device also measures water temperature at the same frequency. The effect of an ice cover on hydraulic conditions was omitted due to the unknown relationship between the discharge and the pressure of the confined flow during this period.

Flow velocity measurements were taken with a propeller current meter (Swoffer

Figure 2.4. Setup of the pressure transducer on a privately-owned bridge (Figure 2.1b)**.**

2001) at each 50 cm laterally to compute discharge and produce a stage-discharge rating curve. When the water was less than 50 cm deep, one measurement was taken at 40% of the water column depth. Otherwise, the average of two measurements, taken at 20% and at 80% of the flow depth, was used. The channel cross-sectional area was estimated by manually measuring bed topography at 20 cm intervals. Discharge estimates derived from velocity and flow depth measurements allowed producing the rating curve at the pressure transducer (Figure 2.5). Thorough analysis of the DEM reveals that the area contributing to the flow discharge observed at this location approaches 80% of the total watershed area.

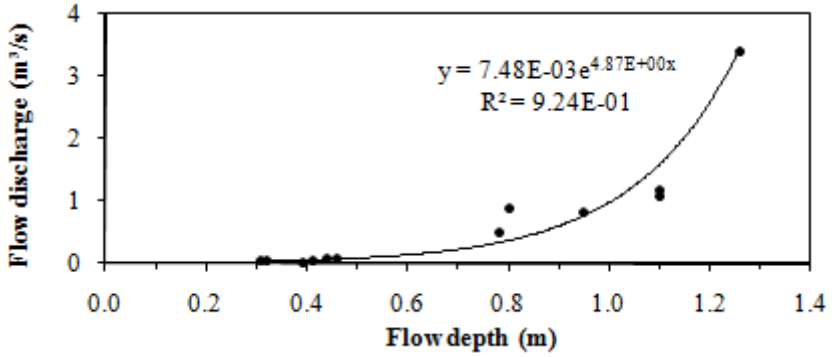

Figure 2.5. Stage-discharge curve at the pressure transducer.

The stage-discharge curve could not be used to extrapolate at higher discharges, as it predicted unrealistically high values for the deepest flow recorded by the pressure transducer, for which the velocity is unknown (22 m^3/s for a depth of 1.64 m reached in August 2008). The Manning equation was thus used to predict flow velocities at stages above which no velocity could manually be measured (due to the challenge of synchronising field visits with low-duration high stage events), assuming constant roughness coefficient and bed slope between the highest measured flow discharge and any other discharge above this value (and below the maximum channel capacity). In the Manning equation, the average cross-sectional velocity (in m/s) is given by:

$$V = \frac{1}{n} \cdot R^{2/3} \cdot S_0^{1/2} \qquad \textit{(Equation 2.1)}$$

where n is the Manning roughness coefficient, R is the hydraulic radius (m) and S_0 is the bed slope. Therefore:

$$V_{ex} = V_{bf} \cdot \left(R_{ex} / R_{bf}\right)^{2/3} \qquad \textit{(Equation 2.2)}$$

where R_{bf} and R_{ex} are bankfull and intra/extrapolated radii, respectively.

Channel and surface sediment size

In order to parameterise the sediment transport model and to complete the characterisation of the channel, samples from cross-sections along the main stem of the Richer watercourse were collected in July 2009. Cross-sections were spread apart by 250 m except where the land owners did not allow access to the stream. Although the Richer channel bed and banks mainly consist of clay, sand particles are found downstream of the residential reach and gravel particles are present sporadically in upstream reaches. Channel bed and bank samples were collected approximately at each 250 m with a shovel. Although a total of 50 samples were acquired (from 23 cross-sections), the analysis was limited to 32 samples. The unused samples were stored in case other analyses are required.

After removing the organic material and drying each sample for a period of 24 hours at 105˚C, a quantity of approximately 100 grams of each sample was crushed with a mortar and pestle. A combination of sieve analysis and hydrometry procedure was followed in order to determine the sediment size and distribution of each analysed sample. The analysis reveals that the samples collected from upstream beds and banks have a clay texture (median particle diameter of 0.0044 mm) whereas downstream

samples consist of clay loam (median particle diameter of 0.0092 mm). Note that many incongruous results from the analysis were observed due to the attraction and agglomeration of clay particles. Therefore, the traditional procedure relying on H-151 type hydrometers was modified to better dissolve particles from the sample and remove sand and larger particles prior to the hydrometry analysis.

Sediment transport

Three types of sediment loads were required for the Richer Stream characterisation and for the validation of the sediment transport model developed for this study: surface sediment runoff, bed load, and suspended load. Surface sediment runoff was estimated at two different locations in the Richer watershed using a series of samplers based on the design of Mathier et al. (1989) (Figure 2.6). The first site was located near a hilly corn crop whereas the second site was located on a flatter terrain with hey crop. Both sets of samplers were installed in June 2009 and removed early in December 2009.

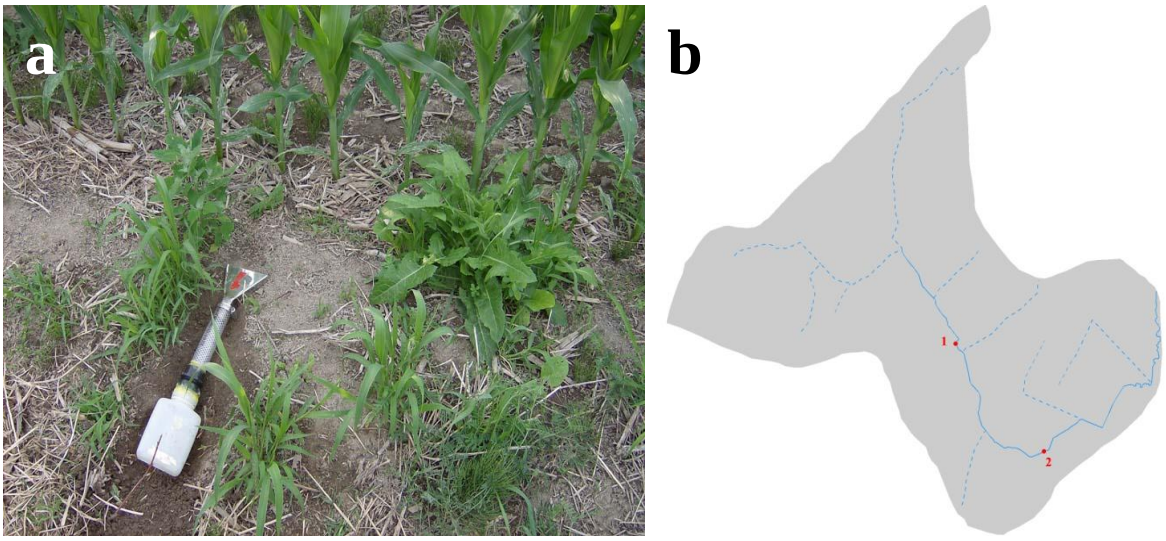

Figure 2.6. (a) Runoff samplers based on the design of Mathier et al. (1989); (b) location of the samplers.

Three temporary bridges were built over the channel to facilitate bed load and suspended load rate measurements. Due to their small length, the bridges were installed at locations

where the channel width is narrow and the banks are steep. Bridge's abutment pairs were built from stainless steel fence hardware. The design of the abutments was different for each bridge due to contrasting channel morphologies (Figure 2.7a-c). A Featherlite lightweight (16 kg) commercially-graded fibreglass ladder hanging between abutments on opposite banks and used as a platform then allowed data to be acquired without standing in the river and without disturbing bed substrate. Due to the proximity of the Richer Stream to main roads and urban centers, the bridge system was designed to fit on a car roof. It was also easy to carry between corn rows over a distance of 1 km, and it could be installed by a single person (even at a high-flow stage). Since it is usually not recommended to use this kind of ladder as a bridge, its flexibility and strength were tested prior to data collection. Some concrete blocks (115 kg) were gradually placed in the middle of the open ladder whose extremities were elevated. With this design, the ladder could be stretched at a length of 21 feet and hold one person. Four U-bolts were added between stair pairs to secure the ladder and thus ensure that it will not open when acquiring data. A permanent private bridge was used as a fourth site of sediment transport data and flow conditions acquisition (Figure 2.7d).

Bedload transport rates were measured during two high-flow discharge events using a Helley-Smith sampler (Figure 2.8a). A custom tool was built to facilitate the transfer of sediment from the collection bags to smaller transport bags (Figure 2.8b). Similarly, water samples were collected for different flow depths using a MSR Sweetwater camping pump, after removing the carbon filter (Figure 2.8c).

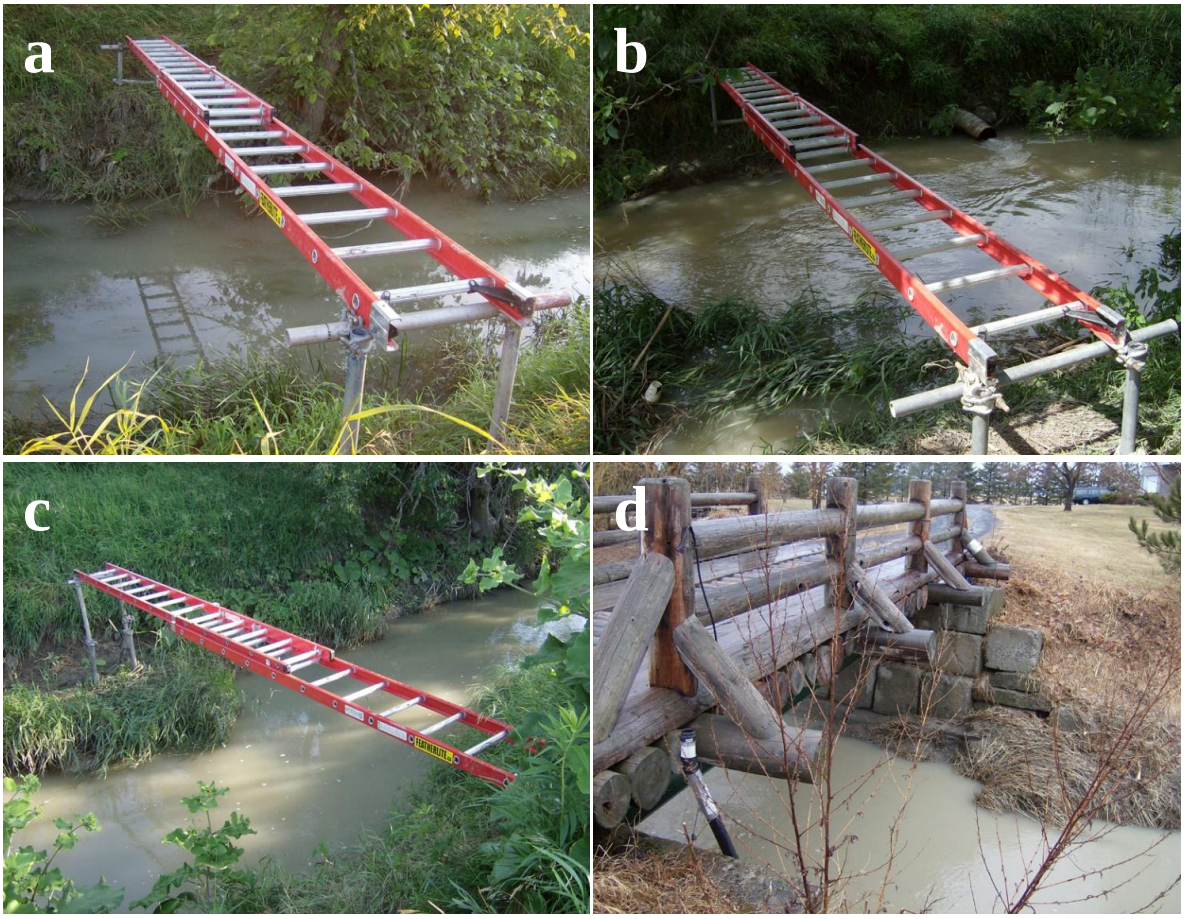

Figure 2.7. Data acquisition (a) bridge #1, (b) bridge #2, (c) bridge #3 and (d) bridge #4. The location of each bridge is mapped in (e).

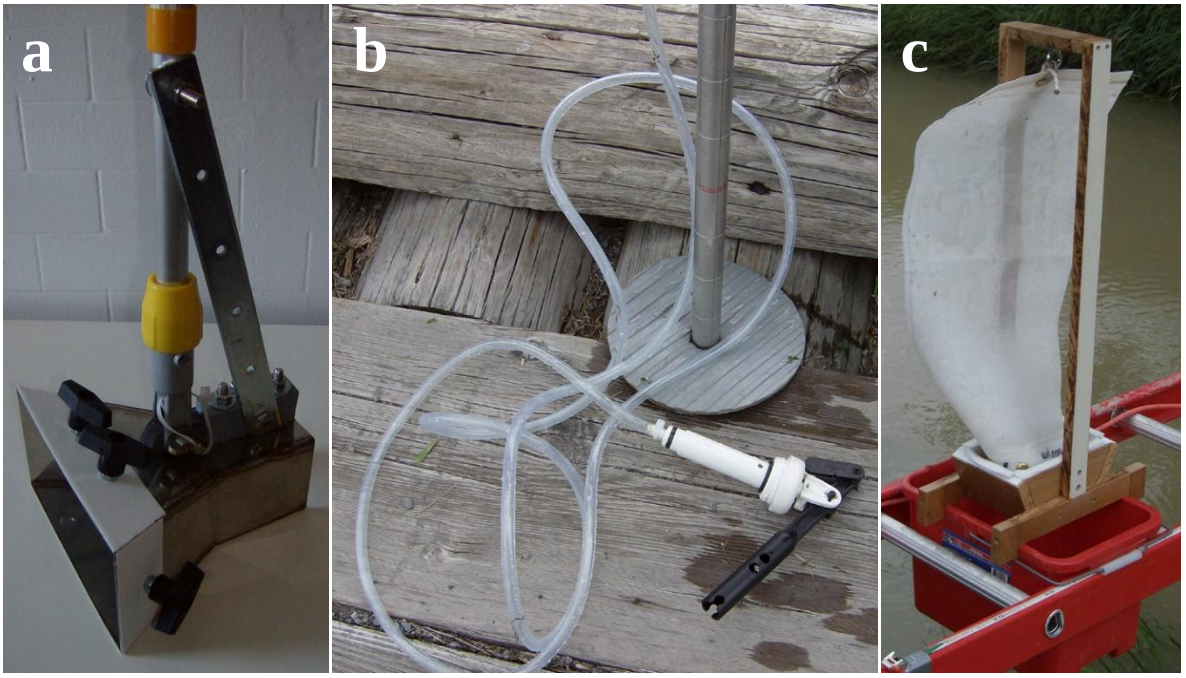

Figure 2.8. Instream sediment transport rate samplers showing (a) a Helley-Smith sampler and (b) a water pump used for collecting bed load sediment and suspended load, respectively. The photograph in (c) shows the hardware used to empty the sediment trapped in the net that can securely be attached to the Helley-Smith sampler.

Climate data

Since weather conditions are not available for the examined watershed, the assumption was made that they are similar to those recorded at Mount St-Hilaire weather station (managed by McGill University). Climate and weather data were obtained from this station that is located 19 km south from the Richer watershed centroid. The provided data include wind speed and direction, atmospheric pressure and precipitation. Through an agreement with McGill University, the station was modified from previous configuration in June 2008 for the duration of this study to record precipitation data each 15 minute and thus take maximum precipitation intensity into account. However, the occasional lack of synchronization between the Richer flow discharge and precipitation data provided by the aforementioned station (attributed to spatial differences in fallen precipitation depth) resulted in a need to use data from supplemental neighbouring

weather stations. The interpolation of precipitation data from these stations (Figure 2.9) significantly improved the correlation.

Figure 2.9. The Richer watershed and surrounding weather stations: (1) St-Amable, (2) St-Antoine, (3) St-Hilaire, (4) Ste-Madelaine and (5) Montreal (Trudeau Airport). Source: Google Earth (2010).

2.3. Numerical modelling

The establishment of exhaustive inventories of stabilisation methods and management strategies was achieved in previous studies (Ahn et al., 2002; Thompson and Stull, 2002; National Cooperative Highway Research Program [NCHRP], 2005). Therefore, it does not constitute one of the main objectives of the current study. However, a literature review was completed above determining the range and conditions of application of some of the methods that could potentially be beneficial to the stability of a watershed located in the St. Lawrence lowlands. This review identified the approaches used in Québec, in Canada and in other similar countries in terms of industrialisation and environmental settings. It also helped understand the legal, social and procedural changes that would be required in Québec before being able to implement the most sustainable available solutions. These methods are assessed using two numerical models used at two different scales. A two-dimensional hydro-morphological model programmed in the Java language is employed to predict the effect of two management strategies on hydrological and sediment transport processes at the watershed scale. In addition, a 3D fluid dynamic numerical model is used to predict the hydraulic effects on the flow field of adding instream structures (weirs and barbs) at the scale of individual reaches.

2.3.1. The hydro-morphological model

2.3.1.1. Purpose and overview of the initial version

In order to predict and compare flow conditions, sediment transport rates and channel evolution resulting from the implementation of various stream management approaches, a numerical model specific to agricultural streams is employed. This model requires few input parameters and was developed by Rousseau (2008) using Stella® model builder software version 9. The hydro-morphological model consists of three modules, each of which deals with a category of physical processes: the weather generator, the hydrological model, and the sediment transport model. The model is thoroughly described in Appendix A but its main characteristics are introduced below.

The weather generator produces a set of daily weather records (statistically derived from the analysis of climate variable averages and distributions). These records are used by the hydrological module to predict instream and surface sediment transport rates. The computed climatic conditions include air temperature (monthly minimum, maximum and average), relative humidity (average monthly), wind speed (average monthly) and precipitation (type, depth and duration). The hydrological module statistically predicts flow discharge peaks and recession rates from water excess depth (i.e. water remaining on the ground after evapotranspiration and snow melt). The sediment transport module forecasts the intensity of overland and instream sediment movement (Figure 2.10). Sediments from the surrounding fields may leach into the stream during intense precipitation events and those within the stream are lifted and entrained towards a downstream section as bed and suspended loads. The variables from the three modules interact as shown in the causal loop diagram (Figure 2.11). A positive feedback

mechanism exists where a change in discharge or slope induces a change in the channel cross-sectional area in the same direction.

Channel representation and evolution

Within the inner representation of the model, individual channel sections have constant slope, dimensions, bank angles, and sediment size. The dimensions include channel depth, basal width bank angles and longitudinal bed slope (Figure 2.12). Increasing the number of sections used in a simulation results in a configuration that more accurately reflects the topography of the channel and watershed. However, increasing the amount of details is time consuming in terms of data acquisition and model parameterisation. Thus, a balance must be found between the duration of simulations and the required level of details. The exported results comprise daily flow characteristics

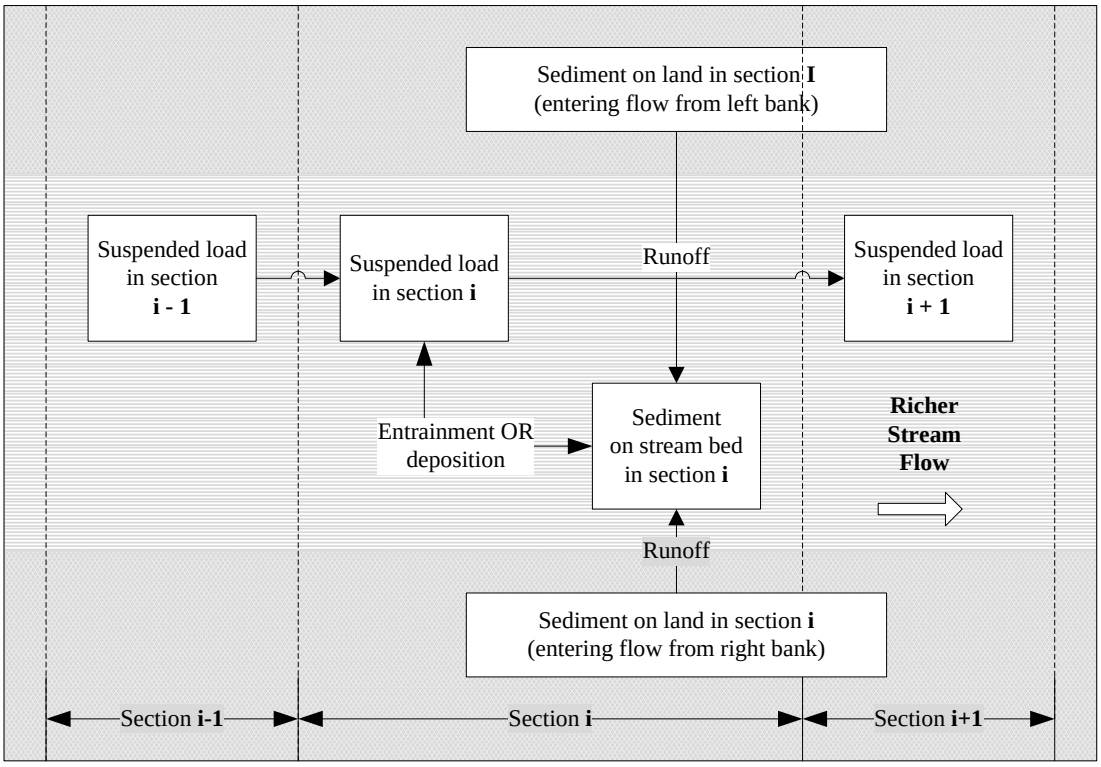

Figure 2.10. Overview of the sediment transport module.

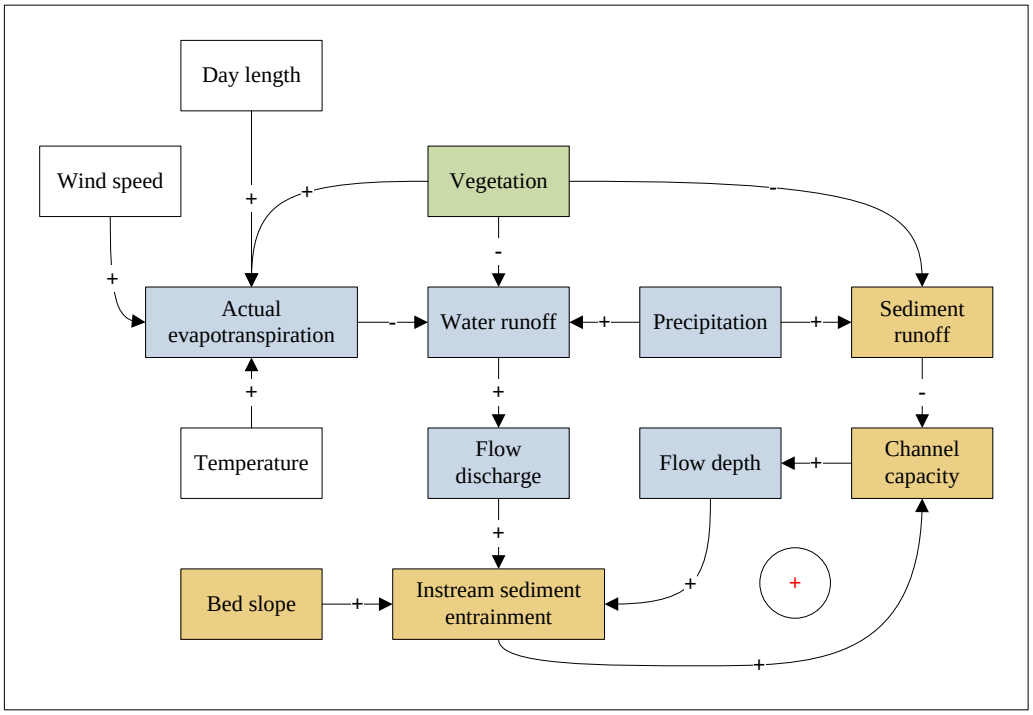

Figure 2.11. Interactions among the main variables of the model.

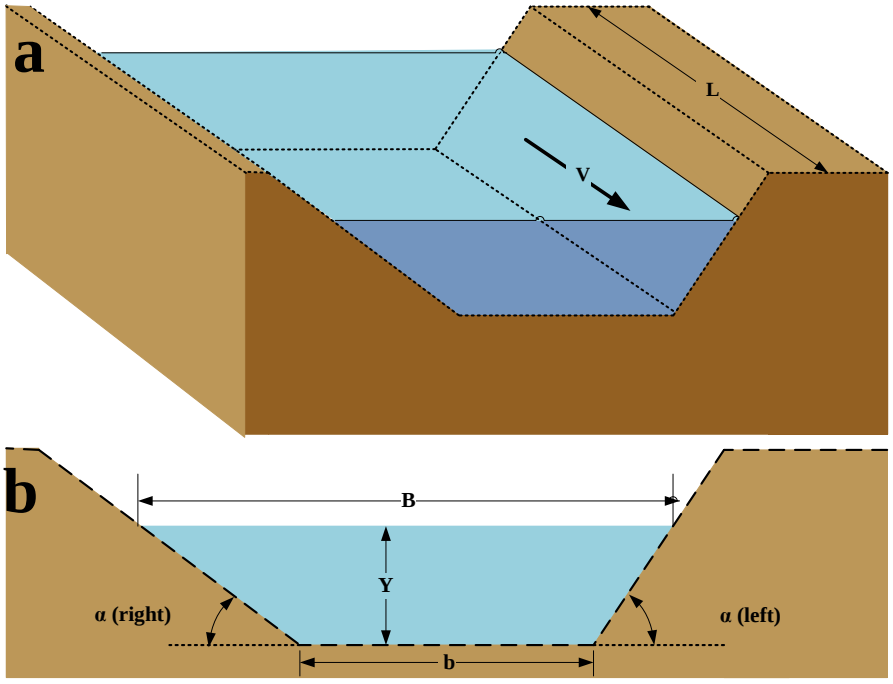

Figure 2.12. (a) Channel representation and (b) cross-sectional dimensions. V: flow velocity, L: section length, B = flow width (surface), b = flow width (bed), α = right and left bank angles.

(i.e. discharge, velocity and depth) and the geometry of each defined section (i.e. depth, basal width and bank angles). Although the cross-sectional area changes, the ratio of dimensions is static in this version of the model. In other words, erosion or aggradation is uniform. Note that this situation would not occur in the Richer Stream due to the accessible sediments being located mainly on the bed; dense vegetation on channel banks holds particle in place.

The model assumes that sediments are always available to be picked up by the flow. This situation is problematic for two reasons. Firstly, the mechanical work performed during dredging has the effect of compacting bed and bank materials, making them less available. Secondly, bank cohesion (which varies with soil particles size and is affected by vegetation type and density and moisture) might prevent sediments from being detached from the banks. Bank erosion processes are lacking in this model, although the flow pressure exerted on channel bed and banks is employed to identify the most vulnerable reaches. Moreover, the effects of wind and ice on sediment transport are also absent. Bank shading caused by channel bank angles and sunlight direction is not incorporated, although unequal soil surface melting is expected to have a significant effect on soil cohesion during spring, when one side of the channel is frozen and the other is not.

2.3.1.2. Improvements

Performance

The model of Rousseau (2008) implemented in Stella® was migrated into a Java application using Eclipse 3.4 development platform and Java 1.6.0 specification language. The migration was achieved to reduce the duration of the simulations and enable batch processing. This modification facilitates the examination of specific management methods

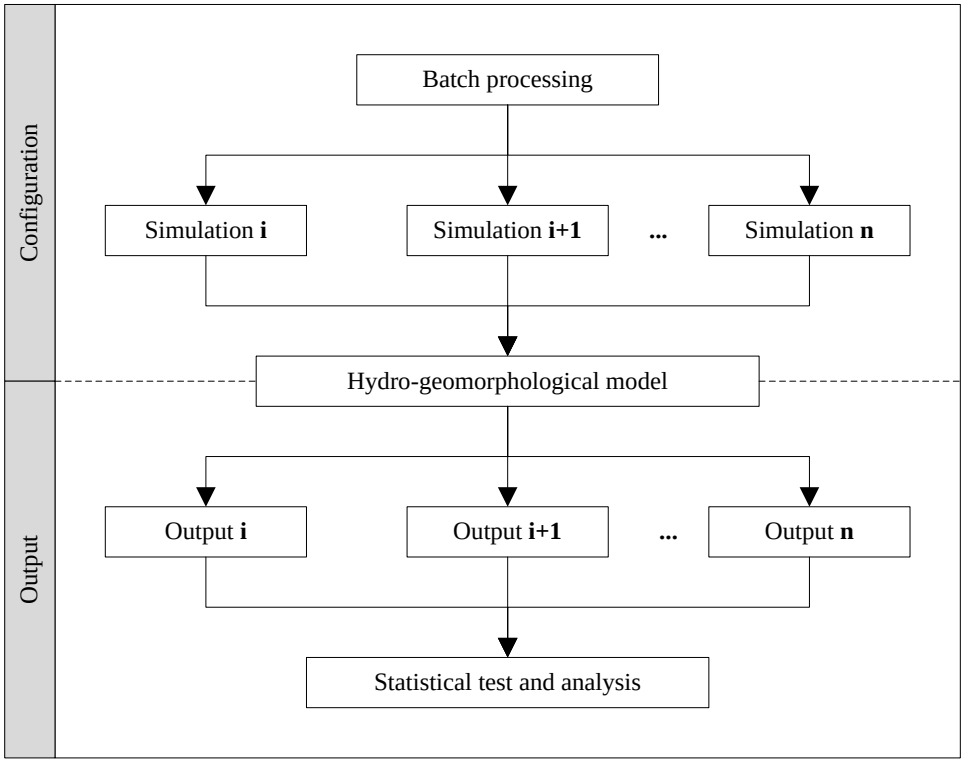

Figure 2.13. Main files of the hydro-morphological model.

over a spectrum of possible configurations and weather conditions (Figure 2.13). The implementation of the model in a standalone application allows solving complex equations that require iterations (e.g. complex integrals, third (or higher) degree polynomial equations). The coding in Java also facilitates releasing the model as an online application. This could easily be done by upgrading the graphical user interface whilst reusing coded functions and object classes. The application is currently constituted from 35 classes for a total of approximately 10,000 lines of coding.

Channel representation and evolution

Five identical sections of 50 meters long each were used to define the channel in the initial version of the model (Rousseau, 2008). In this study, the main stem of the Richer stream is divided in 162 trapezoidal sections. Cross-sectional dimensions were measured at each 250 meters in the fall 2009 to serve as input in the model. Supplemental

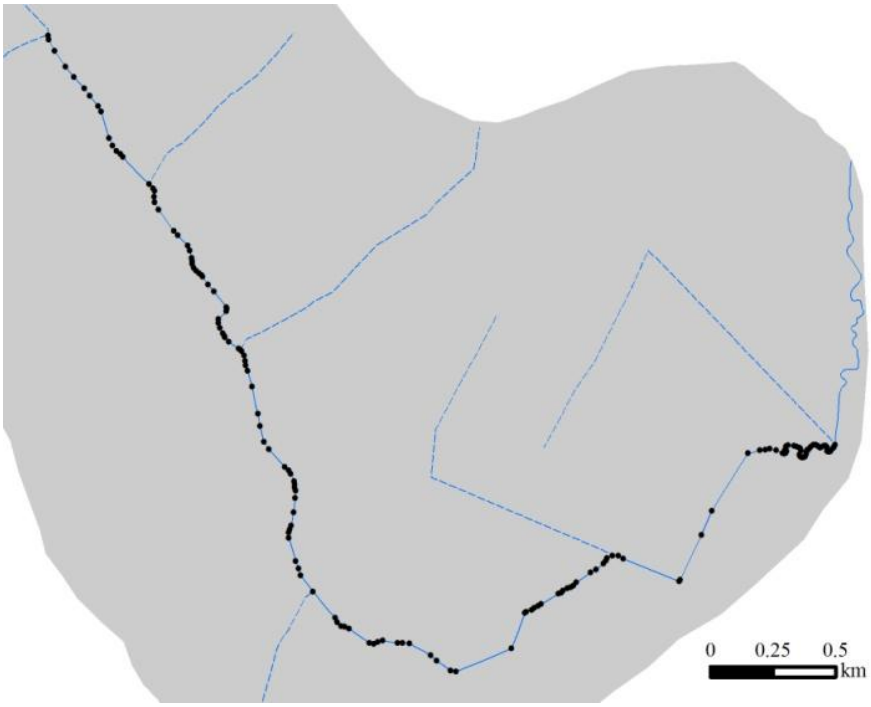

Figure 2.14. Location of the 163 inflection points that define the start and end nodes of the 162 sections used in the hydro-morphological model.

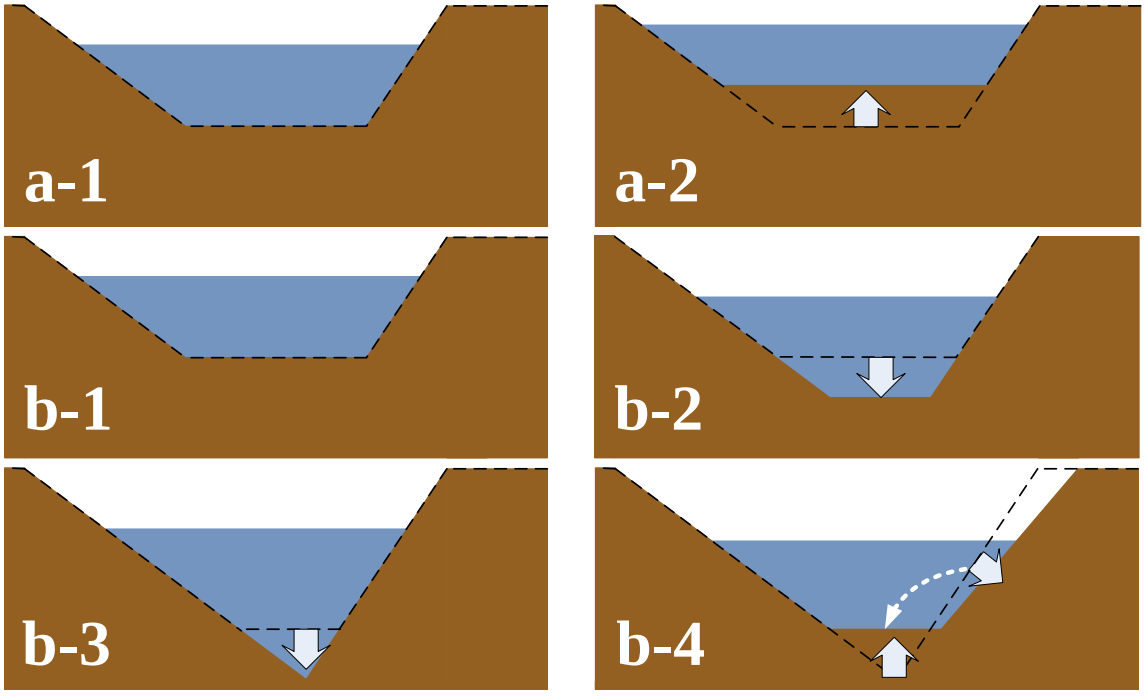

Figure 2.15. Representation of channel evolution within the hydro-morphological model showing (a) bed aggradation and (b) bed erosion followed by bank erosion.

cross-sections were also measured where a significant change existed in channel dimensions. The extension of simulations to the entire stream length is done by considering the most significant inflection points (Figure 2.14). Interpolation of channel dimensions was required since the location of most of the measured cross-sections does not match the location of the inflection points. Channel evolution has been revisited by more adequately representing channel bank erosion. Rather than preserving dimension ratios, sediments accumulate on the bed and erosion occurs first on the bed, then on the steepest bank (Figure 2.15).

Graphical user interface

In Rousseau (2008), a Stella® runtime interface is used to automate parameterisation according to predefined modelling options and thus to reduce the possibilities of introducing errors when manually changing input parameters. In the new model version, the graphical user interface is replaced by a set of configurable Excel worksheets. Field validation is performed both in Excel worksheets and in the Java application. After each simulation, the Java application exports the results into an Excel worksheet. This file can be imported in ArcGIS for display, viewed in Excel for statistical analysis or used as input conditions for a simulation. The exported results include daily weather records, section dimensions, and flow conditions in addition to a climate summary. Furthermore, the model can take historical values (including weather conditions and flow discharge values) as input in addition to generating weather conditions.

The hydrological module was modified to more accurately predict flow discharge. In its initial version, the model based a prediction on daily precipitation depth. However, in reality, instream flow intensity is also dependent upon antecedent soil moisture,

evapotranspiration, temperature and snow melt rate. The new version of the model forecasts a peak discharge based on current and previous recent excess water depths. The model employs a kernel size of 10 days (i.e. days preceding the day for which the prediction is made) to estimate daily flow peak discharge whilst considering the initially omitted variables affecting flow intensity. Although this change significantly improves peak discharge rate predictions for summer months, the predictions in March remain poor, likely due to excess water retention in local topographic depressions in a frozen soil.

2.3.1.3. Validation

Hydrological and geomorphological field data are used to validate the revised version of the model. Sediment transport measurements (i.e. bed load, suspended load and surface runoff) are used to corroborate the rates predicted by the physically-based formulas. The stage-solid discharge curve built from a combination of the data acquired under the four bridges is used to validate suspended load rates. It is, however, difficult to follow the same procedure for the two other types of loads. Surface runoff was only detected once and stream stage does not seem to be the primary factor affecting bed load rate in a clay-bed stream. Rather, the minimum precipitation depth required to initiate sediment runoff is used in validation, whereas the order of magnitude of the predicted bed load is attested by comparing it to measured rates. Similarly, flow stage-discharge curves are used to validate predicted flow conditions (i.e. depth and mean velocity) derived from empirical formulas. Also, predicted flow discharge is a function of excess water depth, which mainly depends on precipitation, evapotranspiration rate and snow melt. Therefore, a single validation step (i.e. excess water depth) accounts for the validation of several variables that are estimated using physically- and empirically-based formulas.

The simulations completed under the new version of the model were improved from initial runs by validating the computed variables over a longer time period. The choice of the validation period is constrained in time by the availability of flow depth recordings (6 June 2008 to 3 December 2009).Validation was achieved by comparing the predicted and actual values within four modelling sections corresponding to the location of the data collection bridges.

2.3.1.4. Modelled management strategies

The hydro-morphological model is employed to predict the hydrological and geomorphological effects of (a) leaving the channel in its current condition or applying alternative strategies to the management of the Richer Stream and watershed: (b) the creation of backwater ponds and (c) the creation of meanders. The effect of each approach on channel stability is illustrated in Figure 2.16.

(a) No action

The status quo strategy corresponds to the condition of the stream that has naturally evolved for a period estimated at 10 years. Banks are covered with herbaceous and arbustive plant species whilst the clay bed lacks vegetation (Figure 2.2b). The "No action" scenario is expected to have little effect on current channel morphology since dimensions are expected to have naturally adjusted following dredging works: bank slopes are shallower and bank roughness has increased due to the colonisation by herbaceous and arbustive species.

(b) Creation of backwater ponds

The installation of retention basins along the channel should decrease peak flow discharge by accumulating water as flow discharge increases and releasing it as it

decreases (Figure 2.17). Such an approach has been used on the Niagarette River near Québec City (Fondation de la Faune, 2010). The accumulation of water in retention basins results in a decrease in peak discharge (Chen et al., 2007). The falling limb has a

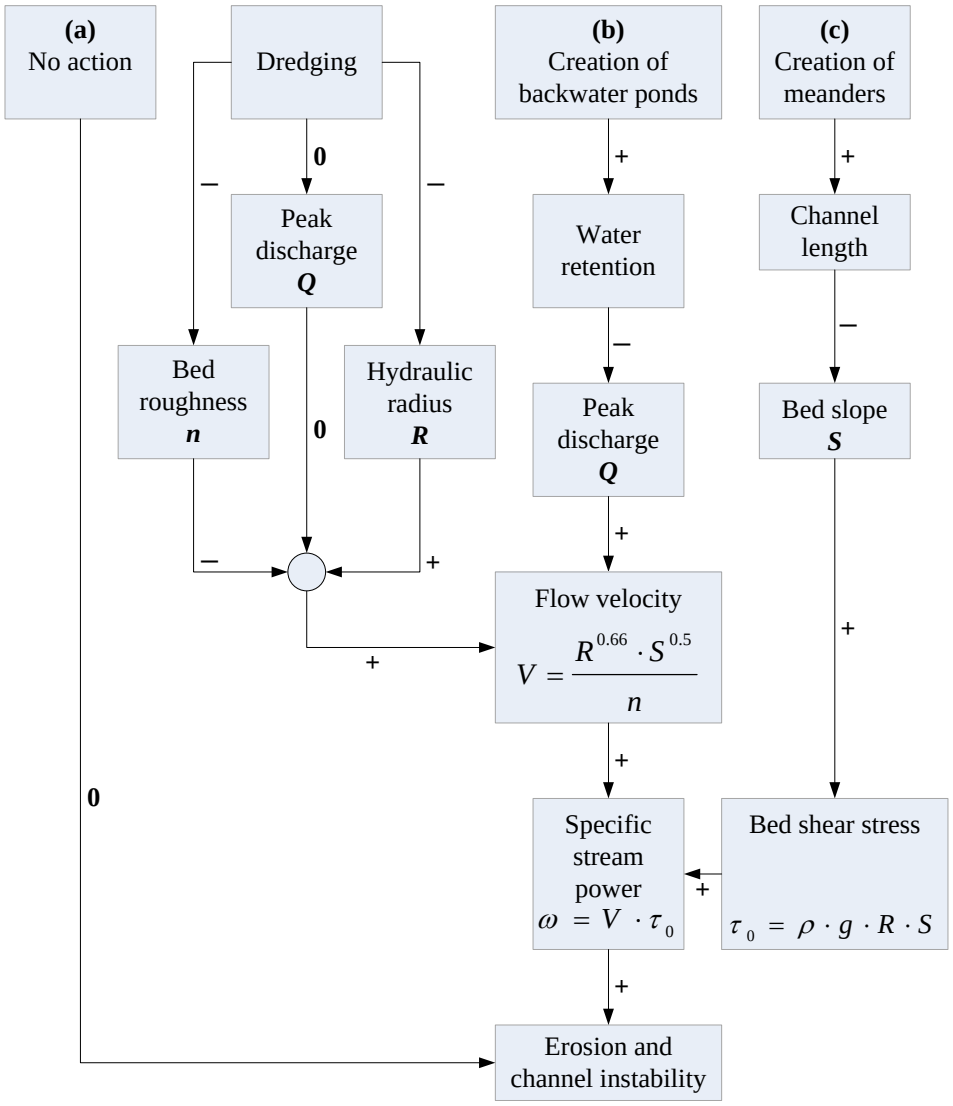

Figure 2.16. Interactions between hydraulic variables for each scenario. A positive relationship (+) between two variables exists when a change in the value of an independent variable causes a change in the same direction in a dependent variable. Conversely, in a negative relationship (-), a change in the independent variables causes a change to the dependent variable in the opposite direction. The impact of dredging on flow velocity is uncertain due to simultaneous positive and negative changes in multiple independent variables. The symbol '0' indicates no change.

gentler slope due to the gradual release of the water temporarily held in the basin. As a result, the maximum unit stream power is expected to decrease. Although the effect of pore water pressure changes on bank stability cannot be assessed by the current version of the model, more gradual changes in flow depth would probably contribute to the greater weight applied on the bed by the flow when the bank is saturated.

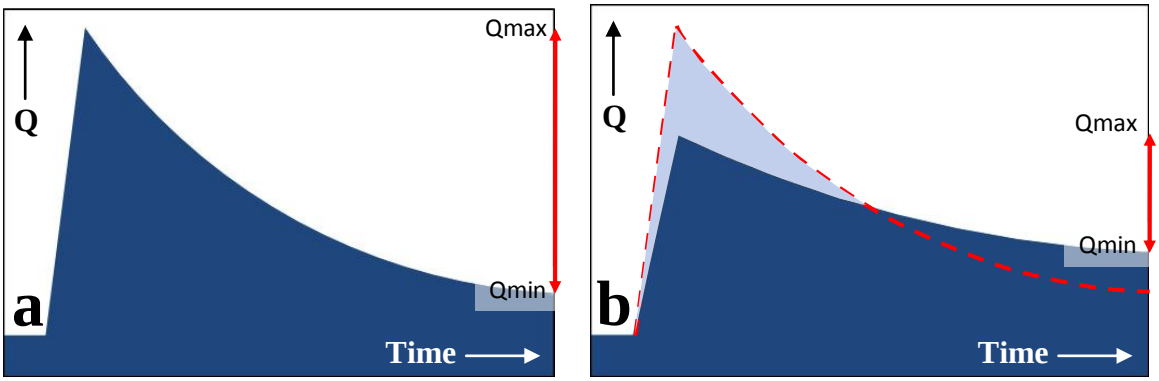

Figure 2.17. Alteration of flow hydrograph from (a) no pond to (b) one or several ponds. Q_{max} and Q_{min} are peak flow discharge and flow discharge at the end of the day, respectively.

(c) Creation of meanders

The reestablishment of meanders within the channel should decrease flow velocity, unit stream power and particle entrainment (due to increased resistance and decreased slope). Manning roughness coefficient was modified proportionally to the increase in sinuosity. A sinuosity of 1.44 corresponds to the situation of the 1932 channel whereas a sinuosity of 1.25 is assumed to be a compromise between no action and full meander restoration.

Parameterisation

The hydro-morphological model allows running simulations in two modes depending if flow and weather conditions are generated or if an existing weather record is read. Due to the difficulty of predicting channel morphology changes in a context in

which only suspended load transport rates could be validated in the field, the model was first run using a static channel and historical weather and flow data, i.e. from 6 June 2008 to 3 December 2009. Flow conditions were extracted and studied in details for August 6th, 2008 since the highest flow depth in 1.5 year was recorded on that day (predicted discharge of 6.6 m^3/s). This discharge is assumed to correspond to the bankfull stage. The same simulations were then run with sediment transport and channel morphology adjustments enabled.

Space requirements

The re-establishment of meanders was tested for sinuosity values varying between 1.00 (current situation) to 1.44 (1932 situation) at intervals of 0.05. The creation of backwater ponds was tested for 3, 6 or 12 ponds occupying a total area of 15,000, 30,000, 60,000 or 120,000 m^2.

The tested methods require removing an area from agriculture to create meanders or backwater ponds. In the case of re-meandering, this area takes the form of a corridor having a certain width and following the main stem of the channel on both sides (Figure 2.18). The width of the corridor depends on the desired degree of sinuosity, bankfull width and the 3-m buffer legally required between bankfull level and crop extent. For instance, the current channel configuration results in a corridor width of 17 m (bankfull width of channel of 11 m and sinuosity of 1.00). The corridor will be 39 m and 50 m wide, respectively with a sinuosity of 1.25 and 1.44. Although the wavelength of the 1932 channel was considered here in the modification of the channel, wavelength can modify the required corridor width (Figure 2.18). An example of a channel modified to retrieve a sinuosity of 1.25 with a wavelength of 80 m is provided in Figure 2.19. Since

the current channel location is problematic near the urban area, the channel was slightly translated north to reduce flooding risks and bank erosion on privately-owned lands. However, the sinuosity was increased by 29% in this area to reduce channel slope to the same level as if a sinuosity of 1.25 was applied to the channel in the urban reach without modifying its location.

The creation of ponds requires space near each pond rather than along the channel. Here it is assumed that the ponds are circular and have the same depth as the adjacent channel. In reality, ponds would certainly have gradual banks with deeper centre. A vegetated buffer strip of ten meters is assumed to surround each pond. For instance, a pond having an area of 5,000 m² will end up occupying 7,821 m² (radius of 49 m) when considering the required buffer strip. Three of the modeled scenarios are mapped in Figure 2.20.

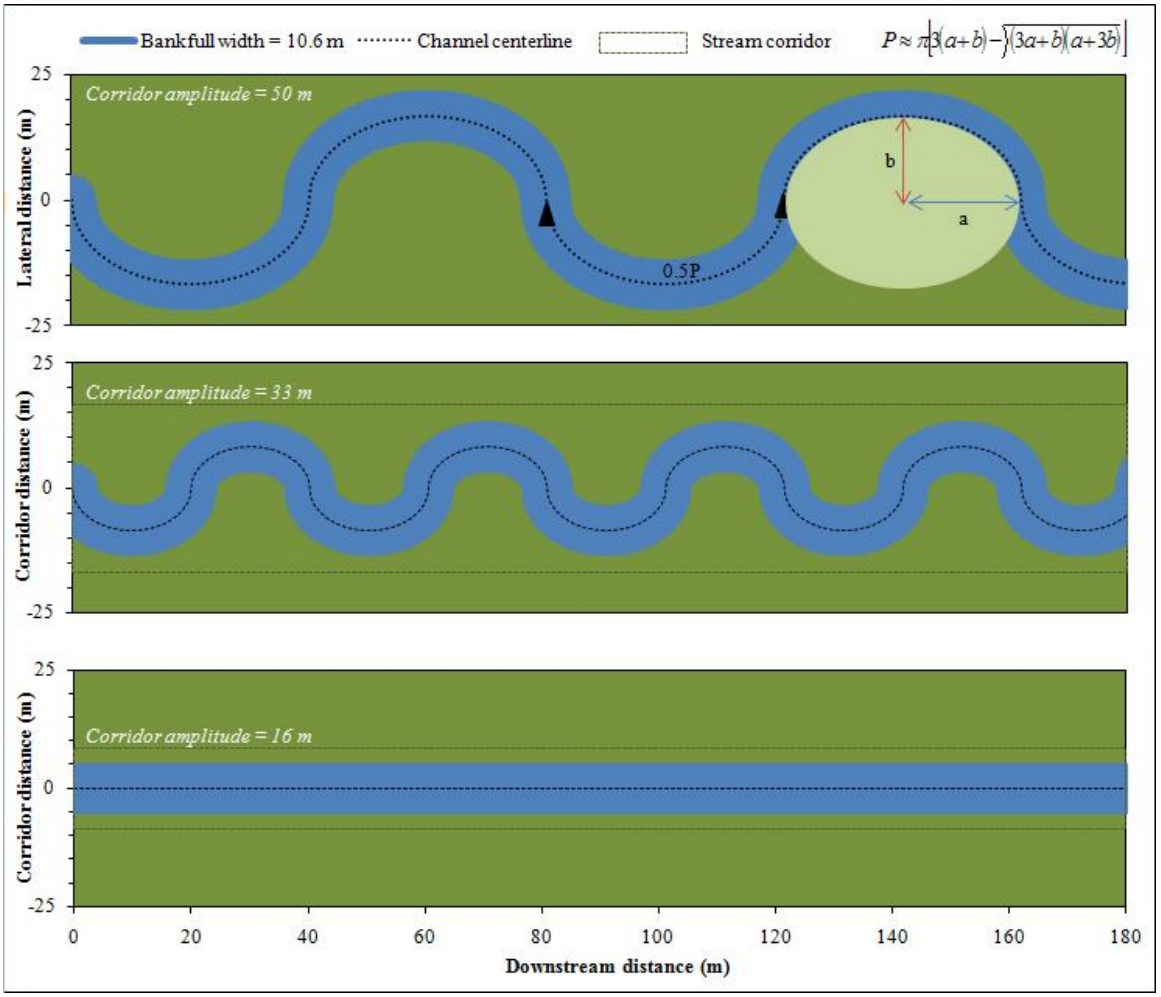

Figure 2.18. Channel design using elliptical meanders. Each wave unit has a length that is equal to the perimeter of an ellipse defined with semi-minor (b) and semi-major (a) axes. The equation used to estimate the perimeter of an ellipse is the first approximation of Ramanujan (1914).

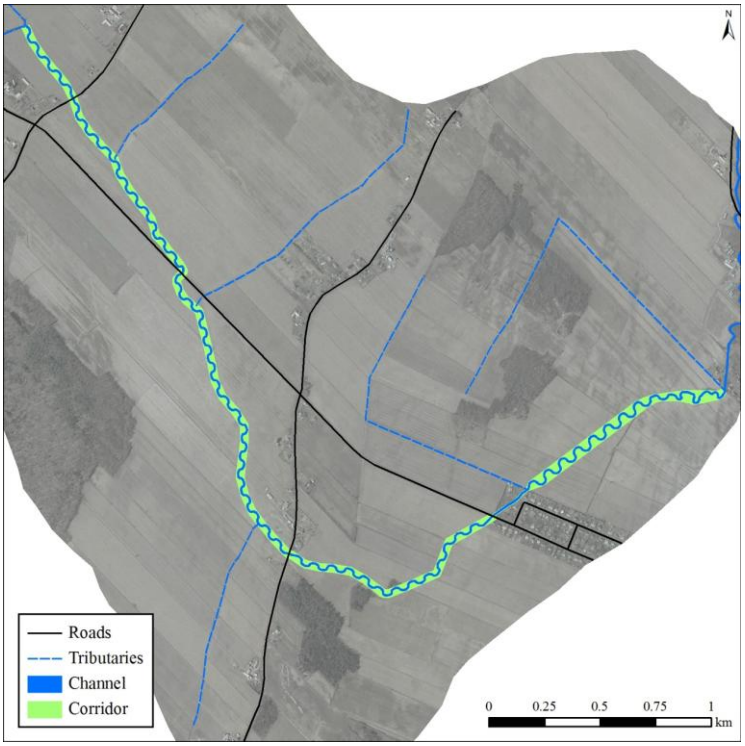

Figure 2.19. Example of a channel re-meandering scenario in which the desired sinuosity is 1.25.

Figure 2.20. (a) Example of backwater pond creation scenario (12 ponds occupying an area of 10,000 m² each).

Figure 2.20. (b) Example of backwater pond creation scenario (6 ponds occupying an area of 20,000 m² each).

Figure 2.20. (c) Example of backwater pond creation scenario (3 ponds occupying an area of 40,000 m² each).

2.3.2. The 3D flow dynamics model

Numerical modelling set-up

The 3D flow dynamics computational model Phoenics (from CHAM) is used to simulate the flow field in the urban reach (Figure 2.1b). The numerical domain is 50 m long and 100 m wide in the bend section, and 225 m long and 17 m wide in the straight section (Figure 2.1b). Grid dimensions are 0.5 m, 0.5 m and 0.1 m in the longitudinal, lateral and vertical dimensions, respectively. An upstream section of approximately 100 m was used to ensure that the 3D flow is fully developed before entering the bend section. Inlet velocity values were set to the values obtained at the outlet of the upstream section. The DEM of bed topography in the urban reach was used to create a bed object in Phoenics, allowing a Cartesian grid to be used. The procedure is explained in Biron et al. (2007) and Haltigin et al. (2007). Variable porosity in the surface layer cell does not restrict the flow to a predefined rigid grid but allows vertical flow surface adjustments (Ouillon & Dartus, 1997). A logarithmic velocity profile is assumed near the bed.

Model validation

In order to attest to the validity of the simulations performed in the 3D numerical model Phoenics, 87 3D velocity measurements were taken with a Sontek Acoustic Doppler Velocimeter (ADV) at a low flow stage (corresponding to a maximum flow depth of 26 cm at the transducer location) in the straight reach (Figure 2.1b) in July 2008. The ADV points were taken at a height above the bed corresponding to 40% of flow depth. The sampling frequency of the ADV was 25 Hz, and the duration of each measurement was one minute. On average, one ADV point was taken per 15 m^2 of water surface whereas channel cross-sections were surveyed at each 2-3 m to generate a

topographic map. Conversely, the density of simulated velocity points in Phoenics was of one point per 0.25 m^2 with the adopted configuration.

A visual comparison of the interpolated data points reveals a reasonably good agreement between measured and simulated velocity magnitudes considering the limited number of ADV and topographic points collected (Figure 2.21). Despite a few differences in the location of high-velocity zones (i.e. mid-reach and second bend), the 3D model Phoenics is able to predict velocity values that are in the range of those measured in the Richer Stream. Also, the ADV measurements were performed during the summer that followed topographic data acquisition. Channel morphology may have been altered by erosion or deposition between topographic and velocity measurements.

Although the acquisition of flow velocity data at medium and high flow stages would have been useful to validate the 3D flow hydraulics simulations, field setup did not allow such measurements to be safely acquired; the 21 foot ladder used in field data collection could not be deployed in the urban reach due to its larger width. Furthermore, this research required significant efforts in field data collection with different types of measurements during the same (rare) high-flow stage events. The decision was taken to concentrate efforts on measuring sediment transport rates rather than 3D flow velocity validation. It is hypothesized that a comparison of measured and simulated velocities at higher stage would result in a better agreement due to the smaller impact of small-scale channel irregularities as flow stage rises.

In-stream structures

The 3D model was used to predict flow velocity changes following the virtual installation of two types of hydraulic structures within the urban reach of the Richer

Figure 2.21. (a) Measured and (b) simulated velocity magnitudes at low flow stage. Flow is to the right. The symbol ✓ indicates a good agreement between measured and simulated velocity values whereas the symbol × represents a poor agreement.

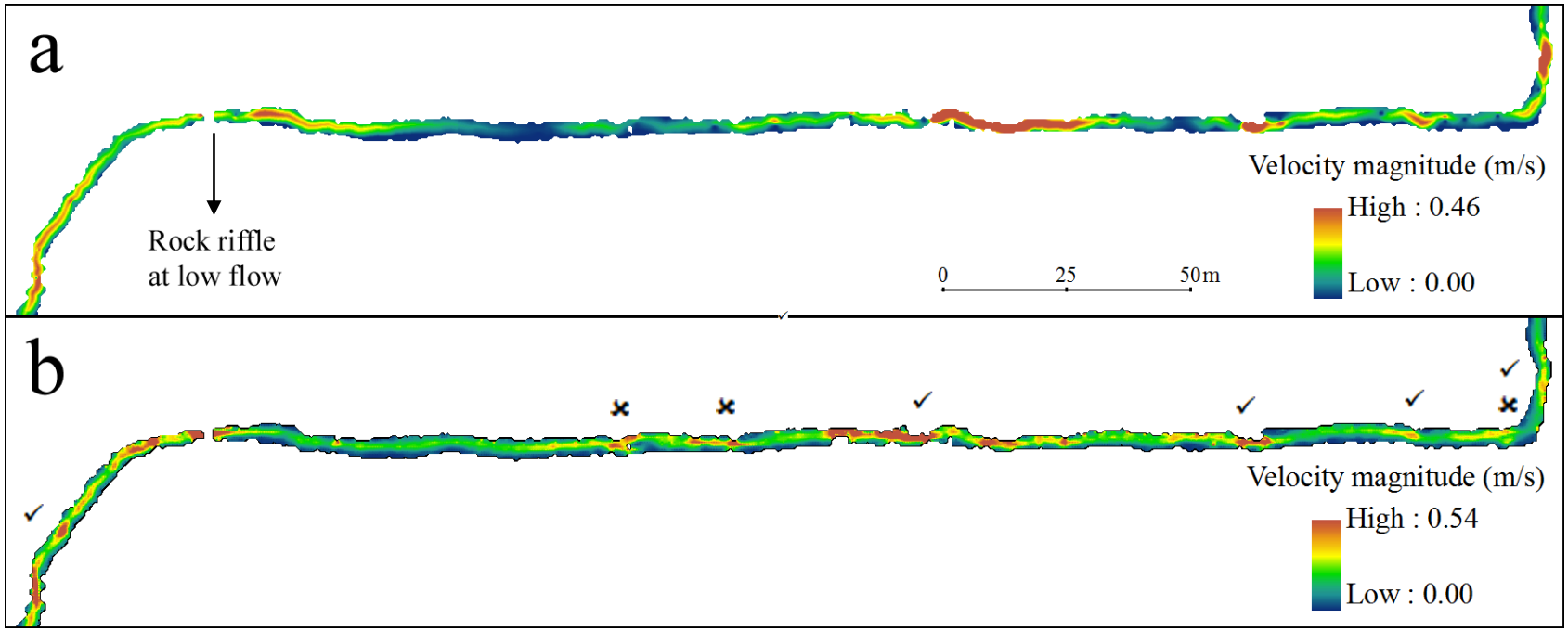

Stream to reduce bank instability (Figure 2.1b). In-stream structures were incorporated to the model by modifying the object bed. The distance between the inlet and the zone where structures were inserted is sufficiently long for a fully-developed flow to develop.

The hydraulic effects of installing these structures are investigated at two flow depths: 0.80 m (0.37 m^3/s) and 1.26 m (3.46 m^3/s), respectively for medium and high stages. These stages were reached 46 (8.4%) and 10 (1.8%) times in the 546-day period spanning 6 June 2008 through 3 December 2009. Although higher flow stages were recorded by the transducer after spring 2009, the highest modelled flow stage nevertheless corresponds to an event of infrequently high magnitude.

Based on the survey of available methods and interviews with practitioners, the tested methods are stream barbs and bed weirs. Stream barbs are expected to redirect the flow towards the center of the channel and away from the outer bank in a channel bend, thus reducing near-bank velocities. Six barbs with a length of 4.5 m, a maximum width of 0.4 m and a maximum height (near bank) equal to 90% of flow depth (in respect to the higher flow stage) are used in this experiment (Figure 2.22). Each structure is oriented upstream at 40º from the bank which causes a lateral constriction of 38%.

Bed weirs should locally modify flow surface slope and concentrate higher velocities in the vicinity of each structure. Four bed weirs were implemented in the model across the channel width at 50 m intervals in the straight reach that follows the 125° bend (Figure 2.23). Low weirs (vertical drop of 0.6 m) were tested at each flow stage whereas high weirs (vertical drop of 1.06 m) were only employed with the highest stage. Flow

characteristics cannot be predicted with steady simulations since high weirs would create a chute at medium stage. Both upstream and downstream parts are perpendicular to flow direction whereas the top is flat. The straight weir has a constant thickness (2 m) whereas the V-shaped type has a minimum thickness of 2 m with the downstream side rotated 45° from the upstream side (Figure 2.23).

It is obviously not possible to validate the simulations using in-stream structures as these constitute virtual modifications. Therefore, they are mainly used here to assess their impact prior to their implementation, and to provide a general assessment of the type of changes to be expected from their installation under medium and high flow conditions.

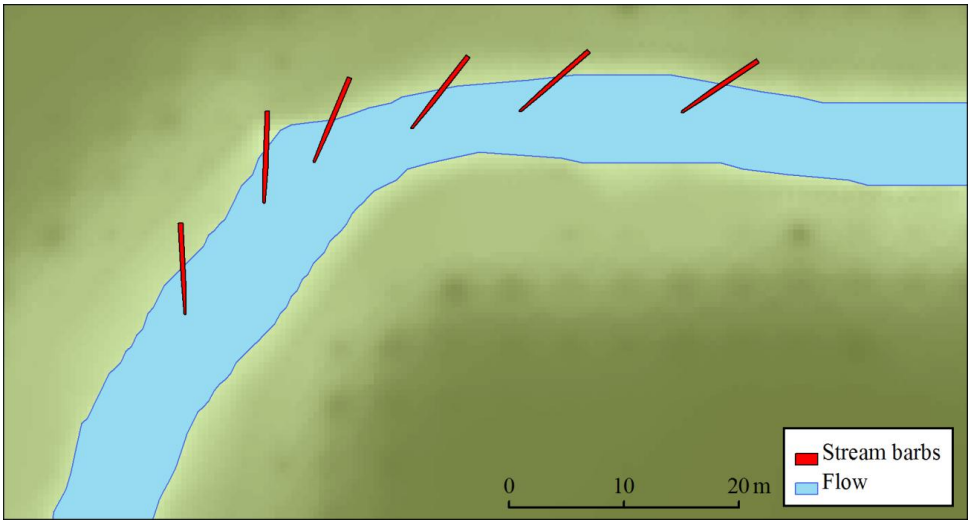

Figure 2.22. Configuration of stream barbs in a 125° bend. Flow (medium stage shown) is to the right.

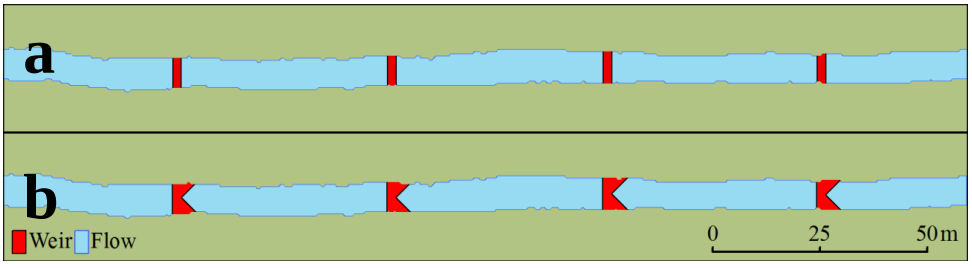

Figure 2.23. Configuration of (a) straight and (b) V-shaped bed weirs in a straight reach. Flow is to the right.

3.1. Watershed characterisation

3.1.1. Stream hydrology

Data from the gauging station installed on the Richer Stream

Figure 3.1 presents the flood hydrograph for 2008 (starting on 6 June) and 2009 (ending on 3 December). Note that the pressure transducer did not record flow depth for the period spanning 5 May to 16 June 2009 because its memory unit was full. Missing minimum and maximum daily discharge values were estimated from the average daily value recorded by a nearby gauging station installed on the Acadie River. The following regression equations were employed to estimate the Richer daily peak discharge:

$$Q_{Richer,average} = 0.0008 \cdot Q^2_{Acadie,average} + 0.0236 \cdot Q_{Acadie,average} \qquad R^2=0.72 \qquad \textit{(Equation 3.1)}$$

$$Q_{Richer,\min} = 0.2275 \cdot Q^{0.6226}_{Richer,average} \qquad R^2=0.77 \qquad \textit{(Equation 3.2)}$$

$$Q_{Richer,\max} = 2.3533 \cdot Q_{Richer,average} - 0.0232 \qquad R^2=0.90 \qquad \textit{(Equation 3.3)}$$

The relationship described by Equation 3.1 was established using the events for which there was a synchronisation in the occurrence of peak discharges in the Richer Stream and Acadie River (59 points). Equations 3.2 and 3.3 are based on the analysis of the complete Richer dataset (504 points). Based on precipitation depth during this period, approximately 130 mm of rainfall reached the watershed. The estimated discharge appears in good agreement with this amount of rain.

Note that the predicted bankfull discharge is twice the value of 3.33 m³/s that was estimated by Rousseau and Biron (2009). In this study, the ratio of Richer and Hurons watersheds were used to predict Richer peak discharge based on the historical discharge

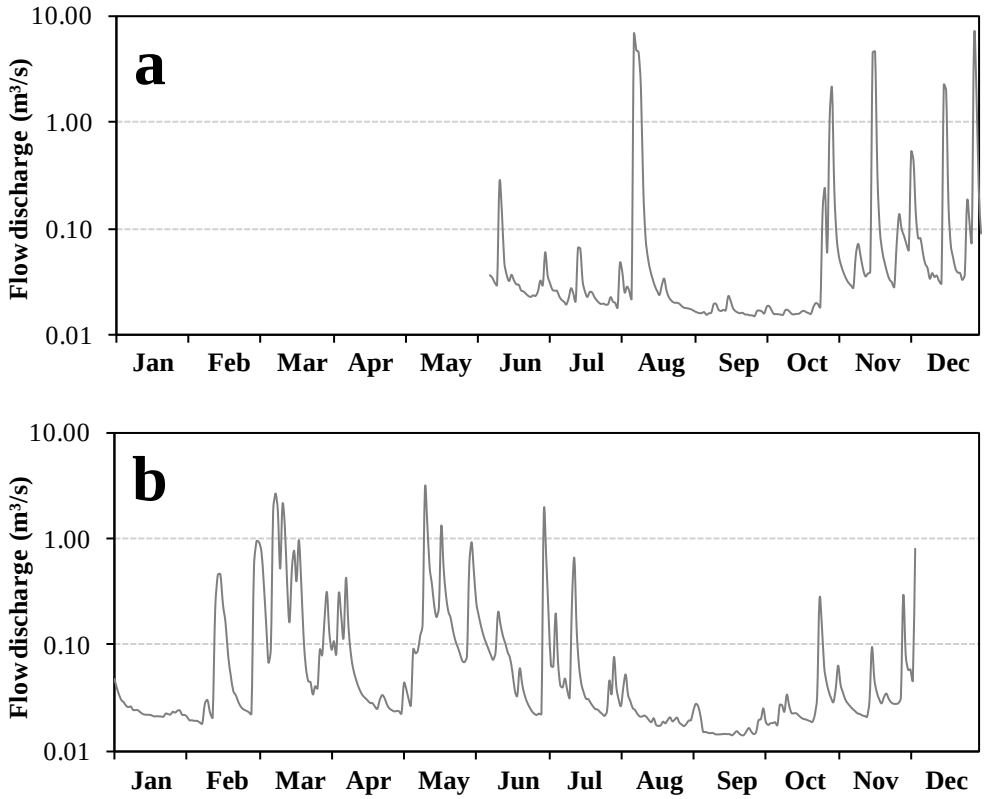

Figure 3.1. Flow hydrograph of the Richer stream at the pressure transducer location in (a) 2008 and (b) 2009. Data associated with the period 5 May 2009 - 15 June 2009 were estimated based on the correlation between the average daily discharge recorded at the Richer Stream and the average daily discharge measured by a gauging station installed on the Acadie River. Note that the timing of occurrence and the magnitude of peak discharge events differ significantly from one year to another.

record of the Hurons River. This highlights the limits of using the watershed ratio approach for small watersheds, and the necessity of installing pressure transducers to obtain accurate discharge estimates.

The maximum discharge (6.6 m³/s) was observed in August 2008 whereas the minimum value (0.014 m³/s) was recorded in September 2009. The daily average in this period was 0.17 m³/s. Overall, there is a general tendency for the flow to be low in the summer months and at the beginning of the year (before snow melt begins). Although the highest discharge was not recorded during spring, several peak values were reached

between February and April with a base flow significantly higher than in other periods of the year. Depending on the amount of precipitation received, the flow discharge rises by ten to one hundred times after a precipitation event. The frequency curve (Figure 3.2) confirms that flow discharge is usually very low with episodic bursts. A flow discharge above 1 m³/s was reached 17 times out of 503 (3.4% of days). The maximum flow discharge did not occur during spring as expected, but in August 2008 after the watershed has been subject to rainfall on a quasi- daily basis for a few weeks. However, the second highest peak (6.2 m³/s in 28 December 2008) was achieved as a result of snow melt and ice cover breakup. In comparison, the estimated peak discharge in spring 2009 was only 2.7 m³/s. From a modelling perspective, the fact that ice broke up at the end of December

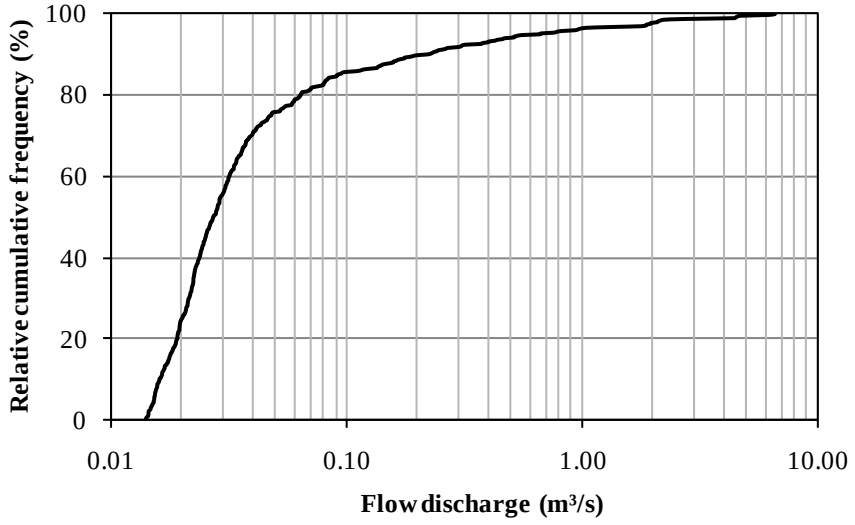

Figure 3.2. Cumulative frequency distribution of maximum daily discharge values from 6 June 2008 to 3 December 2009 (except between 5 May and 16 June 2009).

was unexpected when considering monthly air temperatures. At the St-Hilaire weather station, the air temperature is not expected to rise above zero in December (maximum daily temperature of -1.75ºC). This indicates that randomly generated air temperatures should be used rather than average values in hydrological models.

Water temperature and quality

High water temperatures can hinder fish development by impairing their growth, increasing parasitic diseases and predation rates (Roth et al, 2010). This thermal pollution can also contribute to the development of buoyant algae and favour the invasion of a stream by undesirable species (El-Jabi et al., 1995). Eleven fish species were observed in the Richer Stream in August 2006 (Garceau et al., 2007). The highest temperature recorded in the Richer Stream was 29.3°C, in August 2009. This is above the theoretical survival threshold for three species found in the Richer stream: the White Sucker, the Pumpkinseed, and the Rock Bass. The Golden Shiner and the Brown Bullhead are unlikely to suffer from the direct effect of heat due to their higher tolerance to extreme temperature values.

32 additional fish species were inventoried in the Richelieu River near the outlet of the Richer Stream. Although these species were not observed within the Richer Stream during the survey works performed in August 2006 (at low flow depth) they may inhabit the Richer Stream at certain periods of the year for spawning or feeding. This reinforces the hypothesis that, even in its current state, the Richer Stream has significant ecological functions although it is sometimes referred to as a drainage ditch. 11 of the species for which the maximum tolerated is available may not withstand the maximum recorded temperature.

Temperature is only one of several characteristics that contribute to the quality of a stream. In a previous report (Garceau et al, 2007), the quality index of surveyed reaches within the Richer stream was found to be low (over 74.5% of the length), medium (19.25%) and good (6.25%) in regards to substrate type, cover, sinuosity, pool-riffle

sequence, flow depth and velocity, and the type of a vegetated riparian buffer. Oxygen level was found to be low enough to seriously affect the most vulnerable species (40%). Re-meandering combined with the installation of riparian vegetation (providing shade, cover and colder temperatures) would contribute to improving the biological indices in regards to all aspects. The effect of a mature riparian forest was found to reduce the peak temperature by 1.2°C (compared to an exposed stream) after the modeling of temperatures in the Boiron de Morges River, southwest Switzerland (Roth et al, 2010). In contrast, a reeds cover was found to have little effect (reduction of 0.1°C). The same study reported a 0.7°C increase in maximum water temperature after the removal of vegetation. Since the removal of vegetation is associated with dredging works, fish in the Richer Stream would certainly benefit from the adoption of a program including riparian forest canopy installation.

Thermal pollution in the Richer Stream is currently attributed to land management in regards to agricultural practices and urbanisation. Deforestation exposed the stream to solar radiation and heated the stream. In addition, regular dredging works remove deep pools which could otherwise regulate stream water temperature. As a result, important differences between daily minimum and maximum temperatures exist. A maximum difference of 12.6°C was recorded on 24 April 2009.

Anthropogenic climate changes are also expected to modify stream temperature. Using the relationship between the maximum atmospheric and water temperatures (Figure 3.3) and temperature deltas for the CGCM2 A2x climate change scenario (Figure 3.4), monthly maximum water temperatures are predicted for the period June 2008 to December 2009 (Figure 3.5). These changes could potentially affect the fish

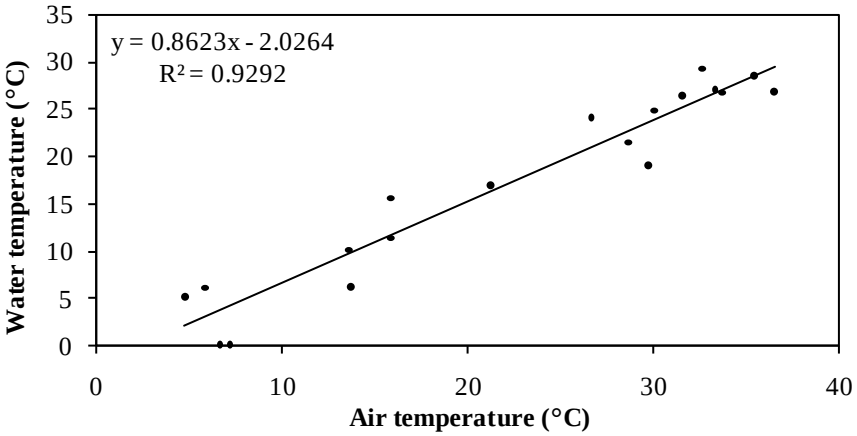

Figure 3.3. Relationship between maximum atmospheric temperature (at Montreal Trudeau Airport according to Canadian Climate Normals 1971-2000 (2010)) and Richer water temperatures.

Horizon	Jan	Feb	Mar	Apr	May	Jun	Jul	Aug	Sep	Oct	Nov	Dec
2020	1.58	1.07	0.64	0.40	2.23	1.18	1.47	1.26	1.32	0.83	1.17	0.48
2050	2.48	2.45	0.93	1.01	4.29	2.52	2.41	2.21	2.36	2.40	2.14	0.68
2080	3.21	3.76	1.58	3.94	6.64	4.04	3.90	3.61	3.89	3.44	3.81	1.21

Figure 3.4. Predicted temperature deltas at (46.39°N, 71.25°W) according to the CGCM2 A2x climate change scenario (Canadian Climate Impact Scenarios, 2010).

community in the Richer Stream. For instance, water temperature would rise from 29.3°C to 30.4°C in 2020, 31.2°C in 2050 and 32.4°C in 2080. Assuming that the fish are unable to adapt to these changes, Smallmouth Bass would be eradicated from the Richer Stream in 2020, the Emerald Shiner in 2050 and the Northern Pike in 2080. From the eleven fish species found in 2006, only four would remain in 2080: the Bluntnose Minnow, the Central Mudminnow, the Golden Shiner and the Brown Bullhead. Assuming that the establishment of a riparian forested canopy decreases water temperature by 1.9°C as in Roth et al. (2010), the Emerald Shiner and Northern Pike could continue to inhabit the Richer Stream.

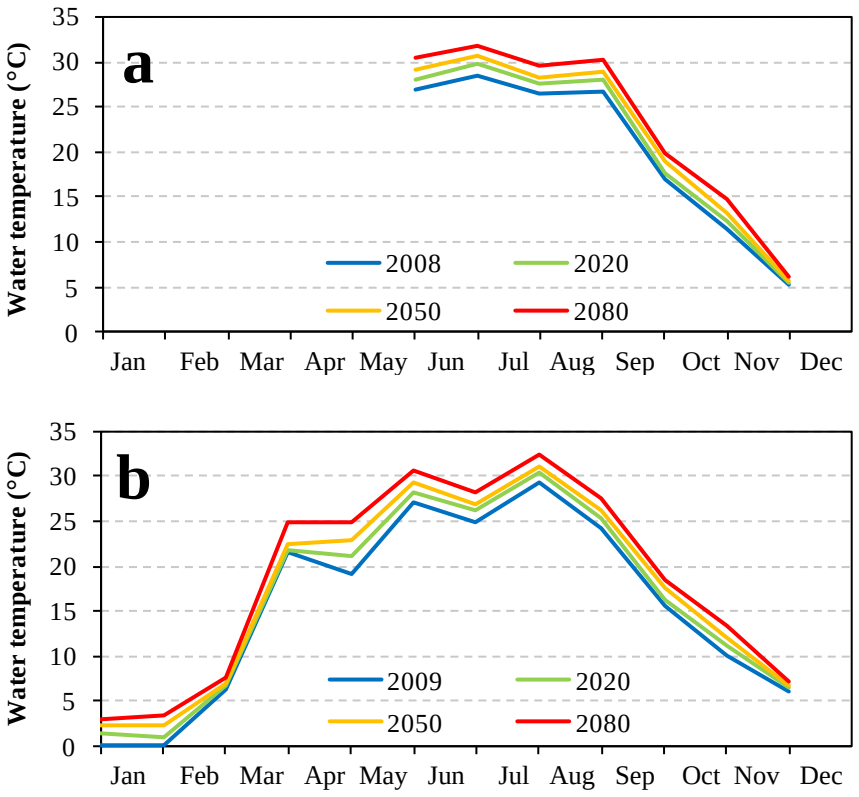

Figure 3.5. Current and predicted monthly maximum water temperature in (a) 2008 and (b) 2009.

3.1.2. Channel and surface sediment size

The analysis of bed and bank sediment samples reveals that the channel material consists on average of 45.6% clay, 33.0% silt and 21.3% sand (clay texture). The median particle size is 0.0137 mm on the banks and 0.0097 mm on the bed (fine silt in all cases). Bank particles are thus slightly sandier than bed particles and contain less clay and silt. Although they both fall into the clay texture category, the color of the solutions in the cylinder during the hydrometry procedure indicated that beds and banks differ in composition (Figure 3.6). Bank samples are darker (more brown) than bed samples (more beige or gray). Although the difference in median sediment size is small, a more significant difference was found when distinguishing between upstream and downstream

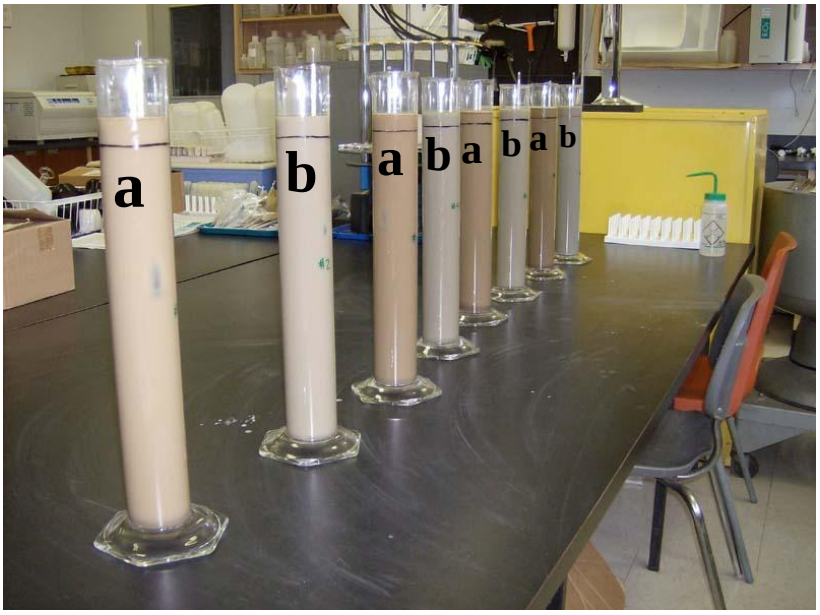

Figure 3.6. Hydrometry procedure setup showing sedimentation occurring simultaneously in eight cylinders and indicating a different composition between bank (a) and (b) bed samples.

samples. Upstream bed and bank samples have a clay texture whereas downstream samples have a clay loam texture (less clay and more silt and sand). The upstream bank particles consist of very fine silt whilst beds consist of coarse clay. Downstream banks and beds are all made of medium silt.

A comparison of soil texture between channel material and the adjacent field (for each analysed sample) was achieved to determine the provenance of bed and bank sediments. This analysis reveals that the differences in the proportion of each sediment size class (i.e. clay, silt and sand) between the channel and the adjacent field are low in upstream cross-sections and higher otherwise (Figure 3.7). The average difference (for all classes combined) is 6.9% in the six upstream cross-sections but 23.9% in the remaining ten cross-sections. This suggests that the downstream channel mainly consists of sediment delivered by upstream reaches, where sediment runoff rates are expected to be larger to steeper field slopes. Another possibility would be that only fine particles are transported at the surface towards the stream, leading with time to a texture that is finer in

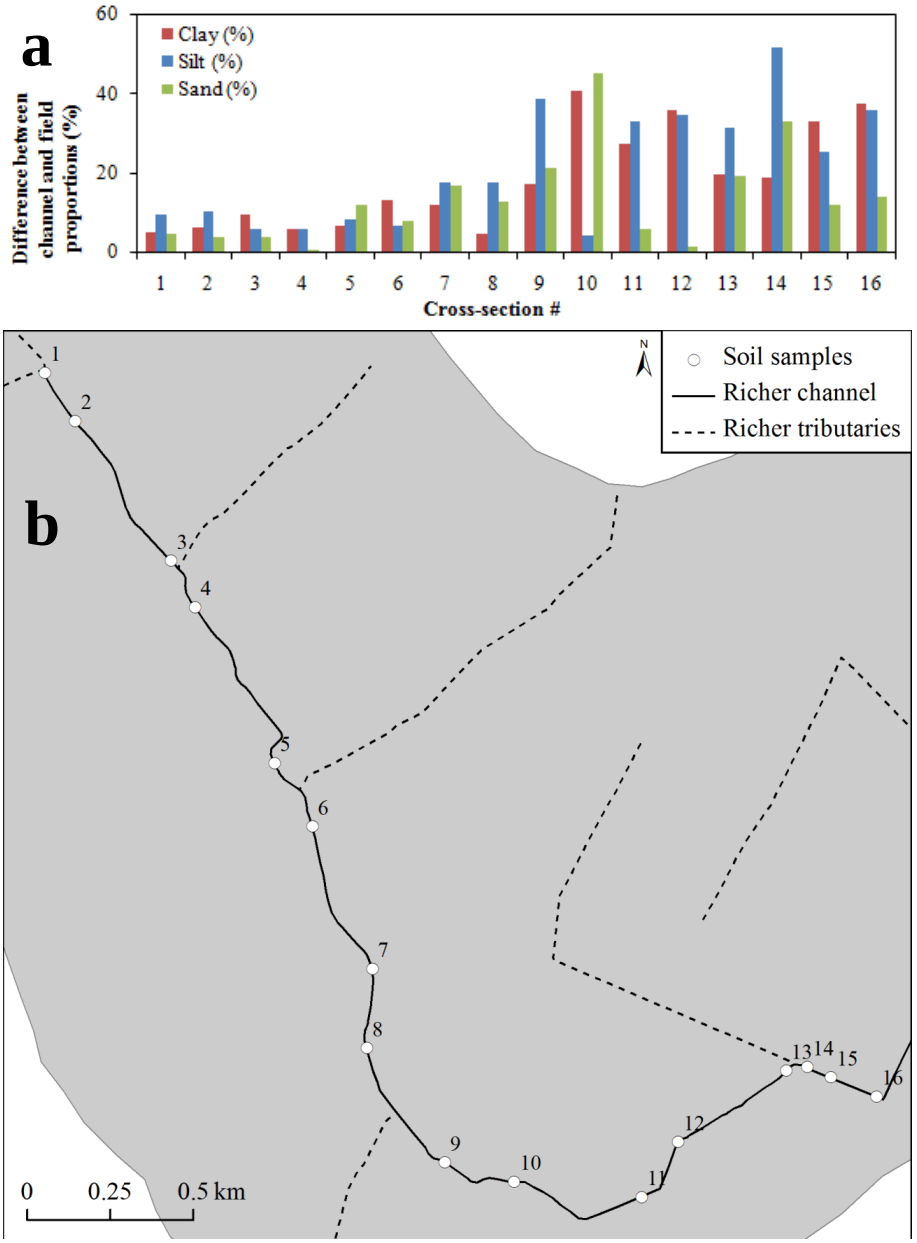

Figure 3.7. (a) Difference between channel and field soil classes. (b) Location of the cross-sections where the samples were collected.

then channel than in the field. A stable bank will facilitate the successful installation of vegetation. In the case of the Richer channel (average soil texture assemblage: 45.6% clay, 33.0% silt and 21.3% sand), the maximum gradient of a stable channel lies between 1:3 and 1:1.5 (D'Auteuil & Dubois, 1994). These values significantly contrast with the desired channel morphology as specified in the most recent stream management Act

(gradient of 1:1). Considering these recommendations, it is not surprising to observe that Richer channel banks have a general tendency to flatten over time (Rousseau and Biron, 2009). The fact that streambanks in the residential area have naturally evolved from a slope of 45º to 22º after 6 years (since the last dredging operation) suggests that a gradient of 1:2 is more stable than one of 1:1 in the case of the Richer Stream. Therefore, the former value should be considered in future interventions.

3.1.3. Sediment transport

Surface runoff

Even if surface runoff samplers were verified and cleaned frequently, only one event rainfall (occurring between 1 and 20 July 2009) produced surface runoff. This 4-hour rain event had a total depth of 52.95 mm with a maximum hourly intensity of 38.5 mm/h (and a 15-minute peak intensity of 18.1 mm/h). This event was the most severe to be observed during the period where the runoff samplers were installed in 2009. In comparison, the 45-minute event of 29 June 2009 (with a maximum 15-minute intensity of 17.51 mm/h) and a total depth of 41.9 mm did not produce any runoff (liquid or solid). This indicates that the duration of an event is as important as the intensity to determine if runoff will occur.

The sample analysis reveals that the concentration of surface runoff was on average 4.69 g/L. Assuming that only the highest 15-minute intensity event could create surface transport, it is estimated that approximately 78 g of soil may have been transported across the 65 m long river reach associated with a 1500 m^2 area contributing to the Mathier samplers. This amount is not significant considering the findings that the rainfall events that create runoff are occasional. Unfortunately, it was not possible to collect runoff samples during spring, when vegetation is sparser, to confirm that runoff sediment

transport is very small throughout the year in the Richer watershed. The low surface runoff rate could also be attributed to the low field slope and to the efficient ground drainage pipe network which encourages infiltration. Furthermore, the use of the semi-direct practice (no ploughing and left-over of plant residuals on the ground after harvest) probably contributes to reducing surface flow velocity in addition of enhancing infiltration rate.

Suspended load transport

A stage-solid discharge curve of suspended load was built after the analysis of the water samples collected over height sampling sessions under the data acquisition bridges (Figure 3.8). Since data collection and laboratory analyses are time consuming tasks, data points were merged into a single curve with a high coefficient of determination. The highest point recorded indicates that the suspended sediment discharge is approximately 1kg/s when the flow discharge approaches 2.5 m^3/s.

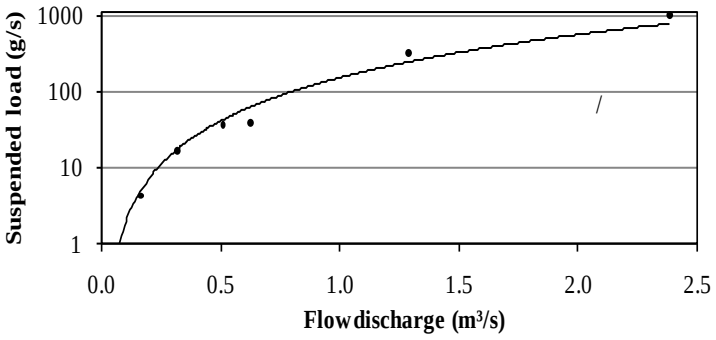

Figure 3.8. Stage-solid discharge curve of suspended load when considering the water samples collected under the four data acquisition bridges.

Bedload transport

An attempt was made to devise a stage-solid discharge rating curve from bedload measurements as was done for the suspended load data (Figure 3.9). However, a low correlation (r^2=0.38) was found between flow discharge and bed load transport rates.

Furthermore, bed load rates were noted to vary considerably under the same bridge from one time interval to another (Table 3.1). This suggests that other variables than the discharge explain the unexpected bed load rates. In general, bed load transport appears negligible compared to the suspended load in this stream.

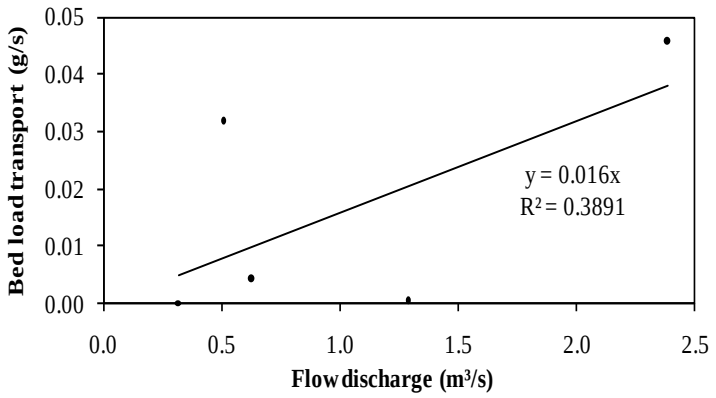

Figure 3.9. Mass of sediment collected using a Helley-Smith sampler.

Sample code	Date (yyyy-mm-dd)	Time interval (minute)	Sediment transport (g/hour)	Average transport (m³/s)	Flow discharge (m³/s)
BR1-1	2009-07-04	10	0.00	0.00	0.31
BR1-2		10	0.00		
BR2-1	2009-07-04	10	130.44	115.14	0.51
BR2-2		10	207.84		
BR2-3		10	147.96		
BR2-4		10	46.68		
BR2-5		10	42.78		
BR3-1	2009-07-04	10	41.76	15.85	0.62
BR3-2		10	13.62		
BR3-3		10	6.54		
BR3-4		10	9.54		
BR3-5		10	7.80		
BR2-1	2009-12-03	10	2.34	2.34	1.29
BR3-1	2009-12-03	10	158.40	165.38	2.38
BR3-2		20	53.94		
BR3-3		20	125.40		

Table 3.1. Suspended transport rate measurements.

3.1.4. Drainage network condition and water quality

A quantification of drainage network suspended load was made in order to verify if agricultural subsurface drainage systems contribute to the stream suspended load. The

results of water samples analysis reveal that load is low as compared to that of the stream, but that this load also depends on antecedent rainfall depths. For instance, 10.4 mm of rain fell three days before 23 November 2009 data collection (Figure 3.10). For the July 12th sample, 41 mm of rain fell the previous day, and a total of 119 mm in the thirteen previous days. Similarly, the analyses of water samples collected on November 28th are linked to a 16 mm rainfall event. Approximately 30 mm of rain in the previous four days are responsible for the water samples collected on December 1st. These values, although not exhaustive, indicate that antecedent soil moisture conditions positively influence the intensity of suspended sediment discharge provided by the drainage systems.

Our quantitative analysis is also supported by visual observations. Water drained by pipe #29 (Figure 3.12) is much more transparent than the stream flow at low-medium discharge (Figure 3.11b). The combination of both observations suggests that drainage pipes reduce the suspended sediment concentration in the river. However, no chemical analysis was achieved in the current study to account for the other possible adverse consequences of agricultural drainage systems on habitat quality, for example in terms of phosphorous or nitrate inputs.

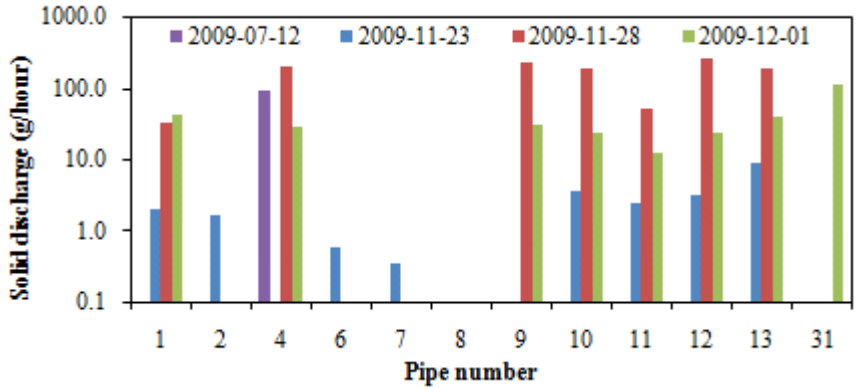

Figure 3.10. Suspended load within drainage pipes obtained from the water samples collected during four data collection sessions for different drainage pipe ends.

The drainage network was found to be generally in a satisfactory condition. However, some problems exist and are associated with bank retreat and bed sedimentation. Firstly, five pipe ends were uncovered as a result of acute bank erosion. In the case of pipe #7 (Figure 3.11a), the pipe end is approximately two-meter long, thus more vulnerable to strong flow events and moving ice. Most pipe ends were partially or significantly blocking pipe flow at various degrees due to algae accumulation. Finally, some old ceramic pipe ends were partially buried in the bed as a result of channel

Figure 3.11. (a) Exposed drainage pipe end #7 is vulnerable to flow and ice due to acute bank erosion. (b) Water draining from pipe end #29 on 28 November 2009 and being more transparent than stream flow, thus indicating lower suspended load.

sedimentation. Our inspection suggests that the efficiency of soil drainage is affected by their maintenance but also by channel instability. However, a more thorough study would be needed to assess the impact of a lack of maintenance on the hydrology and sediment dynamics in this watershed; this was beyond the objectives of this research.

The drainage systems that are directly connected to the Richer Stream are shown in Figure 3.12. This map was built from drainage plans that were not updated since 1986. The fact that many working pipe ends were found that are not linked with any known drainage plan suggests that the watershed is probably more artificially drained than what appears in the data. There is a need to further analyse the impact of drainage network on stream flow quality and event peak.

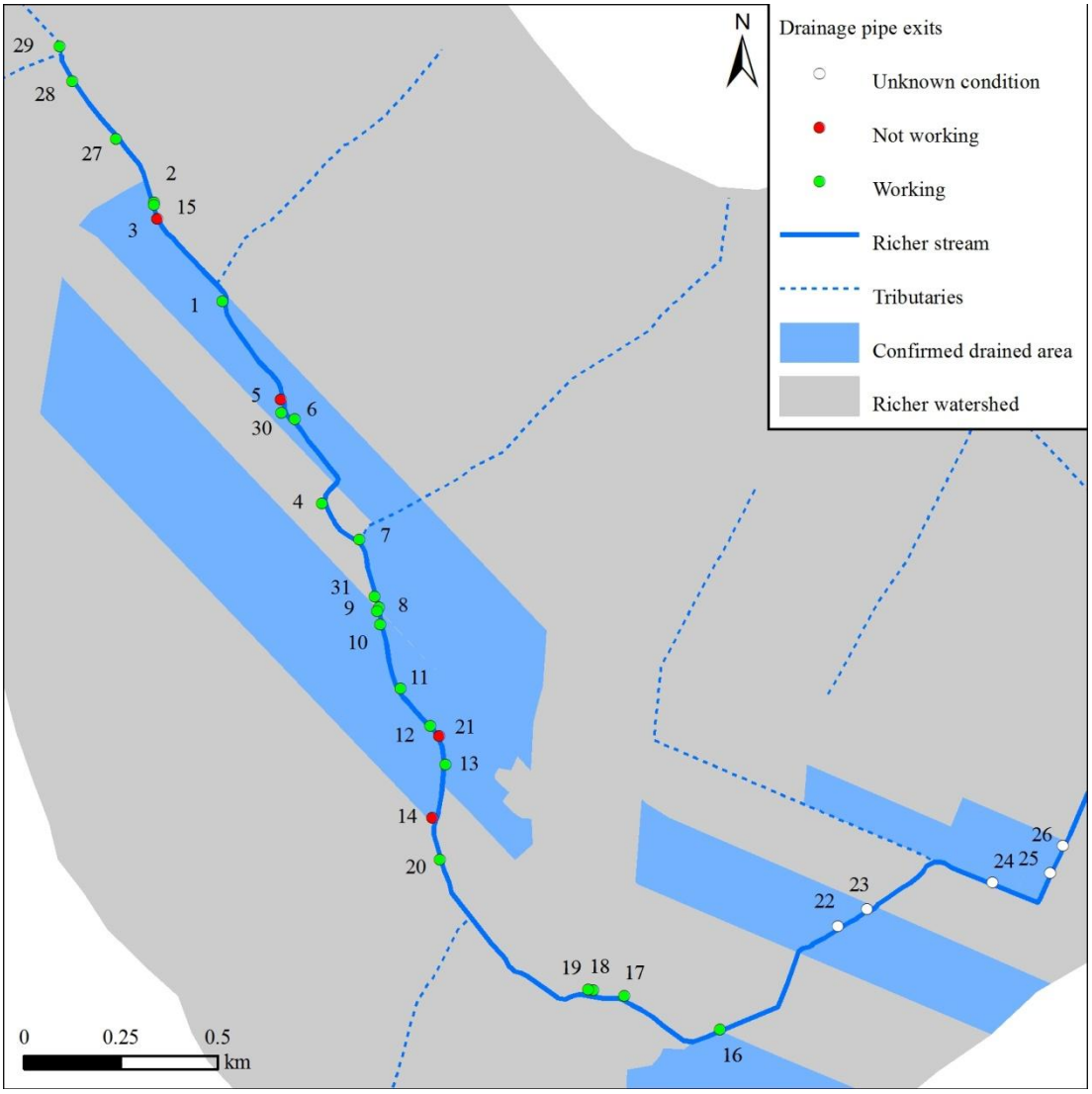

Figure 3.12. Extent of the drained fields near the Richer Stream. References are made to pipe numbers in the text.

3.2. Hydro-morphological modelling

3.2.1. Precipitation data interpolation

Initially, only Saint-Hilaire (Natural Gault Reserve) station was used to relate precipitation to discharge. The fact that it is located at 18.7 km from the Richer watershed Figure 2.9) may contribute to the lack of synchronisation between measured flow

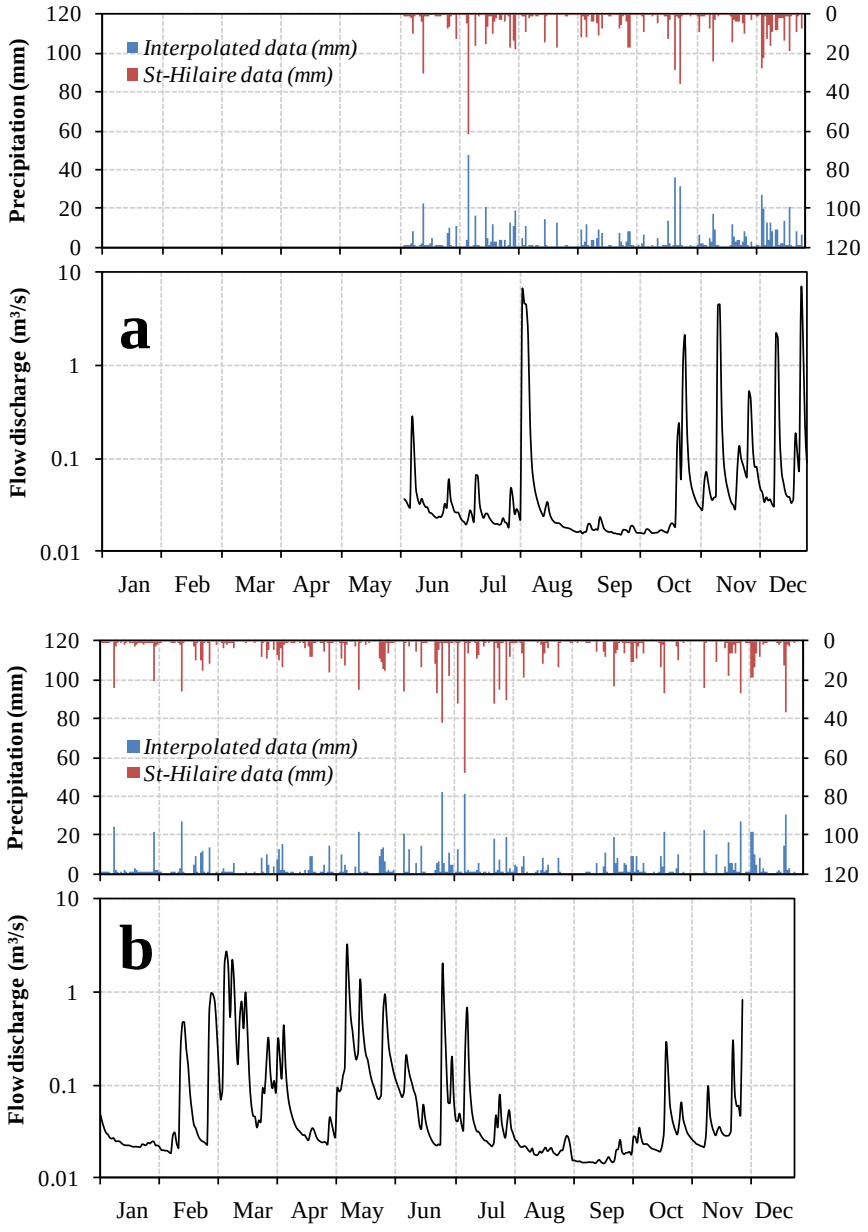

Figure 3.13. St-Hilaire vs. interpolated precipitation data in respect to flow discharge in (a) 2008 and in (b) 2009.

(discharge peaks on the Richer flow hydrograph and measured rainfall depth recorded at the St-Hilaire weather station (Figure 3.13). By interpolating precipitation data from five nearby weather stations (Figure 2.9), the correlation between rain and discharge was greatly improved. This case illustrates the spatial variability in precipitation; a weather station would be required in the Richer watershed to further improve the correlation between precipitation depth and stream flow discharge.

3.2.2. Simulations

3.2.2.1. Hydrological effects on a static channel

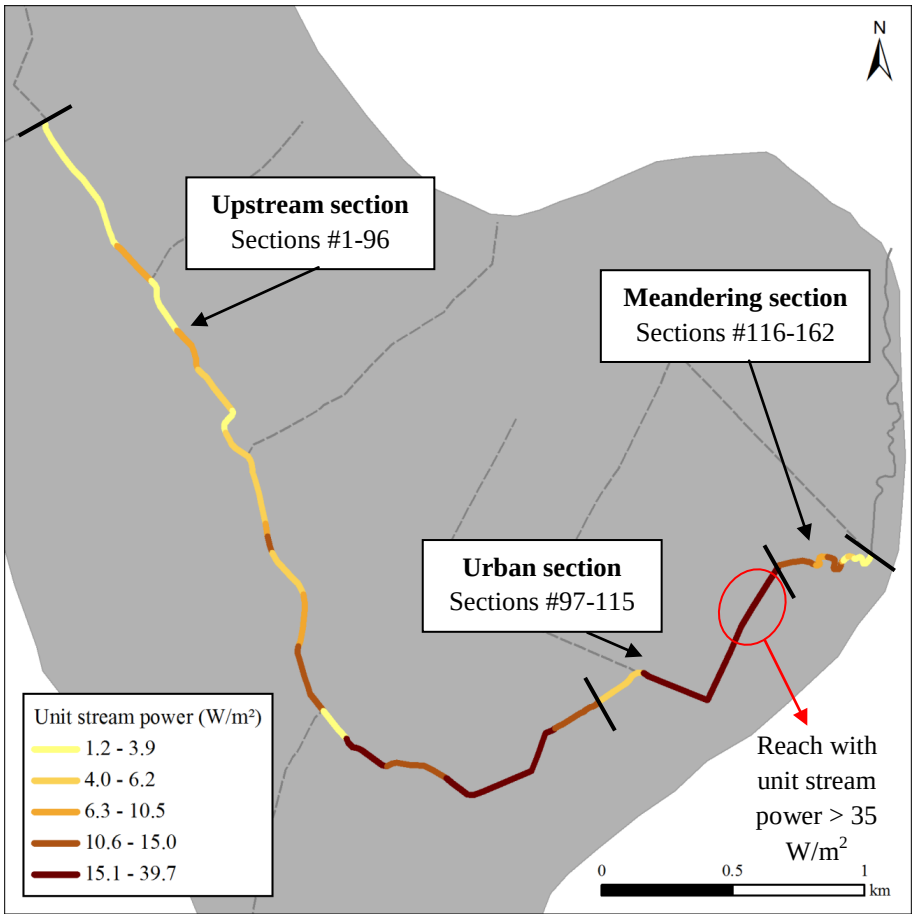

Figure 3.14. Simulated unit stream power using historical weather conditions (6 June 2008 to 3 December 2009) for the no-action scenario.

No action

Figure 3.14 presents the predicted stream power values in each section of the Richer Stream on 6 August 2008 for the current channel configuration. Due to contrasting land uses and channel planform, the stream is divided in three parts for the analysis: the upstream agricultural part (sections 1-96), the residential part (sections 97-115) and the meandering part (sections 116-162). When comparing the predicted stream power values among the three parts, the urban part possesses the highest values, followed by the upstream part. Stream power values in the meandering part are lower than in the two other parts.

Creation of meanders

Channel re-meandering decreases specific stream power, albeit more effectively in the urban part where longitudinal bed slope is the steepest (Figure 3.15a-b). Mean and maximum stream power values are reduced on average by 49.2% and 24.3%, respectively, when restoring a sinuosity of 1.44. The change in the meandering part is minimal since most of the sections already have more than the desired sinuosity. The rate of decrease of the stream power (i.e. with increasing space investment through the re-establishment of channel sinuosity) is the highest between a sinuosity of 1.00 to a sinuosity of approximately 1.06 (Figure 3.15c). After this value, the reduction in stream power is constant (2.5% reduction per additional 10,000 m² protected area when using the wavelength of the 1932's channel).

Creation of backwater ponds

Backwater ponds decrease specific stream power due to the reduced stream power. Mean values (among all sections in the upstream part) are reduced by 24.0% with the

installation of 3 ponds of 40,000 m² each (Figure 3.16a). With the same configuration, maximum values are reduced by 17.4%. The reduction in stream power is more important when using less but larger ponds (for the same total area) (Figure 3.16b). For instance, 12 ponds of 10,000 m² each would only reduce mean specific stream power by 12.2%. Less and larger ponds also have the benefit of reducing stream power more significantly for a specific investment (Figure 3.16c). This situation is attributed to the fact that a constant width of 10 m is proposed for the vegetated riparian strip surrounding each pond regardless of the area of the pond. Since a pond reduces flow discharge values in all sections downstream from its location, it will affect a longer stretch of the stream if it is installed upstream in the watershed.

Improvement per space investment unit

If a predetermined area is to be invested in a watershed management program, a key question is which method is expected to provide the highest return on investment in terms of bank stability. The four scenarios are expected to reduce stream power by the same proportion for a total space investment lower than 25,000 m² (equivalent of 3 ponds of 15,000 m² each or of a sinuosity of 1.07) (Figure 3.17). Above this space investment, re-creating meanders triggers a more important reduction in stream power than installing backwater ponds.

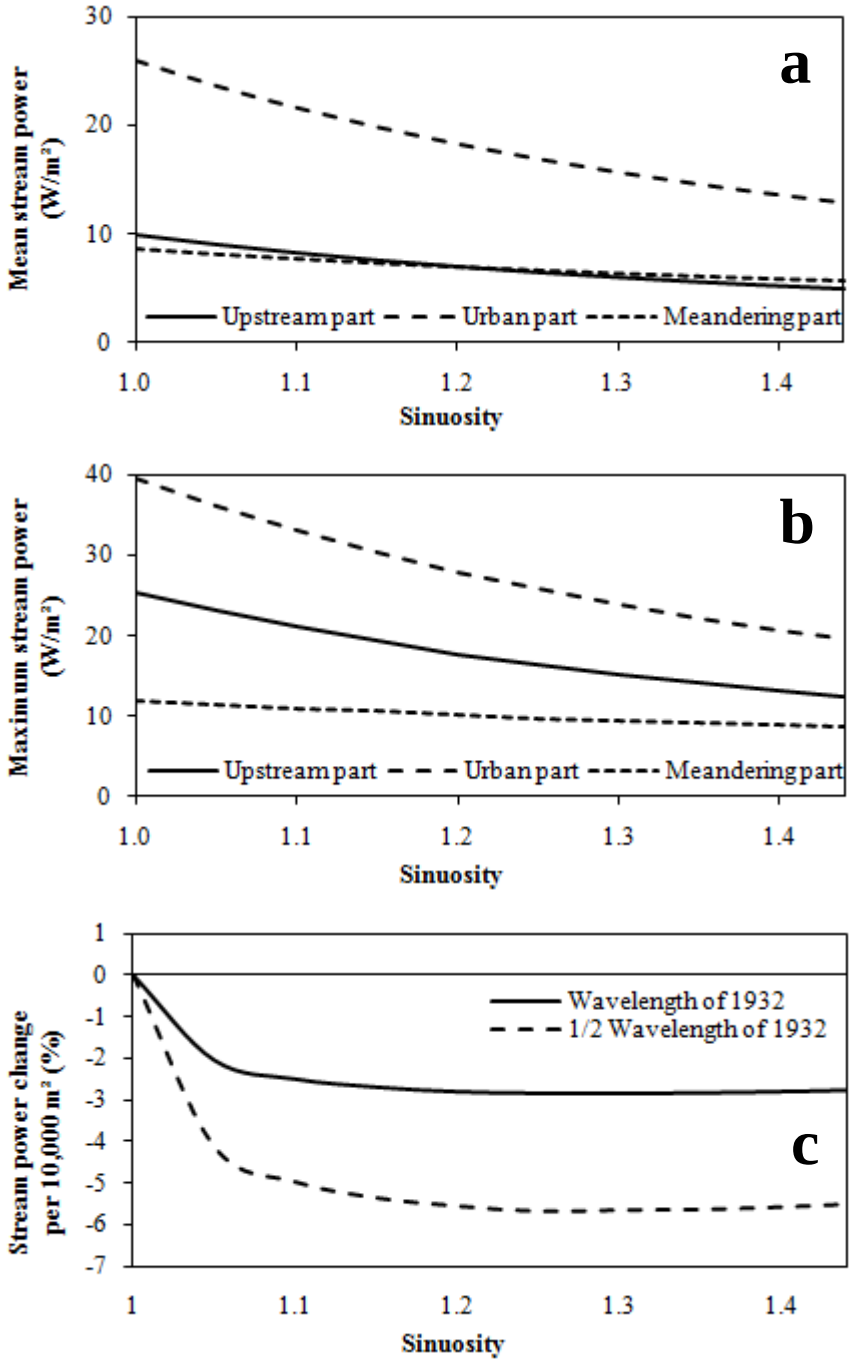

Figure 3.15. Effect of various re-meandering scenarios on (a) mean and (b) maximum stream power for 6 August 2008 peak discharge. (c) Stream power change for various sinuosity and wavelength scenarios.

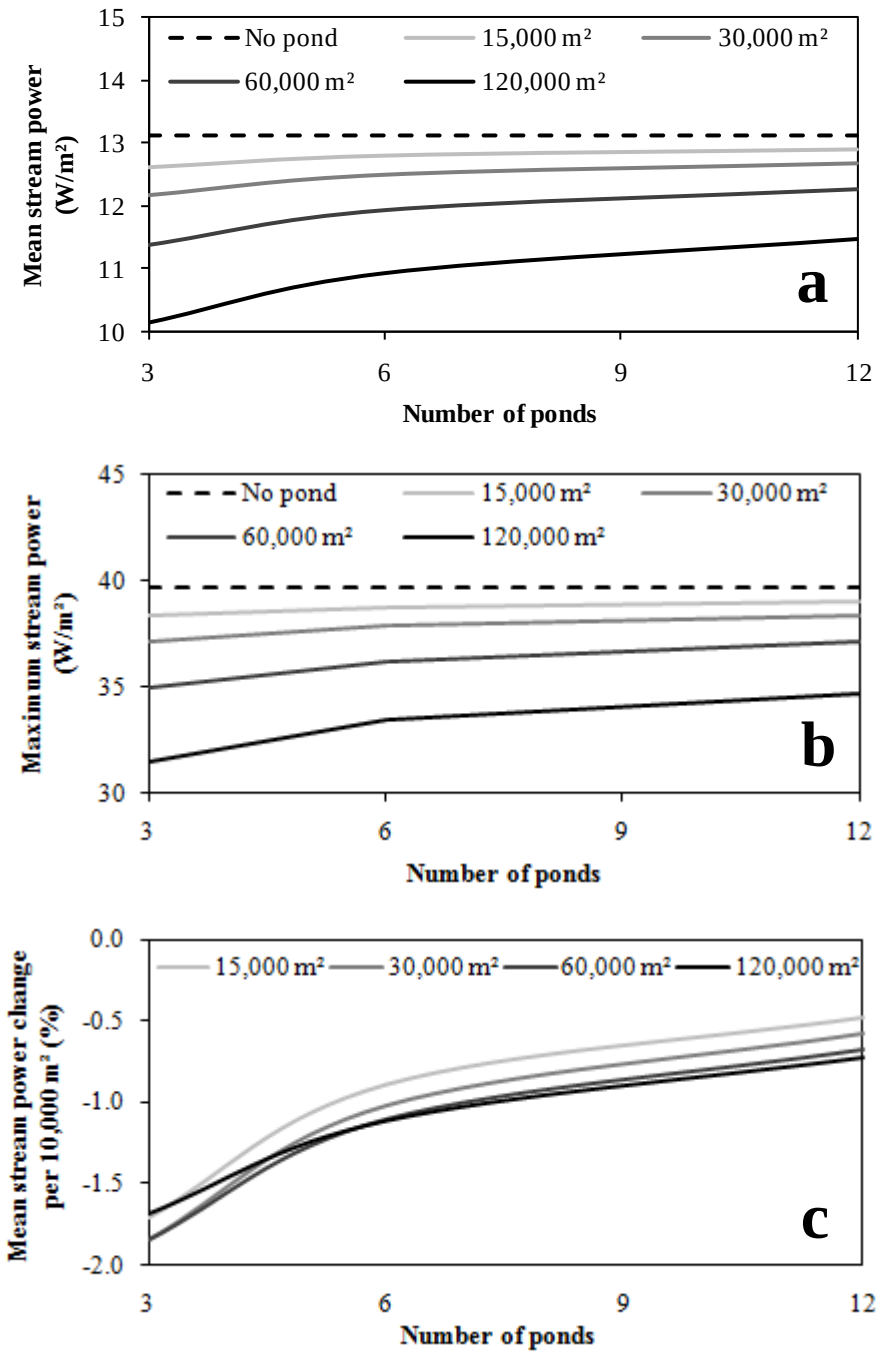

Figure 3.16. Effect of various backwater pond creation scenarios on (a) mean and (b) maximum stream power for 6 August 2008 peak discharge. (c) Stream power change for various configurations.

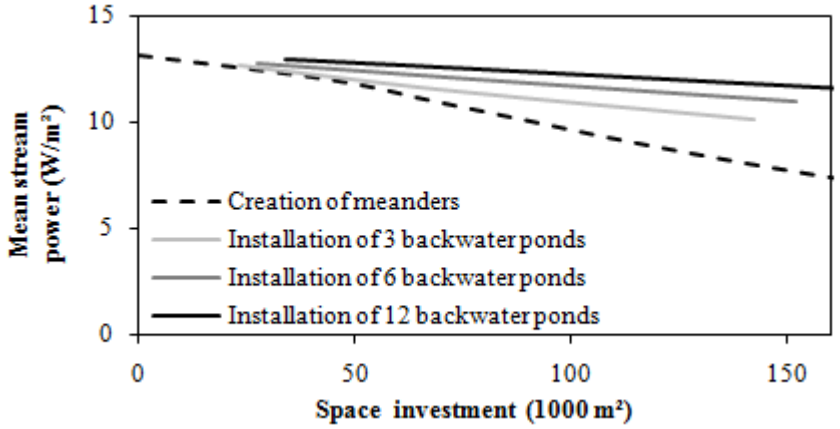

Figure 3.17. Effect of space investment on maximum stream power for four management scenarios.

3.2.2.2. Geomorphological effects on a dynamic channel

The simulations aiming at understanding channel dynamics were achieved by enabling bed and suspended loads whilst not taking account of surface runoff and drainage pipe loads. Instead of using existing empirical equations (e.g. Shen and Hung (1972) for total load and Itakura & Kishi (1980) for suspended load), the solid stage-discharge curves corresponding to the measurements taken in the Richer Stream were used directly in the model to predict transport rates rather than being employed in model validation. This decision was taken because the existing equations gave transport rates that were orders of magnitude larger than the measurements taken in the Richer Stream. This situation is explained by the fact that most of sediment transport equations apply to sand or gravel bed rivers. Little research has been carried out in small clay-bed streams and the variation in transport rates may be too high for the use of general equations due to additional factors affecting cohesion. To the best of my knowledge, no equation can accurately predict sediment transport rates in a small clay-bed watercourse such as the Richer Stream.

Effect on channel capacity

Channel capacity is defined here as the maximum cross-sectional area that the flow would occupy if the channel was completely filled with water. With the current management plan (no action taken between dredging sessions), the hydro-morphological model predicts that the average channel capacity (weighted average of all sections according to the length of each section) of the Richer Stream is expected to have reduced from 12.49 to 12.44 m^2 over a period of 546 days (6 June 2008 to 3 December 2009). This reduction in channel capacity partially explains why dredging works are performed on a regular basis in this stream. Although a 0.42% reduction in channel capacity (i.e. through sediment accumulation on the bed) is negligible, it may contribute to rising water table to a level that can alter field hydrology on the long term if combined with the accumulation rate of sediments derived from failed banks. For instance, considering the average channel dimensions (total width of 10.5 m, depth of 1.73 m and bank angles of 28°) a reach experiencing a 2.78% reduction in capacity would aggrade by 8.5 cm.

The results suggest that the average channel capacity would not have been reduced as much in the aforementioned period with the implementation of alternative approaches such as channel re-meandering or backwater ponds creation (Figure 3.18). Although the tested approaches contribute to maintaining channel capacity, the fact that the final capacity is lower than the initial capacity for all scenarios suggests that supplemental actions would have to be combined with the tested solutions to allow for the preservation of current channel capacity. Channel re-meandering seems however more efficient than the creation of backwater ponds for preserving channel capacity (Figures 3.18-19). This approach is usually associated with the creation of a riparian corridor. The development

of vegetation could contribute to filtering sediments from surface runoff and thus maintaining channel capacity. Conversely, the filtering potential offered by backwater ponds is expected to be much lower.

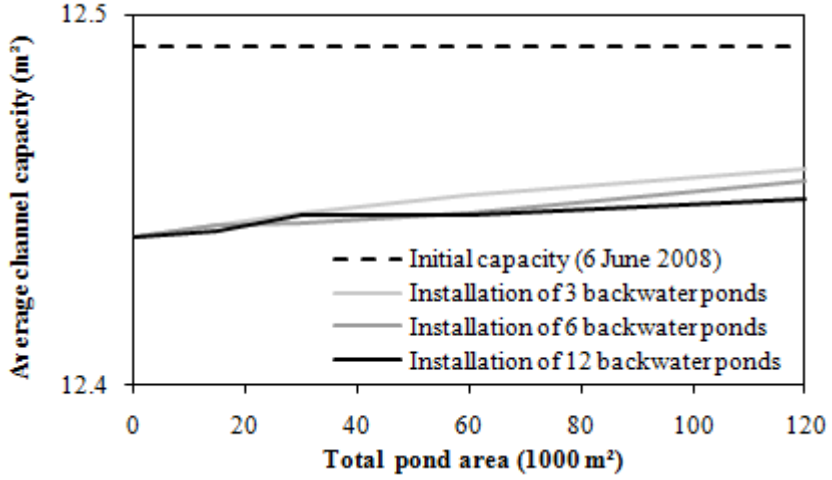

Figure 3.18. Effect of channel re-meandering on maximum capacity.

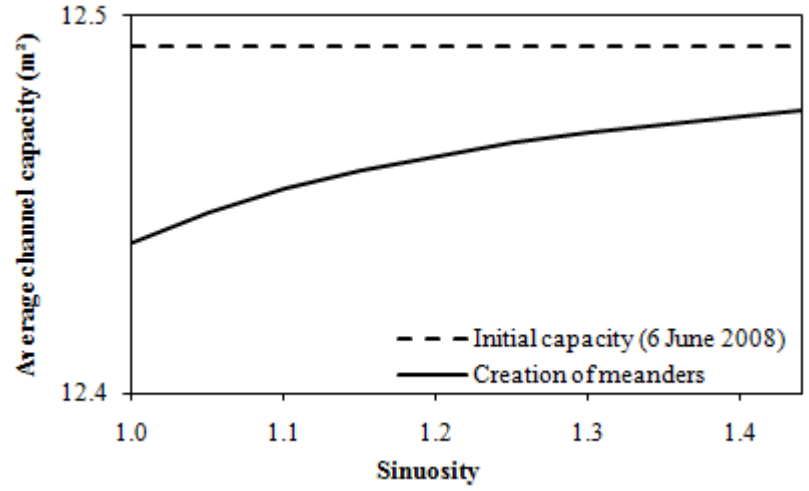

Figure 3.19. Effect of backwater ponds on channel capacity.

Spatial distribution of changes

Maps of predicted channel capacity changes for the two tested scenarios are provided in Figure 3.20. Such maps could be helpful in prioritizing management activities involving the tested approaches. Although the tested methods are intended to

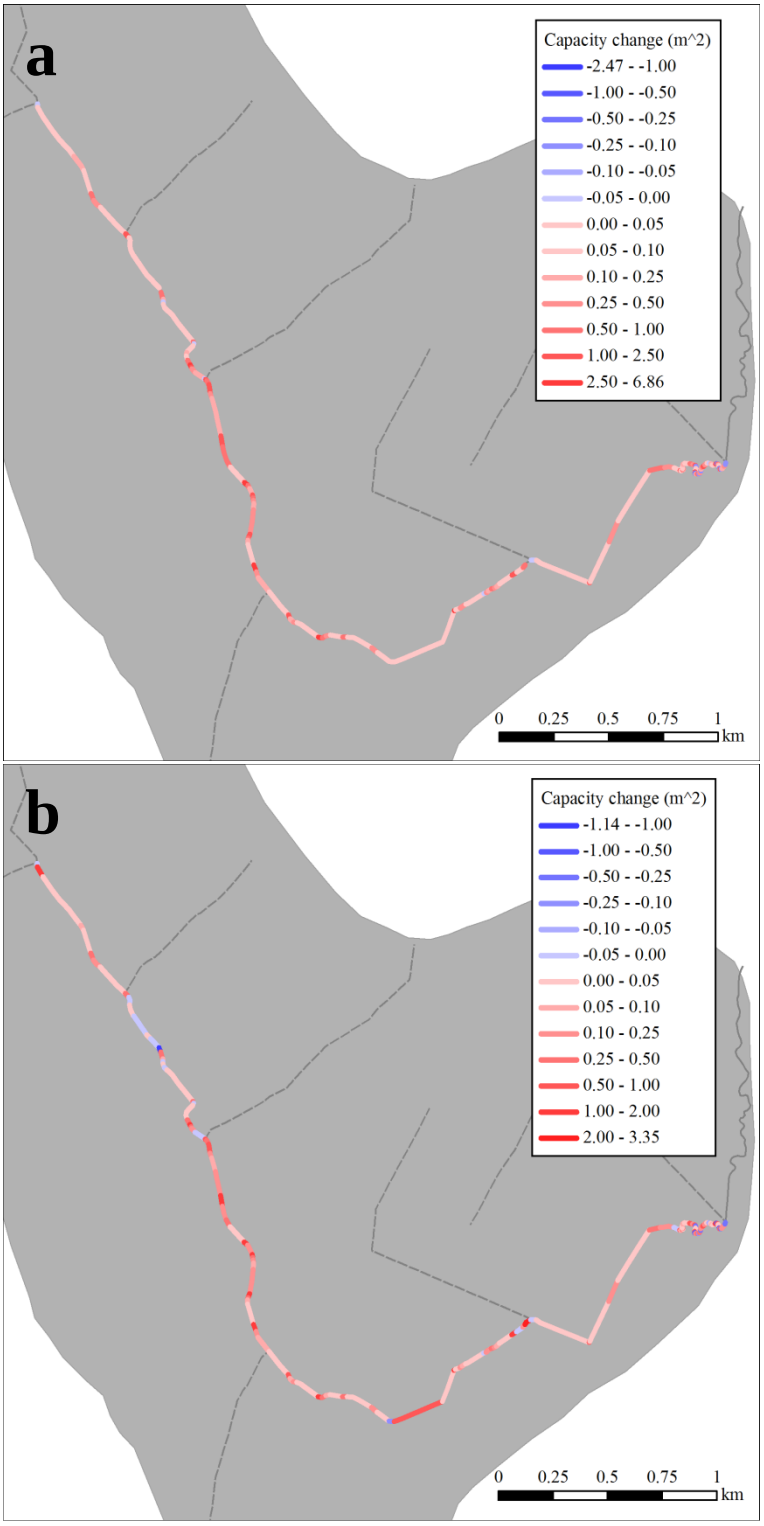

Figure 3.20. Predicted spatial distribution of channel capacity changes (vs. no action scenario) following (a) channel re-meandering (sinuosity of 1.44 shown) and (b) the creation of 3 backwater ponds of 40,000 m² each.

help achieving higher channel stability at the watershed scale, restoration plans could be designed and implemented in such a way as to reduce stream power in the reaches that are expected to experience important reductions in channel capacity (negative and low positive values in the provided maps). In both scenarios, mid-basin reaches seem to suffer the less from channel infilling; some sections may even experience bed incision. Conversely, upper reaches and those near the urban area of Saint-Marc-sur-Richelieu should experience a change that is similar to that operating within the no-action scenario. These latter reaches should therefore be given priority since they are the most at risk due to higher stream power in downstream reaches.

3.2.3. Discussion

The results from the simulations performed with the hydro-morphological model suggest that channel re-meandering is more efficient than the creation of backwater ponds in reducing peak discharge and stream power, for equivalent space investment. However, both solutions contribute to reduce peak discharge by delaying downstream flow progression. The predicted values of unit stream power in the Richer Stream were below 35 W/m^2 in 160 sections (out of 162). As seen in Figure 3.21, this value of stream power is considered a threshold to distinguish between rivers that can recover their original sinuosity (> 35 W/m^2) and those that will require maintenance in order to reinstate a sinuous pattern (Brookes, 1987; 1990; 1995; Sear, 1996). Although the existence of such a threshold remains uncertain (Stacey & Rutherford, 2007), the fact that it was developed for Danish rivers that are similar to the Richer Stream in many respects (e.g. slope, grain size, land use) strengthens our confidence that it is applicable in this case. As seen on Figure 3.14, only the channel reach located between the residential area (municipality of

St-Marc-sur-Richelieu) and the meandering reach (Figure 2.1) would have sufficient stream power to naturally re-create meanders. In the other parts of the channel, some interventions would be required to initiate a sinuous pattern, perhaps using deflectors or emergent vegetation (Bennett et al., 2002).

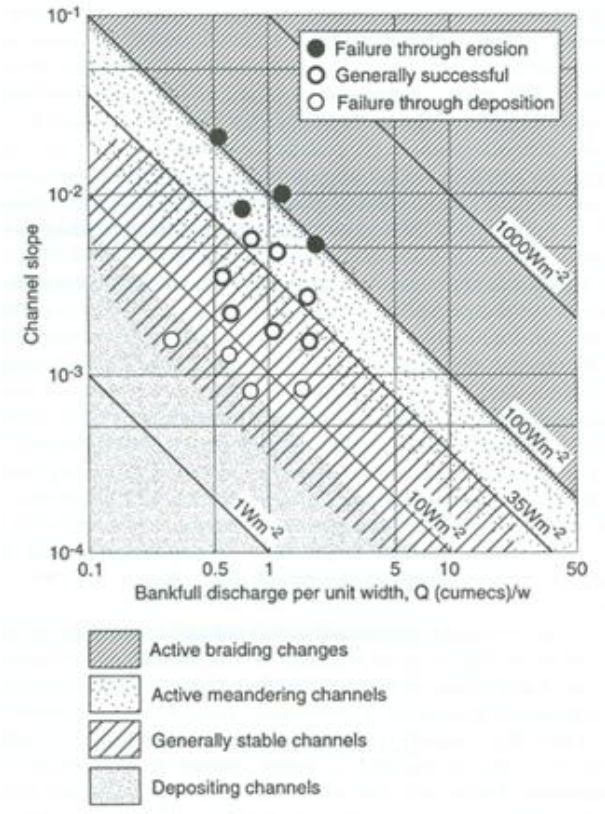

Figure 3.21. River channel adjustment in relation to thresholds of stream power (Sear, 1996).

In the hydro-morphological model used in the current research, the effects of channel re-meandering on stream power is explained by the increase in channel capacity coupled with a reduction in bed slope and a modification of form roughness due to increased sinuosity. Little research has been carried out to quantify the potential hydrological effects of re-meandering straightened rivers. A 14% reduction in peak discharge and 2-hour delay in the occurrence of flood peaks was previously calculated following a 10% modeled increase in channel sinuosity in the Steinsel sub-basin, Luzembourg (Liu et al., 2004). This figure compares well to the 9% reduction predicted in the Richer Stream.

The simulations performed with a physiographic inundation and flood routing model suggest that retention ponds can reduce the intensity of peak flows, especially for events of short returning periods (Chen et al., 2007). The reduction in magnitude of peak

discharges is then expected to reduce fluvial erosion, slide failure and cantilever failure (Luppi et al., 2009). In Cecina, the dominant type of erosion mechanism was found to be seasonally dependent, with fluvial erosion being associated with early autumn events, mass failure with late autumn and winter events and a combination of the three mechanisms with spring events. Although the timing of each mechanism in the Richer Stream may differ from those found in Italy, erosion is likely to be reduced with the installation of retention ponds. The rising and falling limbs of the hydrographs downstream of ponds were equally found to be smoother than those without such facilities (Chen et al., 2007). Since a sudden loss in confining pressure created by the river after the peak flow (when the adjacent soil is still saturated) is responsible for mass failures (Rinaldi et al., 2004), smoother hydrograph slopes could also contribute to stabilising the channel. This approach should facilitate the maintenance of channel capacity and reduce the reliance on environmental adverse techniques such as dredging.

No comparison is possible with regards to pond configuration since, to the best of my knowledge, no previous study examined the selection and number of ponds to be used to optimize the hydrological outcomes of such a solution. The results suggest that less but larger backwater ponds are expected to be more efficient in reducing specific stream power than many small ponds.

Although the hydro-morphological model did not assess the filtering potential of the proposed approaches, both of the tested solutions are likely to prevent sediments and pollutants originating from adjacent fields to reach the stream. In a previous study, a 18 to 82% reduction in suspended solids from the pond water effluent was measured using various types of 3 m wide grassed strips, depending on solid sediment input, bank slope,

and grass species (Ghate et al., 1997). Similarly, a 6 m wide grass strip was found to be efficient in trapping large particles at various degrees depending upon grass length and soil conductivity but also on particle size, grass density and sediment density (Deletic, 2001).

A sustainable channel stabilisation program should seek to let a river self-regulate while minimizing maintenance works. Furthermore, any technical assessment needs to take account a range of possible weather conditions. Since the annual amount of rainfall received in northern Europe during the last century increased over natural variability levels (Scholz, 2007), further research works should equally investigate the hydrological effects of each approach against anticipated climate conditions using one or several of the SRES (Special Report on Emissions Scenarios) families of climate change scenarios defined in The Fourth Assessment Report of the IPCC (Intergovernmental Panel on Climate Change): A1B, A2, B1, and B2. Since current green house gas emissions exceed both the A1 and B2 scenarios and are closer to A2 (Raupach et al., 2007), the A2 scenario should be tested in priority. Adding ponds is expected to attenuate the impacts of anticipated larger floods under climate change scenarios, but it may also help minimizing risks on fish habitat of long periods of low flow with high temperature. The diversification of morphologies associated with increased sinuosity (i.e. pools) reduces low flow risks compared to uniform straight channel. As illustrated in Figure 2.1c, a sinuous channel may also provide additional water storage within higher channel berms.

The effects of installing stream barbs and bed weirs in the urban reach of the Richer Stream are examined through velocity maps. Only part of the simulation domain is shown in each map to properly display streamlines and flow direction vectors. The maps are centered near the zone of maximum velocity in the case of the 125° bend and on the second structure in the case of the straight reach.

4.1. Stream barbs

The objective of redirecting high flow velocities near channel centre to reduce near-bank velocities is partially met with the installation of stream barbs in the 125° bend. As similar patterns were observed at medium flow stage, only high flow stage results are presented here since the overall changes in flow patterns are greater at the highest flow stage. At high flow stage, surface and mean velocity magnitudes are greatly reduced near the outer bank and increased near channel centre compared to the case with no barbs (Figure 4.1). Streamlines are laterally compressed towards the inner bank and are oriented parallel to channel banks instead of being directed to the apex (Figure 4.2*)*. Velocity magnitudes increase with depth near the center of the channel and the lateral symmetry of flow velocities is enhanced between cross-sections 5 and 11 (Figure 4.3). Few changes in secondary current patterns occur throughout the bend. Counterclockwise current forms in cross-section 6 whereas cross-sections 7 and 8 are subject to stronger downwelling currents near the toe of the right bank. The changes in secondary currents in cross-sections 7 and 8 are expected to reduce the rate of near-bed sediment transport towards the right bank and therefore prevent the accumulation of sediment and associated increase in sinuosity at this location. However, cross-section 6 is expected to undergo

opposite morphological changes due to downwelling current near the left bank. Therefore, the net effect of stream barbs on sediment accumulation in this bend is uncertain. Overall, surface velocities are reduced near the outer bank whereas bed velocities are locally increased. Since near-bed velocities are generally much lower than surface velocities (0.01 m/s near the bed compared to 0.45 m/s on the surface on average at high stage) and since velocity reductions are more important than velocity increases, stream barbs are likely to be beneficial to channel stability.

Generally, as flow stage increases, so does maximum velocity at the water surface and the potential for bank erosion. However, because of the trapezoidal shape of the Richer channel, an increase in flow depth leads to a proportionally greater increase in flow cross-sectional area and lower maximum velocities at the surface at high than at medium flow stage. Nevertheless, stream barbs have a marked impact on the location of the high-velocity zone, which is shifted from the left bank to the center of the channel (Figure 4.2), considerably reducing the risks associated with the high surface velocities. Increasing the flow stage whilst preserving stream barbs results in surface flow velocity changes that are mainly located near the right bank (looking downstream) and between each pair of consecutive barbs.

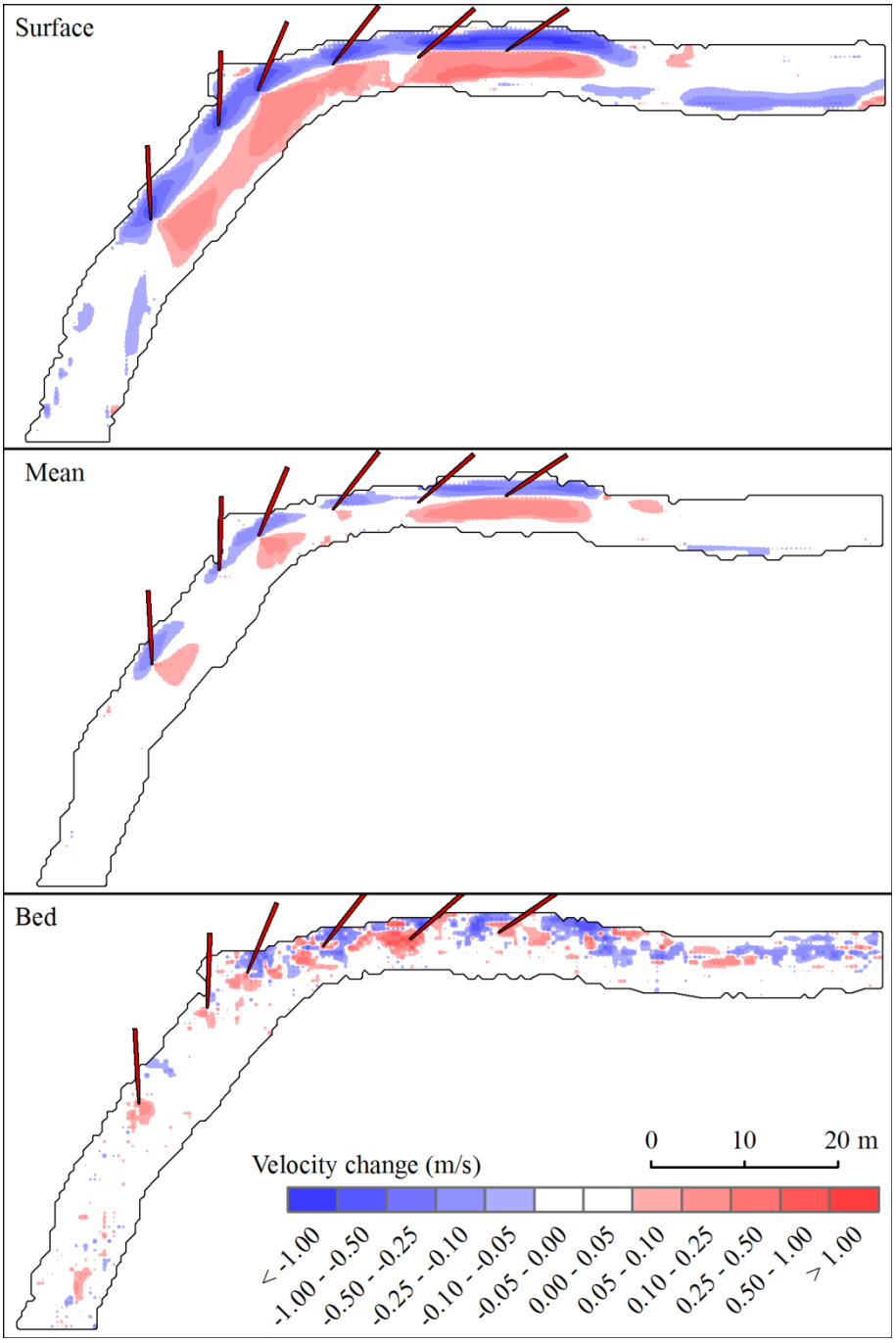

Figure 4.1. Change in velocity magnitude at high stage following the installation of stream barbs in the 125° bend. Flow is to the right.

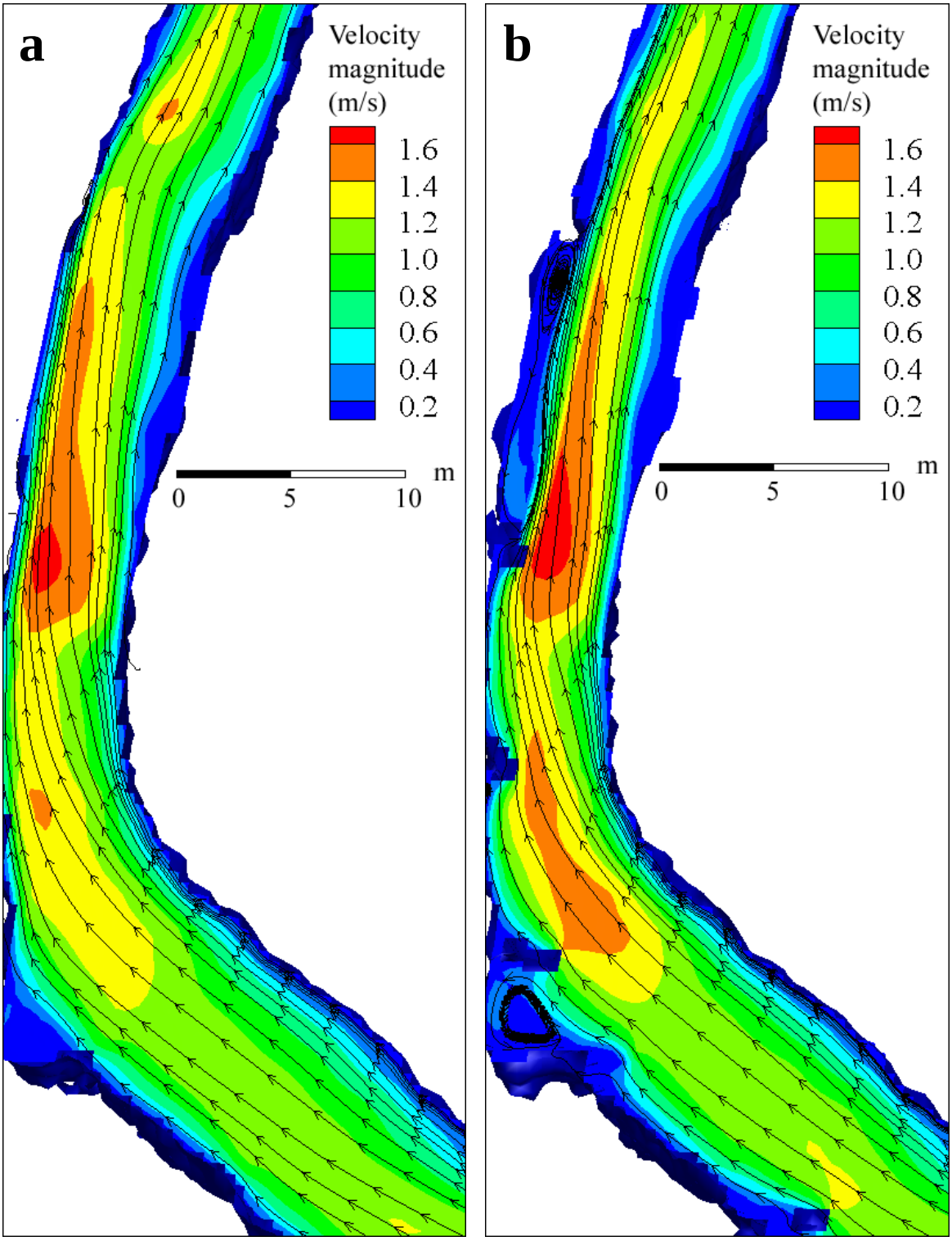

Figure 4.2. Surface velocity magnitudes and streamlines at high flow stage in the 125° bend (a) without barbs and (b) with barbs. Flow is to the top.

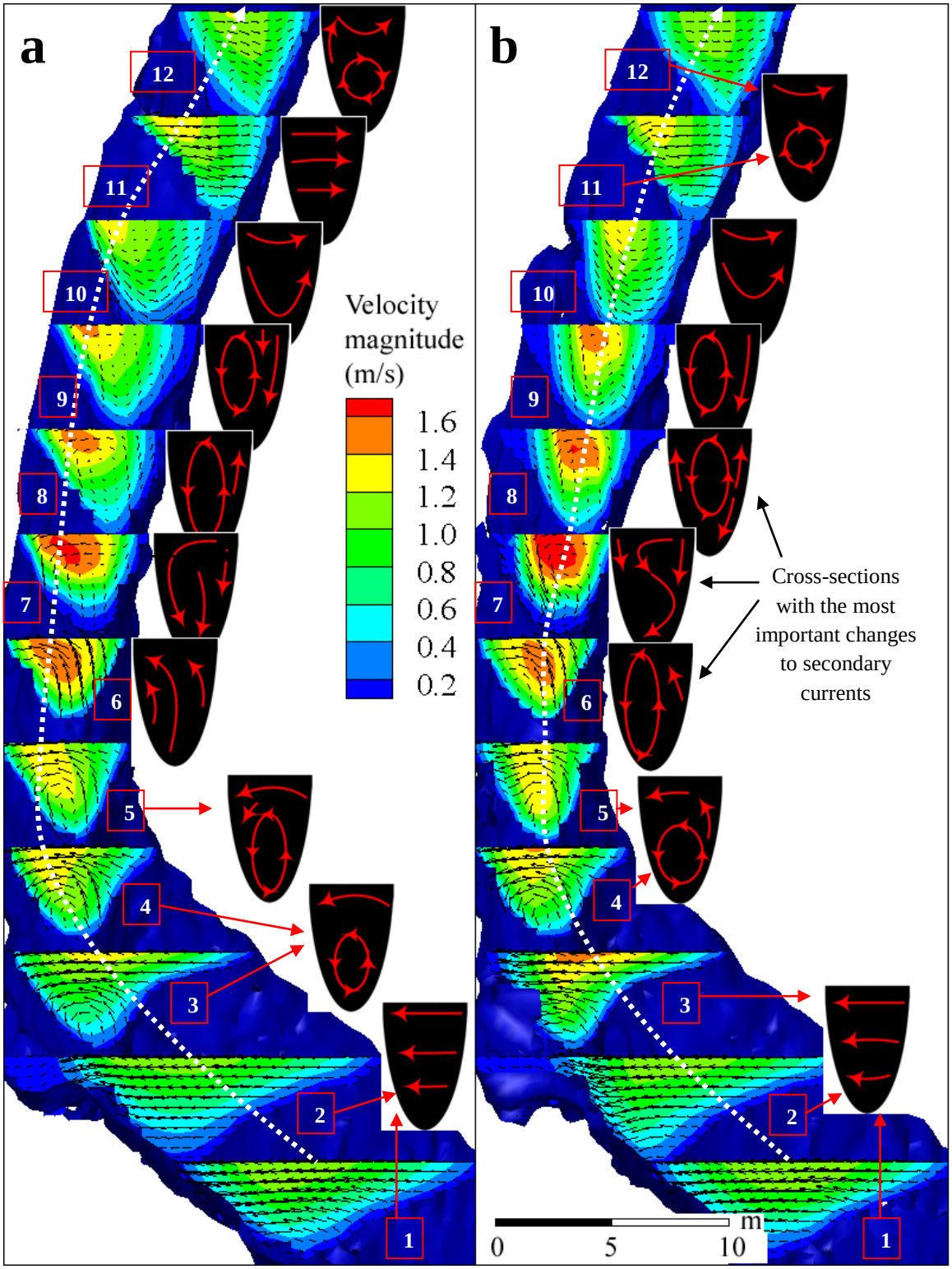

Figure 4.3. Slices of velocity magnitudes at high flow stage in the 125° bend (a) without barbs and (b) with barbs. Flow is to the top. A distance of 4.5 m separates consecutive slices. The white dashed line is the streamline of maximum velocity whereas the black semi-ellipses containing red arrows represent the main patterns of secondary currents in each of the twelve cross-sections.

4.2. Bed weirs

A high velocity zone forms at the center of the channel on the lee side of each V-shaped weir, which gradually fades out downstream (Figure 4.4). This zone is elongated in the case of surface and mean velocities, and elliptical in the case of bed velocities. Flow velocities are reduced downstream of each weir on both sides of the fast flowing central vein. The most important changes in surface velocities occur downstream of the first and fourth weirs, with less change associated with the second and third weirs.

Streamlines indicate flow convergence near channel center (Figure 4.5a). The zone of maximum flow velocities is relocated towards the bed as vertical constriction increases (Figure 4.5b). Upstream of the V-shaped weir (positioned at cross-section 5 on Figure 4.5b), no strong secondary circulation pattern exists. The two symmetrical helical circulation cells that are produced on the lee side of each weir (at cross-sections 6 and 7, rotating clockwise near the left bank and counter clockwise near the right bank) are expected to help the pool morphology self-sustain by preventing sediment accumulation. The two circulation cells then merge in a single counter clockwise-rotating cell at cross-sections 8 and 9. The direction of rotation seems to influence flow orientation towards the left bank in the downstream cross-sections. However, the main vein of the flow remains aligned with the banks in the center of the channel up to more than 28 m downstream of the structure.

Velocity increases near the bed raise a question as to the potential destabilising effects that these structures may have. However, with appropriate bed protection downstream of the V-shaped weirs to protect the bed from downwelling currents (on a distance of about 10 m), the tested structures are expected to reduce bank erosion in the

straight reach.

Important differences exist in the flow patterns resulting from the installation of the straight or V-shaped weirs. Although not illustrated, straight weirs increase flow velocity near stream banks and reduce it near the center of the channel. These changes (which are opposite to those created by V-shaped bed weirs) are likely to promote bank erosion and channel instability. The trapezoidal shape of the channel combined with the small width-to-depth ratio in this agricultural channel may explain this trend. Since the flow is vertically constrained, part of the water that was flowing in the fast central vein prior to the installation of the straight weirs is deviated upward then laterally. This situation results in an increase in the magnitude of near-bank velocities, as is the case with the highest degree of constriction in which the flow is deviated towards the left bank. Two helical cells form downstream of the weirs, but these are not symmetrical (as was the case for the V-shaped weirs). There is overall little evidence that the straight design can be of any utility in stabilising a straight natural reach.

A weir modifies velocity patterns up to the next weir at high flow stage (Figure 4.4). Conversely, the weirs only modify the flow locally at medium flow stage with the main changes found immediately downstream of each structure. The increase in flow stage also affects the change in velocity, with higher stages leading to greater positive and negative velocity changes.

Modifying the degree of obstruction by raising or lowering bed weirs considerably modifies flow velocities and patterns. Although not illustrated here, low V-shaped weirs that are subject to high flow stage produce an increase in velocity magnitude near the left bank and a decrease near the right bank. With high V-shaped weirs, a high-velocity vein

forms at the center of the channel and a decrease is found near the banks (Figure 4.4). The fact that the flow patterns observed at high stage with high weir are similar to those obtained at medium stage with low weir suggests that the degree of vertical constriction is responsible for flow convergence, realignment, and acceleration near channel bed.

Figure 4.4. Change in velocity magnitude at high flow stage following the installation of high V-shaped bed weirs in the straight reach. Flow is to the right.

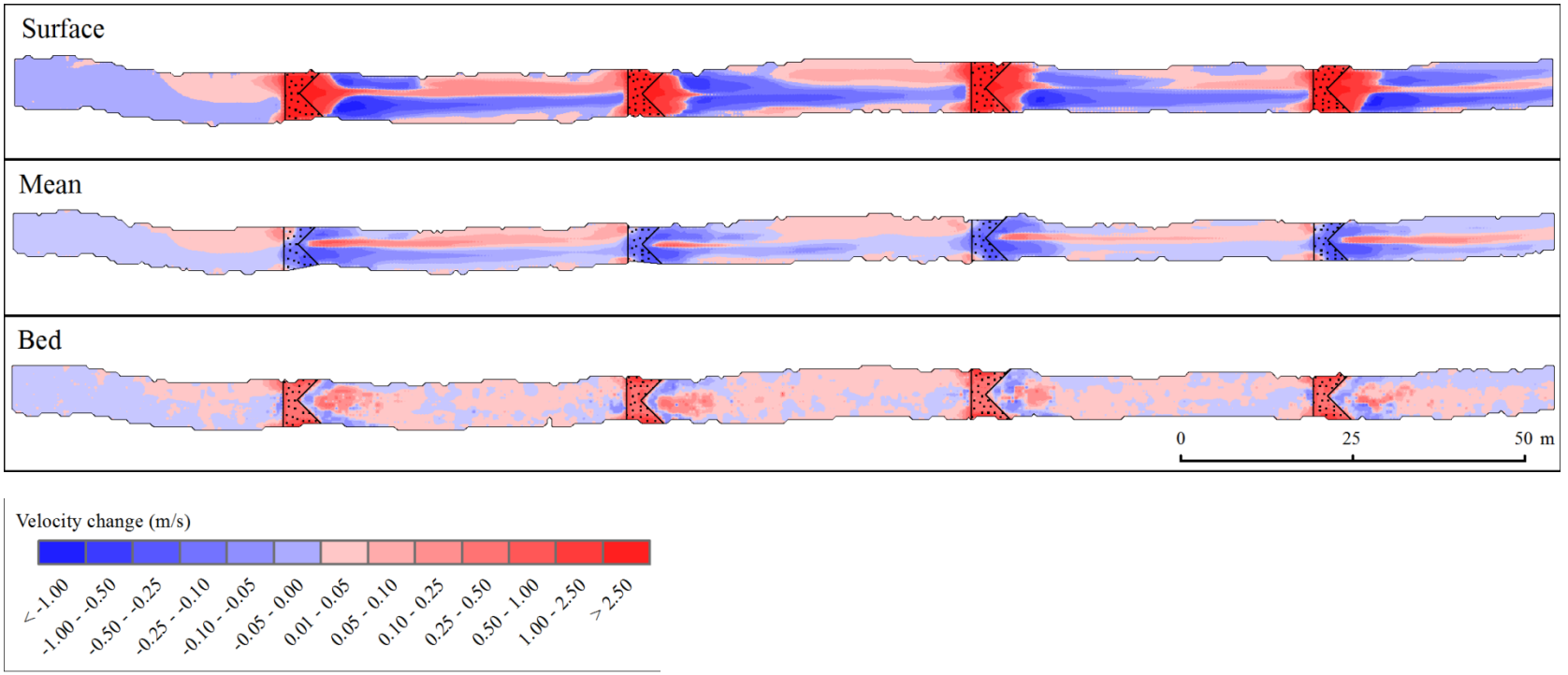

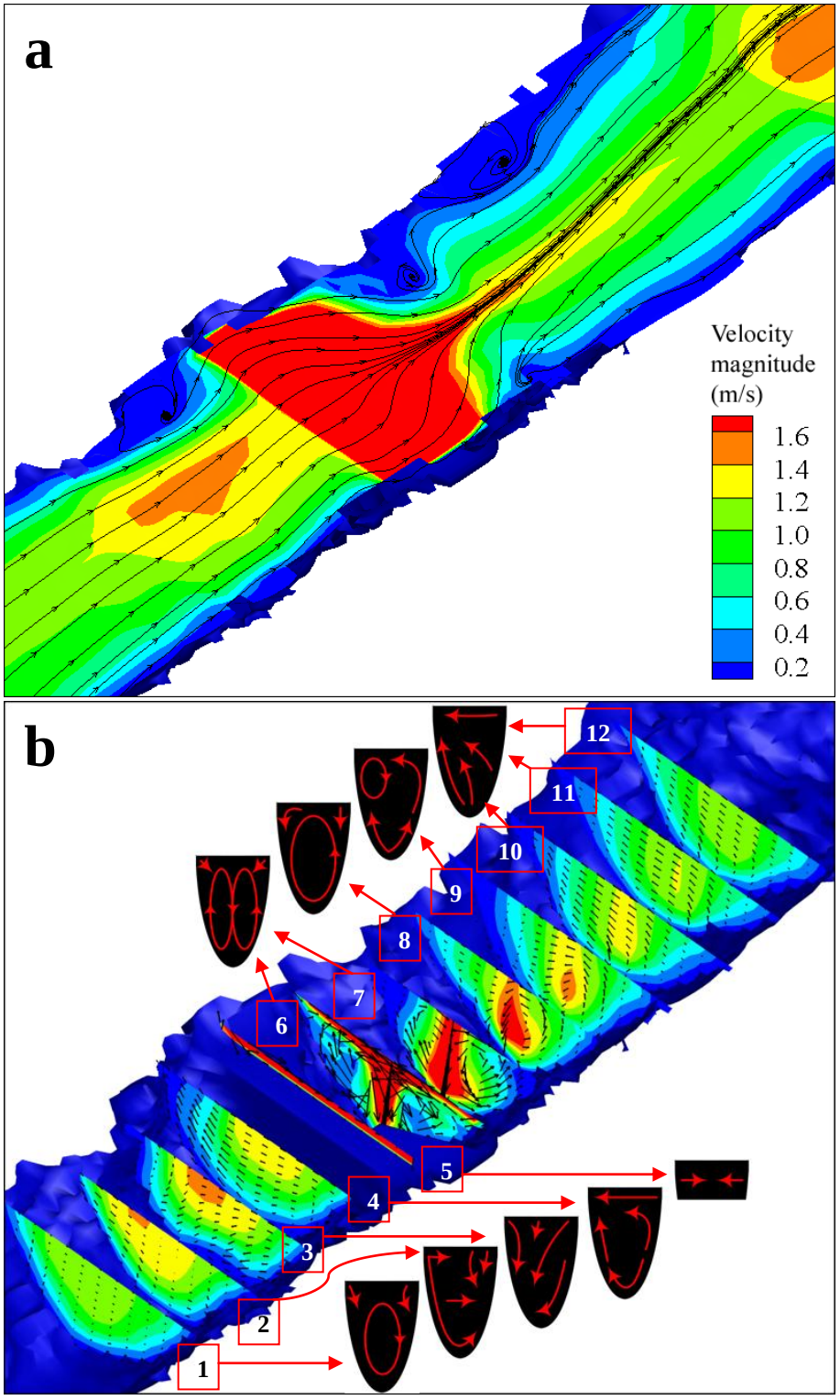

Figure 4.5. (a) Surface and (b) lateral slices of velocity magnitude (in m/s) at high stage following the installation of high V-shaped bed weirs in the straight reach. Flow is to the top. A distance of 4.1 m separates consecutive slices. The black semi-ellipses containing red arrows represent the main patterns of secondary currents in each of the twelve cross-sections.

4.3. Discussion

4.3.1. Stream barbs

The examination of the hydraulic effects of installing stream barbs in a curvilinear experimental reach suggests that these structures can improve channel stability. It was found that stream barbs reduce near-bank velocities on the outer side of the bend by redirecting stronger flow velocities near channel centre. These findings are in agreement with 3D simulations (with the model SSIIM) of flow and sediment patterns in 90° and 135° experimental flumes (Minor et al. 2007a,b) as well as 3D simulations showing the morphological impacts of adding seven barbs in a natural bend, which showed that erosion on the outer bank can be prevented due to reduced velocities and bed shear stress values in this region (Jamieson et al., 2009).

Adding stream barbs may also have undesirable effects, for example due to flow acceleration near the tip of each barb (Figures 4.1) which could limit the effectiveness and durability of the structures. These zones of flow acceleration could locally trigger scour and thus affect the stability of the structures first put in place to stabilise the channel. The morphodynamic simulations performed by Minor et al. (2007a) found that these scour holes develop off the tips of the barbs. Scouring can however be attenuated by lowering the weir section of the barb in respect to bankfull depth (Matsuura & Townsend, 2004). Also, larger velocities near the bank may locally accentuate erosion. Although stream barbs do not break the helical flow, downwelling structures are stronger than without stream barbs but displaced near the channel center (Figure 4.4). This situation could lead to a reduction in the sediment migration rate towards the accumulation zone on the opposite bank (due to the absence of sediment to erode near

barbs) or it could initiate bed incision. However, stream barbs were found to have little impact on deposition along the inner bank (Minor et al., 2007b). Reducing barb spacing and installing vegetation on channel banks could help mitigating potential scour issues.

4.3.2. Bed weirs

According to the 3D flow hydraulics modelling results, the installation of V-shaped bed weirs in a straight reach of the Richer Stream near the urban area of Saint-Marc-sur-Richelieu is expected to improve channel stability. Flow realignment towards channel centre causes a reduction in near-bank and near-bed velocities. The examination of flow patterns around this type of weir using the 3D model SSIIM also revealed the existence of two near-surface merging velocity zones and of two oppositely-rotating secondary current cells (Bhuiyan & Hey, 2007). However, Bhuiyan and Hey (2007) found surface jet to extend further downstream with higher level of submergence, which is contradictory to what was found here: an increase in vertical flow constriction enhances the patterns associated with flow realignment. The analysis of the effects of straight weirs suggests that these structures are detrimental to the stability of the Richer channel due to flow deviation towards the left bank and due to increased near-bank velocities.

The zone located immediately downstream of each bed weir may require bed protection to ensure the stability of each instream structure. This downward flow deflection downstream of the weirs was also noted by Abad et al. (2008) after investigating the effects of bendway weirs using FLOW-3D.

River channelization was mainly undertaken to lower water table in adjacent fields to improve agricultural potential (Brookes, 1987). Since the top of each tested weir lies significantly below field elevation (i.e. weir height of 0.60 and 1.06 m compared to an average channel depth of 1.63 m), the installed structures are unlikely to affect root development in adjacent fields. For instance, yields of soybeans were found to be maximized at suitable water table level (70 cm and 40 cm depths, respectively for wet and dry years) that can be adjusted according to the amount of rainfall received (Shimada et al., 1995). Yield increases up to 6.9% and 37.3% (above free drainage values) were reported with water table level management for corn and soybeans, respectively (Mejia et al., 2000). The same study recommended a water table depth of 0.75 m for corn and soybean, two plants species widely used in the Richer watershed. If the weirs were to be raised further than in the simulations, an assessment of the effects of table rise on root development would be required.

Since field drainage systems are common in the Richer watershed, the impact of locally rising base flow stage (i.e. following the installation of bed weirs) would need to be investigated to make sure that the drainage is still efficient. The modification of drainage systems may increase the costs of this project whilst malfunctions in these systems may affect crop development.

Ecological effects

The straight and V-shaped weirs used in this study were designed so that they could easily be imported in the 3D numerical model. In reality, some modifications to weir thickness, orientation and shape may be desirable to ensure that these structures do not hinder fish migration. Fish passage over unnatural barriers depends on water depth and

velocity (upstream, throughout and downstream of the structure) and fish capabilities to swim and jump (Litvan et al., 2008). Although interspecies differences exist in athletic capabilities among fish species, all these aspects could potentially prevent passage over the employed weirs. Fish ladders are unlikely to ensure smooth fish passage under a range of flow conditions due to the prevailing low flow stage condition in the Richer Stream. Folded weirs were found to help achieving such objective compared to simple straight weirs (Bhuiyan & Hey, 2007). Similarly to vertically-placed screens that are used to dissipate energy below hydraulic structures (Bozkus et al., 2007), the concept of porosity could be incorporated in weir design to enable fish migration under any flow condition whilst ensuring that the weir provides enough flow constriction at medium to higher stages. Screens with a porosity of 40% were found to dissipate more energy than classical nonporous hydraulic jumps (Rajaratnam & Hurtig, 2000). A potential limitation to that solution could arise from infilling with bed material. Channel banks in the Richer Stream were found to be unstable with current steepness and vegetation assemblage (Rousseau & Biron, 2009), leading to bank collapse and the accumulation of bank material on the stream bed. A condition for these structures' suitability is the stabilisation of channel banks, which is partially achieved by the weirs. If efforts are placed on stabilising channel banks (i.e. by installing vegetation and using gentler bank slopes), bed weirs could promote bank stability whilst having only a small impact on fish species.

Bed weirs are also expected to create fish habitat by offering an artificial sequence of pools (before and after each weir) and riffles (over the weir and between two consecutive structures). Such features were found to improve habitat quality in a straightened channel (Rhoads et al., in press). Although a total recovery of the fish

community is unlikely without a true reconnection with the floodplain, the construction of deep pools is expected to make stream communities more similar to those in less degraded stream (Shields et al., 1998).

5.1. Introduction

As part of the CDAQ grant that funded this project, the company Parish Geomorphic Ltd. has produced a cost-benefit analysis for the methods that have undergone flow hydraulics modelling (i.e. installing stream barbs or V-shaped bed weirs) and hydro-morphological modelling (i.e. creating meanders or backwater ponds) (Tables 5.1 and 5.2). The simulated strategies are anticipated to improve channel stability or ecological habitat quality and diversity. Other approaches of bank stabilisation with vegetation and flow retention facilities are also evaluated due to their rising popularity in watershed management. Two additional strategies are evaluated as a comparison basis: 1) letting the stream evolve naturally whilst limiting intervention, and 2) dredging the channel every ten years to re-establish the desired dimensions.

Although several variations of each method exist (e.g. material, shape), the investigated methods adequately represent the main types of strategies used in modern restoration projects and in the management of highly modified channels. For instance, spur dikes and vanes are expected to necessitate similar building material and create a flow field similar to that resulting from the use of stream barbs: these structures all redirect the flow toward the center of a channel in a bend. Therefore, the effort was put on analysing methods that belong to different types of intervention.

In addition to evaluating the anticipated building costs, Parish Geomorphic Ltd. commented on the technical feasibility of some of the proposed methods using their expertise in river restoration planning and enhancement. Furthermore, they have quantified the environmental and cultural benefits at different temporal scales. An overall

W01 - Riparian buffer zone improvement

(A) Setback of cultivated area and subsequent planting of the riparian zone, including trees
(B) Setback of cultivated area and subsequent planting of the riparian zone, not including
(C) Setback of cultivated area and allowing natural regeneration

- Widening of riparian buffer strip over 5.5km to improve riparian vegetation structure and stabilize the
- Riparian strip of 15m on both banks.
- Straight planform of the river remains unaltered.

W02 - Remeandering

- Re-meandering of 5.5km of the channel to increase sinuosity to a value of 1.25 and reduce bed slope to 0.102% within an established river corridor.
- Could be combined with riparian buffer zone planting.
- Calculation of river corridor width : 45.6 m
  - Meander belt width : 33.0 m
  - Factor of safety (10% of belt width) : 6.6 m
  - 3m regulatory buffer (both banks) : 6m

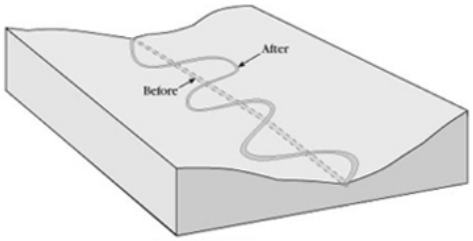

Source: NCHRP, 2005

W03 - Back water ponds

(A) 3 backwater ponds of 40,000 m2 each
(B) 6 backwater ponds of 20,000 m2 each
(C) 12 backwater ponds of 10,000 m2 each

- Addition of backwater, scrapes or floodplain marshes to reduce instream peak flows.
- May have various shapes, capacities and orientations.
- Pond depth is assumed to be equal to adjacent channel depth whilst shape is assumed circular.

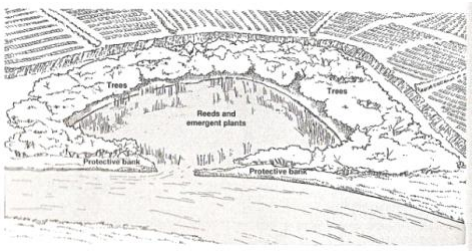

Source: Cowx and Welcomme, 1998

W04 - Multi-stage channel

- Creation of a low flow channel within a larger channel over 5.5km.
- Channel volume assumed to be 200% larger than original.
- Base-flow channel can actively meander within the larger channel.
- Higher discharges are held within the larger channel.

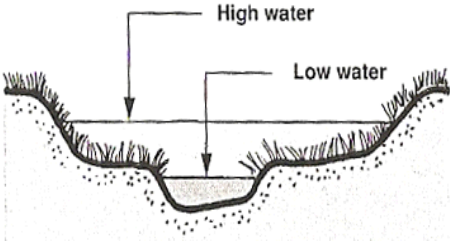

Source: Cowx and Welcomme, 1998

Table 5.1. Potential stabilisation solutions and sub-solutions applying to the watershed scale.

L01 - V-shaped weirs

- 4 weirs placed in a 320 m river reach located between two river bends north-east of St Marc-sur-Richelieu.
- Weir configuration:
  - Thickness: 2m thick in the center
  - Width: same as flow surface width
  - Height: 0.6 m or 1.06 m
  - Spacing: 50m between structures

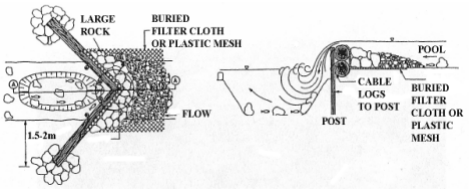

Source: Slaney and Zaldokas, 1997

L02 - Stream barbs

- 6 barbs installed in a 125° upstream bend of the urban area of Saint-Marc-sur-Richelieu.
- Barb dimensions :
  - Length : 4.5 m
  - Width : 40 cm
  - Height : 1.48 m near the outer bank (90% of bankfull depth)

Source: NCHRP, 2005

L03 - Newbury rock riffles

- 4 riffles placed in a 320 m river reach located between two river bends north-east of St Marc-sur-Richelieu.
- Dimensions :
  - Height : 0.6 m at crest with average thickness of 0.3 m.
  - Length : 6 m for the downstream face and 2m for the upstream with a total length of 8m.

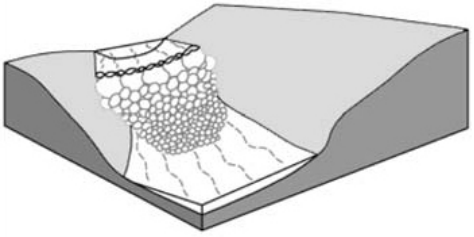

Source: NCHRP, 2005

L04 - Bank stabilisation

- Combined treatment of toe rip-rap, coir and plantings.
- Length of bank treatment between the two river bends north-east of St Marcsur-Richelieu : 320m

Table 5.2. Potential stabilisation solutions and sub-solutions applying to the reach scale.

assessment score is attributed to each method according to the following aspects and weights: technical effectiveness (50%), implementation costs (20%), secondary benefits (10%), ease of implementation (10%), and the timescale required for the achievement of benefits (10%).

5.2. Summary of the cost-benefit analysis

The results of the cost-benefit analysis produced by Parish Geomorphic Ltd. suggest that watershed scale solutions involving riparian buffer zone improvement are expected to provide more benefits than the other investigated solutions (Table 5.3, Figure 5.1). This is especially true for the natural regeneration approach which is cheaper although probably technically less effective than tree planting. The creation of backwater ponds and the creation of multi-stage channel have lower scores. Finally, dredging (which is the method currently employed to temporarily deal with bank instability issues) has the lowest score due to its failure to address the causes of instability and due to the homogenisation of channel morphology and flow conditions that it generates.

On a local scale, V-shaped weirs and Newbury rock riffles are attributed lower scores (Table 5.3). Both solutions contribute to diversifying flow patterns and channel morphology in the modified reach in addition to reducing near-bank velocities. Conversely, stream barbs have similar localized benefits on stability but provide little, if any habitat enhancement. Finally, bank stabilisation protects designated banks in a natural fashion. However, such a method is likely to require maintenance (i.e. supplemental costs) and trigger erosion on the opposite or adjacent bank.

From an economical perspective, riparian buffer zone improvement, the installation of hydraulic structures and dredging are the most affordable techniques when considering

Scale	Method	Overall score (of 5)
Watershed	W01c - Riparian buffer zone improvement - Natural regeneration	4.18
	W01a - Riparian buffer zone improvement - Including trees	4.00
	W02 - Re-meandering of river corridor	3.88
	W01b - Riparian buffer zone improvement - Not including trees	3.75
	W03a - Creation of backwater ponds - 3 x 40,000 m²	3.10
	W04 - Creation of multi-stage channel	3.00
	W03b - Creation of backwater ponds - 6 x 20,000 m²	2.93
	W03c - Creation of backwater ponds - 12 x 10,000 m²	2.75
	Dredging - Once every 10 years	1.60
Local	L01 - V-shaped weirs	3.60
	L03 - Newbury rock riffles	3.50
	L02 - Stream barbs	2.80
	L04 - Bank stabilisation	1.75

Table 5.3. Overall assessment scores of potential solutions (Parish Geomorphic Ltd., 2010).

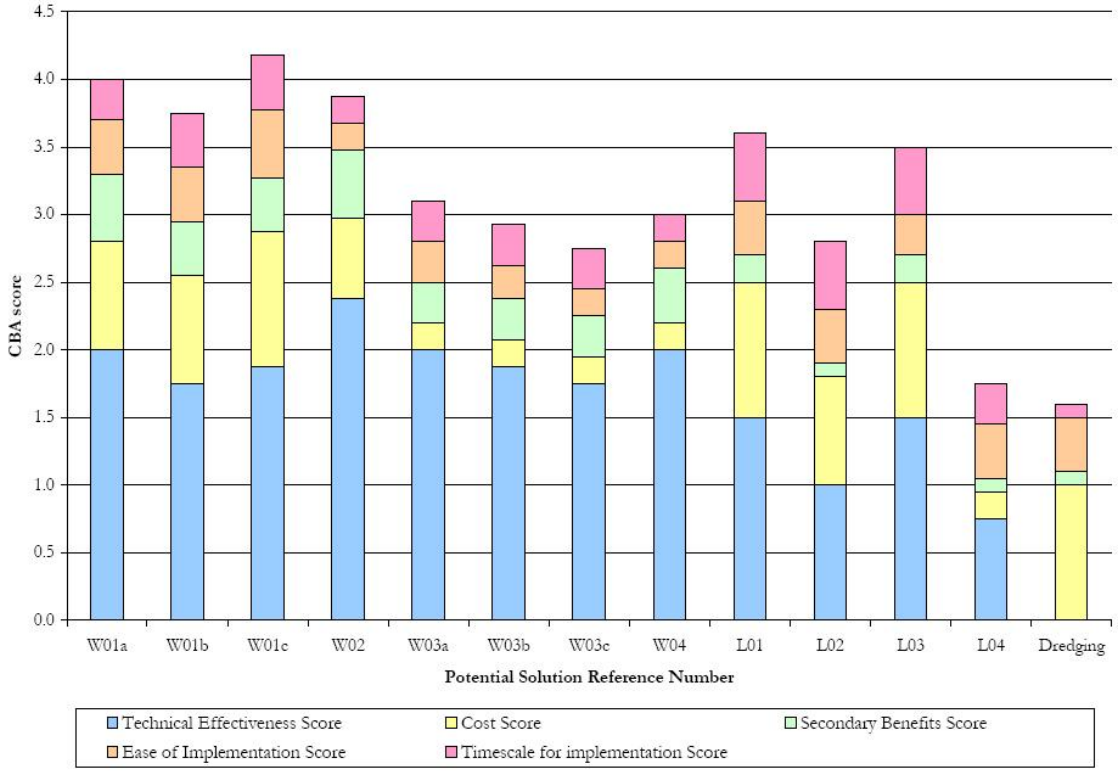

Figure 5.1. Assessment scores for each solution, per criterion (Parish Geomorphic Ltd., 2010).

the spatial extent to which they apply. Conversely, bank stabilisation with vegetation and the creation of backwater ponds or of a two-stage channel have lower cost effectiveness, as illustrated in the assessment score diagram (Figure 5.1).

5.3. Funding sources for restoration projects

Obtaining funding is a key step in river restoration and can alone decide on the degree of intervention (from emergency to preventive or enhancement actions) that is possible for a specific project. A review of the funding programs offered in Québec was undertaken to locate the existing sources within governmental agencies and other private organisations, understand the underlying conditions linked to their attribution, and determine the type of costs for which funding is available. The following organisations can financially support local initiatives: Fondation de la faune du Québec, Wildlife Habitat Canada, Ducks Unlimited, Conseil pour le développement de l'Agriculture au Québec (CDAQ), Ministère de l'Agriculture, des Pêcheries et de l'alimentation du Québec (MAPAQ), Financière agricole du Québec.

Although the eligibility conditions for financial support vary among the foundations and programs, there are however some trends. Many foundations are involved in wetland protection and habitat recovery but not necessarily in river rehabilitation. Fish habitat enhancement activities are usually well supported but they are often primarily intended to support fisheries activities which have significant economic benefits for some regions. Overall, smaller projects tend to receive more support.

Channel straightening and enlargement works have been undertaken in the 20th century to promote faster water evacuation from agricultural lands and to facilitate crop maintenance and harvest. Later, the installation of underground soil drainage networks further improved the drainage of fine-textured soils. Recent interventions in lowland watersheds near Montréal have largely focussed on solving local issues including bank collapse and bed incision rather than elaborating management plans at the watershed scale. The methods used to counter the natural tendency of a formally-meandering channel to redevelop a sinuous pattern after being straightened mainly include dredging and the installation of riprap on unstable banks. Although innovative solutions are sometimes employed in pilot projects, they remain only marginally used.

At the watershed scale, the hydro-morphological model predicts that the installation of backwater ponds and the creation of a sinuous layout would both significantly reduce stream power at bankfull stage. However, the cost-benefit analysis undertaken by Parish Geomorphic Ltd. suggests that any type of re-meandering solution would be more efficient than installing backwater ponds in reducing stream power when considering other aspects such as financial costs, implementation ease and environmental benefits.

At the local scale, the 3D hydrodynamic model was employed to test the impact on the flow field of implementing stream barbs in a bend and bed weirs in a straight reach. The simulations reveal that stream barbs reduce near-bank velocities on the outer side of the bend whereas V-shaped weirs appear efficient in reducing the magnitude of near-bank velocities in the straight reach. From a cost-benefit point of view, the V-shaped weirs however obtained a higher overall assessment score due to potential environmental

benefits derived from flow and morphological diversification.

In addition to river stability issues, the ecological impacts of various management strategies should be taken into account. For example, the water retention created by the weirs would provide greater volume of water for fish and possibility colder and more stable temperatures. If fish migration under any flow condition is a concern, a fish passage structure could be used, although it may require additional maintenance.

Farmers and agro-environmental consultants have put significant efforts in minimising fertilisation requirements. However, some of the chemicals are not entirely absorbed by crops and reach the hydrological network, leading to the spread of blue-green algae. The absence of intolerant and intermediately-tolerant fish species within the Richer Stream is a good indicator that habitat quality could be improved. The homogenisation of channel morphology and the destruction of habitat resulting from the recurrent dredging works are equally inefficient in stabilising the channel and fatal for intolerant fish species. The required costs of the current management strategy (even in the short term) in this watershed suggest that public money could be more efficiently spent.

The implementation of watershed scale solutions may appear as a move backwards, at a time when farming was difficult due to the presence of fine-textured soils (poor drainage) and complex river layout. However, since the underground drainage systems greatly improves soil drainage, a more natural layout with bends and backwater ponds appear as reasonable alternative management solutions. In zones that are highly sensitive, or where space requirements are not available (e.g. in the urban development zone), barbs and bed weirs would limit instability problems.

Although alternative approaches to channelization exist, there are currently some

limitations to the accuracy of the predictions associated with their implementation. The very limited number of published monitoring reports contributes to this source of uncertainty. Also, some hydraulic structures such as bed weirs were solely tested in flumes rather than in natural settings. Finally, the agricultural context is only one of several contexts in which a stabilisation approach can be applied. Simulation cases involving vegetation were found to be the most promising in the cost-benefit analysis with regards to their anticipated low level of maintenance and environmental benefits. Properly including the effects of vegetation in models remains, however, a challenge. Vegetation affects both the flow field and bank cohesiveness and stability, but the complexity of these physical processes precluded their inclusion in the model. More field measurements in straightened channels with both vegetated and unvegetated banks would be a first step in improving our understanding of these impacts, which could also be used to verify and validate a more powerful hydro-morphological model that would take vegetation into account.

Abad, J. D., Rhoads, B. L., Güneralp, I., & Garcia, M. H. (2008). Flow structure at different stages in a meander-bend with bendway weirs. *Journal of Hydraulic Engineering, 134*(8), 1052-1063.

Abam, T. K. S. (1995). Factors affecting performance of permeable groins in channel bank erosion control. *Environmental Geology*, *26*(1), 53-56.

Abernethy, B., & Rutherfurd, I. D. (1998). Where along a river's length will vegetation most effectively stabilise stream banks? *Geomorphology*, *23*(1), 55-75.

Abernethy, B. & Rutherfurd, I. D. (2000). The effect of riparian tree roots on the mass-stability of riverbanks. *Earth Surface Processes and Landforms, 25*(9), 921-937.

Abernethy, B. & Rutherfurd, I. D. (2001). The distribution and strength of riparian tree roots in relation to riverbank reinforcement. *Hydrological Processes, 15*(1), 63-79.

Ahn T.B., Cho S.D., & Yang S.C. (2002). Stabilisation of soil slope using geosynthetic mulching mat. *Geotextiles and Geomembranes. 20*(2), 135-146.

ArcGIS, version 9.2, ESRI, Redlands/CA/U.S.

Beaulieu, R. (2007). Historique de l'aménagement des cours d'eau (Stream developement history). Poster presented at l'Atelier de formation sur l'hydrodynamique, la biodiversité et la mise en valeur des cours d'eau agricoles (Training workshop on hydro-dynamics, biodiversity and agricultural stream developement), Drummondville, QC, Canada.

Beechie, T.J., Sear, D.A., Olden, J.D., Pess, G.R., Buffington, J.M., Moir, H., Roni, P. & Pollock, M.M. (2010). Process-based principles for restoring river ecosystems. *Bioscience*, *60*, 3, 209-222.

Bennett, S. J., Pirim, T., & Barkdoll, B. D. (2002). Using simulated emergent vegetation to alter stream flow direction within a straight experimental channel. *Geomorphology*, *44*, 115-126.

Bennett, S. J., Wu, W., Alonso, C. V., & Wang, S. S. Y. (2008). Modeling fluvial response to in-stream woody vegetation: implications for stream corridor restoration. *Earth Surface Processes and Landforms, 33*(6), 890-909.

Bernhardt, E.S., Palmer, M.A., Allan, J.D. Alexander, G. et al. (2005). *Synthesizing U.S. river restoration efforts. Science, 308*(5722), 636-637.

Bhuiyan, A. B. M. F. & Hey, R. (2007). Computation of three-dimensional flow field created by weir-type structures. *Engineering Applications of Computational Fluid Mechanics, 1*(4), 350-360.

Biron, P. M., Haltigin, T. W., & Hardy, R. J. (2007). Assessing different methods of generating a three-dimensional numerical mesh for a complex stream bed topography. *International Journal of Computational Fluid Dynamics, 21*(1), 37-47.

Biron, P. M., Robson, C., Lapointe, M. F., & Gaskin, S. J. (2004). Deflector designs for fish habitat restoration. *Environmental Management, 33*(1), 25-35.

Boutin, C., Jobin, B. & Bélanger, L. (2003). Importance of riparian habitats to flora conservation in farming landscapes of southern Québec, Canada. *Agriculture, Ecosystems & Environment, 94*(1), 73-87.

Bozkus, Z., Cakir, P., & Ger, A. M. (2007). Energy dissipation by vertically placed screens. *Canadian Journal of Civil Engineering, 34*(4), 557-564.

Bravard, J. P., Landon, N., Peiry, J. L, (1999). Principles of engineering geomorphology for managing channel erosion and bedload transport, examples from French rivers. *Geomorphology, 31*(1-4), 291-311.

Brent Council. (2010). *Brent River Park Regeneration Project.* Retrieved 11 April 2010 Brent website: http://www.brent.gov.uk/RiverBrent.nsf

Brookes, A. (1985). Downstream morphological consequences of river channelization in England and Wales. *The Geographical Journal, 151*(1), 57-62.

Brookes, A. (1987). Restoring the sinuosity of artificially straightened stream channels. *Environmental Geology and Water Sciences, 10*(1), 33-41.

Brookes, A. (1988). *Channelized rivers: perspectives for environmental management*. Chichester: Wiley.

Brookes, A. (1995). River channel restoration: Theory and practice. In: Gurnell, A. & Petts, G. E. (eds) *Changing River Channels*, John Wiley & Sons, Chichester, 369-388).

Brookes, A. & Sear, D.A. (1996). Geomorphological principles for restoring channels. In A. Brookes A. & Shields F. D (Eds.). *River channel restoration: Guiding principles for sustainable projects*. (pp. 75-101). Chichester, New York: J. Wiley.

Brookes, A. & Shields, F.D. Jr. (1996). River Channel Restoration: Guiding Principles for Sustainable Projects, John Wiley & Sons.

Brooks, S. S. & Lake, P. S. (2007). River restoration in Victoria, Australia: change is in the wind and none too soon. *Restoration Ecology, 15*(3), 584-591.

Campbell, K.L., Kumar, S., & Johnson, H.P. (1972) Stream straightening effects on flood-runoff characteristics. Trans. Am. Soc. Agric. Eng., 15, 94.

Canadian Climate Impact Scenarios. (2010). Retrieved 31 May 2010, from http://www.cics.uvic.ca/scenarios.

Canadian Climate Normals 1971-2000. (2010). *National Climate Data and Information Archives*. Retrieved 31 May 2010, from Environment Canada Web site: http://climate.weatheroffice.gc.ca/climate_normals/index_e.html.

Carline, R. F. & Walsh, M. C. (2007). Responses to riparian restoration in the Spring Creek watershed, Central Pennsylvania. *Restoration Ecology*, *15*(4), 731-742.

Chang, H. H. (1988). Fluvial Processes in River Engineering. Malabar, Florida: Krieger.

Chen, C.-N., Tsai, C.-H., & Tsai, C.-T. (2007). Reduction of discharge hydrograph and flood stage resulted from upstream detention ponds. *Hydrological Processes, 21*, 3492-3506.

Chow, V.T. (1959). *Open Channel Hydraulics.* New York: McGraw-Hill.

Chu-Agor, M.L., Wilson, G. V., & Fox, G. A. (2008). Numerical modeling of bank instability by seepage erosion undercutting of layered streambanks. *Journal of Hydrologic Engineering, 13*(12), 1133-1145.

Church, M. (1992) Channel morphology and typology. In Calow, P. & Petts,

G. E. (Eds.), *The river's handbook: Hydrological and ecological principles*.

Oxford, Blackwell, 126-143.

Coulthard, T. J. & Van De Wiel, M. J. (2006). A cellular model for river meandering. *Earth Surface Processes and Landforms, 31*, 123-132.

Cowx I.G. & Welcomme R.L. (1998). *Rehabilitation of rivers for fish*. Oxford, UK, Fishing News Books, Blackwell Science. 260 pp.

Darby, S. E., Van de Wiel, M. J. (2003). Models in fluvial geomorphology. In Kondolf, G. M. & Piégay, H. (Eds.), *Tools in fluvial geomorphology* (pp.503-537). New York: John Wiley & Sons.

D'Auteuil, C, & Dubois, J.-M.M. (1994). Érosion des berges et stabilisation par les végétaux (Erosion and bank stabilisation with vegetation). Département de géographie et télédétection, Université de Sherbrooke, Bulletin de recherché no. 113-114, 94 p.

Deletic, A. (2001). Modelling of water and sediment transport over grassed areas. *Journal of Hydrology, 248*, 168-182.

Dingman, S. L. (1984). *Fluvial hydrology*. New York: W. H. Freeman and Company.

El-Jabi, N., El-Kourdahi, G., & Caissie, D. (1995). Stochastic modeling of water temperatures in running waters. *Revue des sciences de l'eau, 8*, 77-95.

Fish base (2010). Retrieved 31 May 2010, from http://www.fishbase.org.

Fishes of Canada's National Capital Region. (2010). *Dictionary of Ichthyology*. Retrieved 31 May 2010, from http://www.briancoad.com.

Florsheim, J. L., Mount, J. F., & Chin, A. (2008). Bank erosion as a desirable attribute of rivers. *Bioscience, 58*(6), 519-529.

Fondation de la Faune du Québec (2010). Des actions pour la faune en milieu agricole : les habitats du poisson. Retrieved 14 July 2010, from http://www.fondationdelafaune.qc.ca/documents/File/FICHE_POISSONS.pdf.

Frothingham, K. M. (2008). Evaluation of stability threshold analysis as a cursory method of screening potential streambank stabilisation techniques. *Applied Geography, 28*(2), 124-133.

Frothingham, K.M., Rhoads, B.L., & Herricks, E.E. (2002). A multiscale conceptual framework for integrated ecogeomorphological research to support stream naturalisation in the agricultural Midwest. *Environmental Management, 29*(1), 16-33.

Garceau, S., Rioux, S., Letendre, M., & Chagnon, Y. (2007). Caractérisation du ruisseau Richer et de ses tributaires en fonction de la communauté ichtyologique (août 2006). Étude réalisée pour le compte du ministère des Ressources naturelles et de la Faune, Direction de l'aménagement de la faune de l'Estrie, de Montréal et de la Montérégie, Longueuil – Rapport technique 16-31, vi + 28 pages.

Géomont (2009). *Correlator 3D : une nouvelle technologie de modélisation de surface en support aux intervenants de la région (Correlator 3D: a new surface modelling technology to support local stakeholder)* [Brochure]. Belvisi, J.: Author.

Ghate, S. R., Burtle, G. J., Vellidis, G., & Newton, G. L. (1997). Effectiveness of grass strips to filter catfish (Ictalurus punctatus) pond effluent. *Aquacultural Engineering, 16*, 149-159.

Gu, R. C., Voegele, D. M., & Lohnes, R. A. (1999). Evaluation of stream grade control structures in loess soil region. *Journal of Hydraulic Engineering-ASCE, 125*(8), 882-885.

Gurnell, A. M., Morrissey, I. P., Boitsidis, A. J., Bark, T., Clifford, N. J., Petts, G. E., & Thompson, K. (2006). Initial adjustments within a new river channel: Interactions between fluvial processes, colonizing vegetation, and bank profile development. *Environmental Management, 38*, 580-596.

Haltigin, T.W., Biron, P.M. & Lapointe, M.F. (2007) Three-dimensional numerical simulation of flow around stream deflectors: The effects of obstruction angle and length. *Journal of Hydraulic Research, 45*(2), 227-238.

Hassett, B. A., Palmer, M. A., & Bernhardt, E. S. (2007). Evaluating stream restoration in the Chesapeake Bay Watershed through practitioner interviews. *Restoration Ecology, 15*(3), 563-572.

Hey, R. D. (1987). Regime stability. In Brandon TW (Ed.) *River Engineering*, *Part 1*, *Design Principles*, pp. 139-147. The Institution of Water and Environmental Management, London.

Hey, R. D. (1996). Environmentally sensitive river engineering. In Petts, G. E. & Calow, P. (Eds.), *River Restoration*. (pp. 80-105). Blackwell Science, Oxford, UK.

Hupp, C. R. (1992). Riparian vegetation recovery patterns following stream channelization: a geomorphic perspective. *Ecology, 73*(4), 1209-1226.

Hupp, C. R. & Osterkamp, W. R. (1996). Riparian vegetation and fluvial geomorphic processes. *Geomorphology, 14*(4), 277-295.

IPCC (Integovernmental Panel on Climate Change) (2010). The SRES emissions scenarios. Retrieved April 12, 2010 from IPCC Data Distribution Centre website: http://sedac.ciesin.columbia.edu/ddc/sres/.

Jamieson, E. C., Rennie, C. D., & Townsend, R. D. (2009). Design of stream barbs for field scale application at Sawmill Creek, Ottawa. *WIT Transactions on Ecology and Environment, 124*, 281-292.

Jia, Y., Scott, S., Xu, Y., Huang, S., & Wang, S. S. Y. (2005). Three-dimensional numerical simulation and analysis of flows around a submerged weir in a channel bendway. *Journal of Hydraulic Engineering, 131*(8), 682-693.

Jia, Y. & Wang, S. S. Y. (1999). Numerical model for channel flow and morphological change studies. *Journal of Hydraulic Engineering, 125*(9), 924-933.

Jueyi S., Daxian F., & Karney, B. W. (2006). An experimental study into local scour in a channel caused by a 90° bend. *Canadian Journal of Civil Engineering, 33*(7), 902-911.

Kline, M. & Cahoon, B. (2010). Protecting river corridors in Vermont. *Journal of the American Water Resources Association, 46* (2), 227-236

Knighton, A. D. (1998). *Fluvial Forms and Processes: A New Perspective*. London: Arnold.

Kondolf, G.M. & Yang, C.-N. (2008). Planning river restoration projects: social and cultural dimensions. In: *River Restoration: Managing the Uncertainty in Restoring Physical Habitat*, Darby, S.E. & Sear, D. (eds)., Wiley, 43-60.

Kuhnle, R., Alonso, C., & Shields, D., Jr. 1999. Geometry of scour holes associated with 90° spur dikes. *ASCE Journal of Hydraulic Engineering, 125*(9): 972–978.

Landwehr, K. & Rhoads, B. (2003). Depositional response of a headwater stream to channelization, East Central Illinois, USA. *River Research and Applications, 19*, 77-100.

Lane S. N., Ferguson, R. I. (2005). Modelling reach-scale fluvial flows. In *Computational Fluid Dynamics: Applications in Environmental Hydraulics*, Bates, P. D., Lane, S. N., & Ferguson, R. I. (eds). Wiley: New York; 217-269.

Larsen, E. W., Fremier, A. K., & Greco, S. E. (2006). Cumulative effective stream power and bank erosion on the Sacramento River, California, USA. *Journal of The American Water Resources Association, 42*(4), 1077-1097.

Lau, J. K., Lauer, T. E., & Weinman, M. L. (2006). Impacts of channelization on stream habitats and associated fish assemblages in East Central Indiana. *American Midland Naturalist, 156*(2), 319-330.

Li, M. H. (2006). Learning from streambank failures at bridge crossings: A biothechnical streambank stabilisation project in warm regions. *Landscape and Urban Planning, 77*(4), 343-358.

Licursi, M. & Gómez, N. (2009). Effects of dredging on benthic diatom assemblages in a lowland stream. *Journal of Environmental Management, 90*(2), 973-982.

Litvan, M. E., Pierce, C. L., Stewart, T. W., & Larson, C. J. (2008). Fish passage in a Western Iowa Stream modified by grade control structures. *North American Journal of Fisheries Management, 28*(5), 1384-1397.

Liu, Y. B., Gebremeskel, S., De Smedt, F., Hoffman, L., & Pfister, L. (2004). Simulation of flood reduction by natural river rehabilitation using a distributed hydrological model. *Hydrology and Earth System Sciences, 8*(6), 1129-1140.

Luppi, L., Rinaldi, M., Teruggi, L. B., Darby, S. E., & Nardi, L. (2009). Monitoring and numerical modelling of riverbank erosion processes: a case study along the Cecina River (central Italy). *Earth Surface Processes and Landforms, 34*, 530-546.

MacWilliams, M.L., Wheaton, J.M., Pasternack, G.B., Kitanidis, P.K., & Street, R.L. (2006). The flow convergence-routing hypothesis for riffle-pool maintenance in alluvial rivers. *Water Resources Research, 42*, W10427.

Malkinson, D. & Wittenberg, L. (2007). Scaling the effects of riparian vegetation on cross-sectional characteristics of ephemeral mountain streams; a case study of Nahal Oren, Mt. Carmel, Israel. *Catena, 69*(2), 103-110.

Mathier, L., Roy, A. G., & Paré, J. P. (1989). The effect of slope gradient and length on the parameters of a sediment transport-equation for sheetwash. *Catena, 16*(6), 545-558.

Matsuura, T., & Townsend, R. (2004). Stream-barb installations for narrow channel bends - a laboratory study. *Canadian Journal of Civil Engineering, 31*(3), 478-486.

Mejia, M. N., Madramootoo, C. A., & Broughton, R. S. (2000). Influence of water table management on corn and soybean yields. *Agricultural Water Management, 46*(1), 73-89.

Mendrop, K. B. & Little, C. D. (1997). *Grade stabilisation requirements for incised channels*. Proceedings of Conference on Water Management of Landscapes Distributed by Channel Incision, Oxford, Mississippi, 1997. (The Center for Computational Hydroscience and Engineering, Univ. of Mississippi).

Micheli, E. R., Kirchner, J. W., & Larsen, E. W. (2004). Quantifying the effect of riparian forest versus agricultural vegetation on river meander migration rates, Central Sacramento River, California, USA. *River Research and Applications, 20*(5), 537-548.

Millar R. G. (2000). Influence of bank vegetation on alluvial channel patterns. *Water Resources Research, 36*(4) 1109-1118).

Ministry of Agriculture, Food and Fisheries (2001). Historique des travaux de drainage au Québec et état du réseau hydrographique (Historical aspects of drainage works and state of the hydrographic network in Québec) (Publication no. 6211-12-007). Sainte-Martine, QC: Robert Beaulieu.

Ministry of Agriculture, Food and Fisheries (2009). Étang épurateur et régulateur de l'eau en milieu agricole. Direction régionale du centre du Québec: Savoie, V., Chrétien, F., & Desmarais, C.

Ministry of Natural Resources and Fauna, Direction of Fauna Planning of Eastern Township, Montréal and Montérégie (2007). Caractérisation du ruisseau Richer et de ses tributaires en fonction de la communauté ichtyologique (août 2006) (Characterisation of Richer watercourse as a function of the ichthyologic community (August 2006)) (Technical report no. 16-31). Longueuil, QC, Canada : Garceau, S., Rioux, S., Letendre, M., & Chagnon, Y.

Minor, B., Jamieson, E., Rennie, C. D., & Townsend, R. D. (2007b). Three-dimensional flow in a barb field. *WIT Transactions on Ecology and the Environment, 104*, 371-380.

Minor, B., Rennie, C. D., & Townsend, R. D. (2007a). "Barbs" for river bend bank protection: application of a three-dimensional numerical model. *Can. J. Civ. Eng., 34*, 1087-1095.

MNRF (Ministry of Natural Resources and Fauna). (2008). Le PCHE au Québec : Bilan 1987-2007. Québec, QC: Michel Lepage and Normand Traversy.

Montgomery, D. R. & Piégay, H. (2003). Wood in rivers: interactions with channel morphology and processes. *Geomorphology, 51*(1-3), 1-5.

Morris S., & Moses T. (1998). *Channel and streambank stabilisation in a steep colluvial valley, Lake Oswego, Oregon*. Proceedings of the winning solutions for risky problems, Conference 29, Reno, 1998. (International Erosion Control Association). 367-371.

Mutz, M., Piégay, H., Gregory, K.J., Borchardt, D., Reich, M., & Schmieder, K. (2006). Perception and evaluation of dead wood in streams and rivers by German students. *Limnologica, 36*(2), 110-118.

National Research Council. (1992). Restoration of aquatic ecosystems: science, technology, and public policy. Washington, DC, USA: National Academy Press.

NCHRP (National Cooperative Highway Research Program). (2005). Environmentally sensitive channel- and bank-protection measures (Report no. 544). Washington, DC: McCullah J. and Gray D.

Newbury, R. & Gaboury, M. N. (1993). Stream analysis and fish habitat design: a field manual. *Newbury Hydraulics*.

Nielsen, M. B. (1996). Lowland stream restoration in Denmark. In Brookes, A. & Shields, F. D. (Eds.), *River channel restoration: Guiding principles for sustainable projects* (pp.269-289). Chichester, England: John Wiley & Sons.

Ouillon, S. & Dartus, D. (1997). Three-dimensional computation of flow around groyne. *Journal of hydraulic Engineering-ASCE, 123*(11), 962-970.

Pagliara, S. & Chiavaccini, P. (2006). Energy dissipation on reinforced block ramps. *Journal of Irrigation & Drainage Engineering, 132*(3), 293-297.

Paice, C. and Hey, R.D. (1989). Hydraulic control of secondary circulation in meander bend to reduce outer bank erosion. In Albertson, M.L. and Kia, R.A. (Eds), *Design of hydraulic structures*. Balkema, Rotterdam, 249-254.

Parish Geomorphic Ltd. (2010). Richer Stream - Cost-Benefit Analysis, Report to Concordia University, July 2010, 27 pp.

Phoenics, version 5.8, CHAM, Wimbledon Village/London/UK.

Piégay, H., Darby, S. E., Mosselman, E., & Surian, N. (2005a). A review of techniques available for delimiting the erodible river corridor: a sustainable approach to managing bank erosion. *River Research and Applications, 21*(7), 773-789.

Piégay, H., Gregory, K. J., Bondarev, V., Chin, A., Dalhstrom, N., Elosegi, A., et al. (2005b). Public perception as a barrier to introducing wood in rivers for restoration purposes. *Environmental Management, 36/5*, 665–674.

Pollen, N. (2007). Temporal and spatial variability in root reinforcement of streambanks: Accounting for soil shear strength and moisture. *Catena, 69*(3), 197-205.

Practical Action Nepal (2007). Spurs and dykes for flood water protection. *Appropriate Technology, 34*(2), 34-37.

Rajaratnam, N. & Hurtig, K. I. (2000). Screen-type energy dissipator for hydraulic structures. *Journal of Hydraulic Engineering-Asce, 126*(4), 310-312.

Ramanujan, S. (1914). Modular equations and approximations to π. *Quarterly Journal of Pure and Applied Mathematics, 45*, 350–372.

Raupach, M. R., Marland, G., Ciais, P., Le Quéré, C., Canadell, J. G., Klepper, G., & Field, C. B., 2007. Global and regional drivers of accelerating CO2 emissions. *Proc. Natl. Acad. Sci. U.S.A. 104*(24): 10288–10293. doi:10.1073.

Rey, F. et al. (2004). Role of vegetation in protection against surface hydric erosion. *C. R. Geoscience, 336*(11), 991-998.

Rhoads, B. L, Engel, F. L., & Abad, J. D. (in press). Geomorphologically based design for naturalizing straight stream channels. In *Stream Restoration in Dynamic Fluvial Systems: Scientific Approaches, Analyses, and Tools.* A. Simon, S. J. Bennett, J. M. Castro, and C. Thorne (eds.). AGU Monograph.

Rhoads, B. L. & Herricks, E. E. (1996). Naturalisation of Headwater Streams in Illinois: Challenges and Possibilities. In Brookes, A. & Shields, F.D. (Eds.), *River channel restoration: Guiding principles for sustainable projects*. (pp. 331-367). Chichester, New York: J. Wiley.

Rhoads, B. L., Schwartz, J. S. & Porter, S. (2003). Stream geomorphology, bank vegetation, and three-dimensional habitat hydraulics for fish in midwestern agricultural streams. *Water Resources Research, 39*:1218, doi:10.1029.

Rinaldi, M., Casagli, N., Dapporto, S., & Gargini, A. (2004). Monitoring and modelling of pore water pressure changes and riverbank stability during flow events. *Earth Surface Processes and Landforms, 29*, 237-254.

Rodriguez, J. F., Bombardelli, F. A., & Garcia, M. H. (2004). High-resolution numerical simulation of flow through a highly sinuous river reach. *Water Resources Management, 18*(3), 177-199.

Roth, T. R., Westhoff, M. C., Huwald, H., Huff, J. A., Rubin, J. F., Barrenetxea, G., Vetterli, M., Parriaux, A., Selker, J. S., & Parlange, M. B. (2010). Stream temperature response to three riparian vegetation scenarios by use of a distributed temperature validated model. *Environ. Sci. Technol., 44*, 2072-2078.

Rousseau, A. N., Mailhot, A., Turcotte, R., Duchemin, M., Blanchette, C., Roux, M., Etong, N., Dupont, J., & Villeneuve, J.-P. (2000). GIBSI - An integrated modelling system prototype for river basin management. *Hydrobiologia, 422*, 465-475.

Rousseau, Y. (2008). Modelling sediment transport in a small straightened agricultural watershed, southwestern Québec. *Final paper in the course GEOG 498 - Environmental Modeling, Department of Geography, Planning and Environment, Concordia University*.

Rousseau, Y. & Biron, P. M. (2009). Geomorphological impacts of channel straightening in an agricultural watershed, Southwestern Québec. *The Northeastern Geographer, 1*, 91-113.

Sawyer, A. M., Pasternack, G. B., Moir, H. J., & Fulton, A. A. (2010). Riffle-pool maintenance and flow convergence routing observed on a large gravel-bed river. *Geomorphology, 114,* 143-160.

Scheumann, W. & Freisem, C. (2002). The role of drainage for sustainable agriculture. *Journal of Applied Irrigation Science, 37*(1), 33-61.

Scholz, M. (2007). Expert system outline for the classification of sustainable flood retention basins (SFRBs). *Civil Engineering and Environmental Systems, 24*(3), 193-209.

Schultz, R. C., Colletti, J. P., Isenhart, T. M., Simpkins, W. W., Mize, C. W., & Thompson, M. L. (1995). Design and placement of a multispecies riparian buffer strip system. *Agroforestry Systems, 29*(3), 201-226.

Schumm, S.A. (1977). *The Fluvial System.* New York, NY: Wiley-Interscience.

Schwartz, J. S. & Herricks, E. E. (2007). Evaluation of pool-riffle naturalisation structures on habitat complexity and the fish community in an urban Illinois stream. *River Research and Applications, 23*(4), 451-466.

Scobey, F.C. (1933). The flow of water in flumes. U.S. Department of Agriculture, Technical Bulletin 393.

Sear, D.A. (1996). The sediment system and channel stability. In: Brookes, A. & Shields, F.D. Jr. (Eds) *River Channel Restoration: Guiding Principles for Sustainable Projects,* John Wiley & Sons, 149-177.

Shields, F. D., Copeland, R. R., Klingeman, P. C., Doyle, M. W., & Simon, A. (2003). Design for stream restoration. *Journal of Hydraulic Engineering, 129*(8), 575.

Shields, F. D., Knight, S. S., & Cooper, C. M. (1998). Rehabilitation of aquatic habitats in warmwater streams damaged by channel incision in Mississippi. *Hydrobiologia, 382,* 63-86.

Shields, F. D., Lizotte, R. E. J., Knight, S. S., Cooper, C. M., & Wilcox, D. (2010). The stream channel incision syndrome and water quality. *Ecological engineering, 36,* 78-90.

Shields, F. D. & Rigby, J. R. (2005). River habitat quality from river velocities measured using acoustic Doppler current profiler. *Environmental Management, 36,* 4, 565-575.

Shih, H. M. & Yang, C. T. (2009). Estimating overland flow erosion capacity using unit stream power. *International Journal of Sediment Research, 24*(1), 46-62.

Shimada, S., Kokubun, M., & Matsui, S. (1995). Effects of water-table on physiological traits and yield of soybean. 1. Effects of water-table and rainfall on leaf chlorophyll content, root-growth and yield. *Japanese Journal of Crop Science, 64*(2), 294-303.

Simon, A. (1989). A model of channel response in disturbed alluvial channels. *Earth Surface Processes and Landforms, 14*, 11-26.

Simon, A., Bennett, S. J., & Neary, V. S. (2004). Riparian vegetation and fluvial geomorphology: Problems and opportunities. In Bennett, S. J. & Simon, A. (Eds.), *Riparian vegetation and fluvial geomorphology* (pp.1-10). Washington, DC: American Geophysical Union.

Simon, A. & Collison, A. J. C. (2002). Quantifying the mechanical and hydrologic effects of riparian vegetation on streambank stability. *Earth Surface Processes and Landforms*, *27*, 527-546.

Simon, A., Curini, A., Darby, S. E., & Langendoen, E. J. (2000). Bank and near-bank processes in an incised channel. *Geomorphology, 35*(3-4), 193-217.

Simon, A. & Darby, S. E. (2002). Effectiveness of grade-control structures in reducing erosion along incised river channels the case of Hotophia Creek Mississippi. *Geomorphology*, *42*(3-4), 229-254.

Simon, A., Langendoen, E. J., & Thomas, R. (2003). *Incorporating bank-toe erosion by hydraulic shear into a bank-stability model: Missouri River, Eastern Montana*. Proceedings of World Water & Environmental Resources Congress, Honolulu, Hawaii, 2003. (EWRI-ASCE).

Simon, A., Pollen, N. & Langendoen, E. (2006). Influence of two woody riparian species on critical conditions for streambank stability; Upper Trukee River, California. *Journal of The American Water Resources Association, 42*(1), 99-113.

Simon, A. & Rinaldi, R. (2006). Disturbance, stream incision, and channel evolution: The roles of excess transport capacity and boundary materials in controlling channel response. *Geomorphology, 79*(3-4), 361-383.

Simons, D.B. & Richardson, E.V. (1966). Physiographic and hydraulic studies of rivers: resistance to flow in alluvial channels. *U. S. Geological Survey,* Prof. Pap. 422-J.

Skaggs, R. W., Brevé, M. A., & Gilliam, J. W. (1994). Hydrologic and water quality impacts of agricultural drainage. *Critical Reviews in Environmental Science and Technology, 24*(1), 1-32.

Slaney, P.A. & Zaldokas, D. (1997). Fish Habitat Rehabilitation Procedures (Watershed Restoration Technical Circular No. 9). Ministry of the Environment, Vancouver, BC.

Spackman, S. C., & Hughes, J. W. (1995). Assessment of minimum stream corridor width for biological conservation: Species richness and distribution along mid-order streams in vermont, USA. *Biological Conservation, 71*(3), 325-332.

Stacey, M., & Rutherfurd, I. (2007). Testing specific stream power thresholds of channel stability with GIS. *Proceedings of the 5th Australian Stream Management Conference. Australian rivers: making a difference*. Charles Sturt University, Thurgoona, New South Wales.

Stefanovic, J. R. & Bryan, R. B. (2009). Flow energy and channel adjustments in rills developed in loamy sand and sandy loam soils. *Earth Surface Processes and Landforms, 34,* 133-144.

Stella, version 9, ISEE Systems, Lebanon/NH/U.S.

Sudduth, E. B. & Meyer, J. L. (2006). Effects of bioengineering streambank stabilisation on bank habitat and macroinvertebrate in urban streams. *Environmental Management, 38*(2), 218-226.

Surian, N. & Rinaldi, M. (2003). Morphological response to river engineering and management in alluvial channels in Italy. *Geomorphology, 50,* 307–326.

Thompson D. M. (2006). Did the pre-1980 use of in-stream structures improve streams? A reanalysis of historical data. *Ecological Applications, 16*(2), 784-796.

Thompson D. M, & Stull G. N. (2002). The development and historic use of habitat structures in channel restoration in the United States: The grand experiment in fisheries management. *Géographie physique et Quaternaire*, *56*(1), 45-60.

Tilman, D. (2000). Causes, consequences and ethics of biodiversity. *Nature, 405*(6783), 208-211.

Toth, L. A. (1996). Restoring the Hydrogeomorphology of the Channelized Kissimmee River. In Brookes, A., Shields, F.D. (Eds.), *River Channel Restoration: Guiding Principles for Sustainable Projects*. (pp. 369-383). Chichester, New York: J. Wiley.

Trenhaile, A. S. (2007). Geomorphology: a Canadian Perspective, 3rd ed. Don Mills, Ontario: Oxford University Press.

Van De Wiel, M. J., Coulthard, T. J., Macklin, M. G., & Lewin, J. (2007). Embedding reach-scale fluvial dynamics within the CAESAR cellular automaton landscape evolution model. *Geomorphology, 90,* 283-301.

Van De Wiel, M. J., & Darby, S. E. (2004). Numerical modeling of bed topography and bank erosion along tree-lined meandering rivers. In Bennett, S. J. & Simon, A. (Eds.), *Riparian vegetation and fluvial geomorphology* (pp.267-282). Washington, DC: American Geophysical Union.

Vermont Agency of Natural Resources, Department of Environmental Conservation (2010). A Guide to river Corridor Easements. Mike Kline.

Wu, W. M., Shields, F. D., Bennett, S. J., & Wang, S. S. Y. (2005). A depth-averaged two-dimensional model for flow, sediment transport, and bed topography in curved channels with riparian vegetation. *Water Resources Research, 41*(3), W03015.

Wyzga, B. (2001). A geomorphologist's criticism of the engineering approach to channelization of gravel-bed rivers: Case study of the Raba River, Polish Carpathians. *Environmental Management, 28*(3), 341-358.

Yeh, S.-C., Wang, C.-A., & Yu, H.-C. (2006). Simulation of soil erosion and nutrient impact using an integrated system dynamics model in a watershed in Taiwan. *Environmental Modelling & Software, 21*, 937-948.

Zawiejska, J. & Wyzga, B. (2010). Twentieth-century channel change on the Dunajec River, southern Poland: Patterns, causes and controls. *Geomorphology, 117,* 234-246.

Appendix A - Specifications of the hydro-morphological model

A.1. Overview

The current section technically describes the hydro-morphological model. It was developed in Stella in 2008 (and converted into a Java standalone application in 2010) to predict sediment transport rates and the location of accumulation/erosion zones for various watershed configuration schemes involving channel morphology, planform or vegetation cover alteration and for various climate change scenarios. The model is composed of three modules dealing with climatologic, hydrological, and sediment transport physical processes. The model was developed to use few variables and to require climatic / weather data that are available online at no cost. The *National Climate Data and Information Archive from Environment Canada* was used to parameterize and calibrate the hydro-morphological model. Two sections of this online database are particularly relevant to this model: (1) *Climate Data Online* and (2) *Climate Normals & Averages*. The first section provides historical weather conditions for the major weather stations in Canada whereas the second section displays climate statistics for an extended number of stations.

Running modes

The model can either run under historical or randomly-generated conditions. In the random mode, atmospheric conditions are generated based on climate statistics available from any weather station. Instream flow conditions are predicted for a specific section of the river, based on the amount of precipitation received in the previous days. Flow discharge is then calculated for each section and is a function of the area contributing to the flow observed at the section for which the discharge is evaluated.

Channel morphology and morphodynamism

The channel is defined as a series of interconnected trapezoidal sections in which each section empties both liquid and solid discharges in the adjacent downstream section. Each section has unique length, bed width, depth, bank angles, bed slope, sinuosity and floodplain characteristics (average depth and slope). Channel morphological adjustments are a function of the sign and magnitude of the imbalance between the sediments entering and leaving a section. Here, bank failure mechanisms are simplified in the following manner. If the volume of sediments entering a section is larger than the volume leaving it, the sediments uniformly accumulate on the bed. Otherwise, the bed erodes until its width is equal to zero, after which the steepest bank erodes.

A.2. The weather generator

The input parameters required by the weather generator (with the exception of precipitation depth) are generated from monthly climatic averages. Daily wind speed, snow depth, relative humidity and atmospheric pressure are simply interpolated from monthly values. However, the air is assumed to be saturated during precipitation events. Snow depth is only required the first day of simulation; in any other day, it must be consistent with antecedent snow depth and daily snowmelt, sublimation and snowfall. Daily average atmospheric temperature is generated from the climatic average value and its standard deviation. Minimum / maximum daily temperatures are adjusted using the difference between monthly average and minimum / maximum temperatures. Minimum and maximum temperatures are assumed to occur at the same hour every day.

Since temperature varies during the day and that certain processes depends on its

value, namely the type of precipitation and evaporation, the model splits each day in numerous parts (2 to 6 parts, in which the conditions are assumed to be constant) depending on the range of temperatures encountered during the day. For instance, a complex situation can result from a range of temperatures including both positive and negative values (Figure A.1).

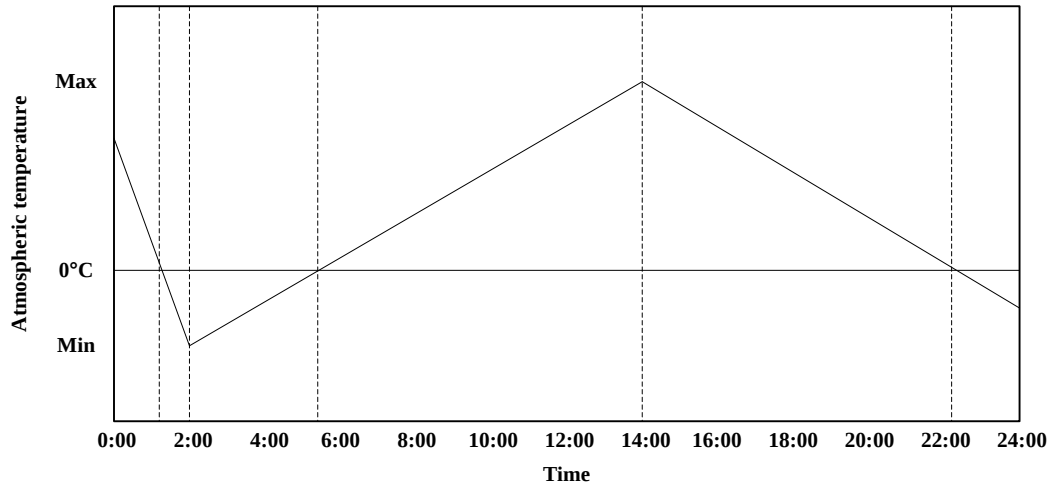

Figure A.1. Division of a single day as a function of atmospheric temperature extremes and of the temperature at 0:00 and 24:00.

Stream water temperature

Maximum daily stream water temperature is predicted using the atmospheric temperature of a certain day of the year and the normal water temperature for the same day and the two previous days. The normal trend in water temperatures (referred below as the annual component) is described by a combination of Fourier and Sine functions whereas the short-term departures from normal values are predicted using a second order Marcow process (Caissie et al., 2001). The residual of air temperature Ra_{jd} (departure from normal temperature) is given by:

$$Ra_{jd} = Ta_{jd,simulated} - Ta_{jd,normal} \qquad \textit{(Equation A.1)}$$

where $Ta_{jd,simulated}$ and $Ta_{jd,normal}$ are the modeled and normal air temperatures for the Julian day *jd*, respectively. The current residual of water temperature Rw_{jd} is given by:

$$Rw_{jd} = A_{jd-1} \cdot Rw_{jd-1} + A_{jd-2} \cdot Rw_{jd-2} + k \cdot Ra \qquad \textit{(Equation A.2)}$$

where R_1, R_2 and k are constants and:

$$Rw_{jd-1} = Tw_{jd-1,simulated} - Tw_{jd-1,annual\_component} \qquad \textit{(Equation A.3a)}$$

$$Rw_{jd-2} = Tw_{jd-2,simulated} - Tw_{jd-2,annual\_component} \qquad \textit{(Equation A.3b)}$$

$$A_{jd-1} = \frac{R_{jd-1} \cdot \left(1 - R_{jd-2}\right)}{1 - R_{jd-1}^2} \qquad \textit{(Equation A.4)}$$

$$A_{jd-2} = \frac{R_{jd-2} - R_{jd-1}^2}{1 - R_{jd-1}^2} \qquad \textit{(Equation A.5)}$$

The predicted water temperature $Tw_{jd,simulated}$ is then given by:

$$Tw_{jd,simulated} = Tw_{jd,annual\_component} - Rw_{jd} \qquad \textit{(Equation A.6)}$$

where the annual component of water temperature $Tw_{jd,annual\_component}$ is given by:

$$Tw_{jd,annual\_component} = a + b \cdot \sin\theta \qquad \textit{(Equation A.7)}$$

where a and b are constants and θ is the position associated with the day *jd* within the annual component of water temperature (in radians) :

$$\theta = \frac{2 \cdot \pi}{365} \cdot \left(jd - 1 + t_0\right) \qquad \textit{(Equation A.8)}$$

where and t_0 is a constant. The value of each coefficient used was determined for the Richer watershed by minimizing the root-mean square error between predicted and actual values for all days comprised in the historical dataset. The optimal values are R_1=0.507; R_2=0.183; k=0.312, a=9.10, b=11.03 and t_0=-114.20. The curves of actual and predicted water temperatures are provided in Figure A.2.

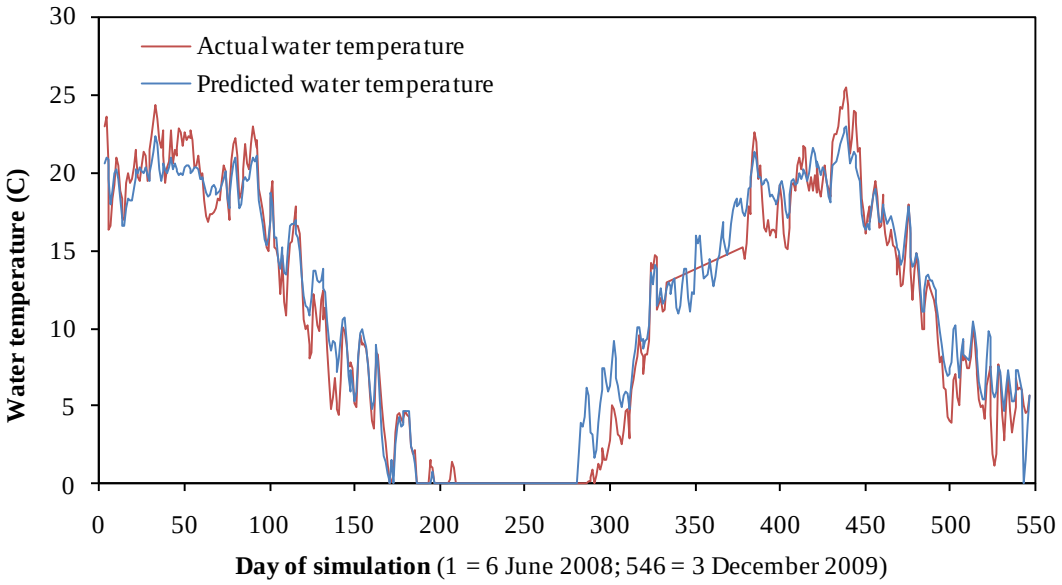

Figure A.2. Historical and predicted water temperature in the Richer Stream between 6 June 2008 and 3 December 2009 after Marcow chain analysis.

A.3. The hydrological module

The hydrological processes included in the current version of the model are transpiration, evaporation, sublimation, snow melt, and strem flow. Evapotranspiration is calculated using three different equations to account for the monthly variations in the vegetation cover. Two assumptions were made. Firstly, vegetation is present only during the summer months in the agricultural fields. Secondly, crops are always harvested before snow begins to fall. In the months were no vegetation is present and the soil is not frozen, a simple evaporation equation is used. When vegetation is absent but the soil is frozen, a sublimation equation is used. When vegetation is present, an evapotranspiration equation is used. The current section details the required equations for the three cases.

Cloud cover and precipitation

The approach followed to generate cloud cover and precipitation depth, duration and start time reflects the irregular character of precipitation events. Firstly, a precipitation

index (with a value between 0 and 1) is generated to influence the degree of cloudiness and the amount of precipitation received. An index of 1 involves a low cloud cover without any precipitation whereas an index of 0 translates in a dense cloud cover and heavy precipitation. Note that cloudiness also affects the proportion of solar radiation reaching the ground and therefore influences the evapotranspiration rate. Cloudiness is solved considering the number of daylight hours, the precipitation index and the normal proportion of hours with low (0 to 25%, average of 12.5%), medium (25 to 75%, average of 50%) and high (75 to 100%, average of 87.5%) cloud cover for the current month. The following equations are solved:

$$H_{total} = H_{low,i} + H_{medium,i} + H_{high,i} \qquad \textit{(Equation A.9)}$$

$$C \cdot H_{total} = 0.125 \cdot H_{low,i} + 0.500 \cdot H_{medium,i} + 0.875 \cdot H_{high,i} \qquad \textit{(Equation A.10)}$$

$$C = 1 - I_p \qquad \textit{(Equation A.11)}$$

$$R_1 = H_{medium,monthly} / H_{low,monthly} \qquad \textit{(Equation A.12a)}$$

$$R_2 = H_{high,monthly} / H_{low,monthly} \qquad \textit{(Equation A.12b)}$$

$$R_3 = H_{high,monthly} / H_{medium,monthly} \qquad \textit{(Equation A.12c)}$$

where H_{total} is the number of daylight hours and $H_{low,i}$, $H_{medium,i}$ and $H_{high,i}$ are the calculated number of hours with low, medium and high cloud cover, respectively during daylight for the solution $1 \leq i \leq 3$. $H_{low,monthly}$, $H_{medium,monthly}$ and $H_{high,monthly}$ are the monthly number of hours with low, medium and high cloud cover. Cloudiness C is a function of the precipitation index I_p. Equations A.12a-c are used to respect the proportions between the expected type of cloud cover according to monthly statistics. Then:

$$H_{low} = \frac{\sum_{i=1}^{3} H_{low,i}}{n} \qquad \textit{(Equation A.13a)}$$

$$H_{medium} = \frac{\sum_{i=1}^{3} H_{medium,i}}{n} \qquad \textit{(Equation A.13b)}$$

$$H_{high} = \frac{\sum_{i=1}^{3} H_{high,i}}{n} \qquad \textit{(Equation A.13c)}$$

where n is the number of possible solutions. H_{low}, H_{medium} and H_{high} are the predicted number of hours with a low, medium and high cloud cover, respectively for the precipitation index I_p.

Precipitation depth, duration and scheduling

Precipitation depth, duration and start time are randomly generated from the precipitation index. The distribution of precipitation intensity is well represented by a two-part gamma function, applying either to the lower or higher range of *fx* values. Duration is represented by a single part. The gamma function is given by:

$$fx = x'^{(k-1)} \cdot \frac{e^{-x'/\theta}}{\theta^k \cdot (k-1)!} \cdot k_{fx} + \Delta_{fx} \qquad \textit{(Equation A.14)}$$

$$x' = x \cdot k_x + \Delta_x \qquad \textit{(Equation A.15)}$$

where k and θ describe the shape and scale of the curve ($\geq$1), respectively. The variables k_x, k_y, Δ_x and Δ_{fx} are used to adjust further the shape and scale of the curve with historical values. The variable *fx* is the dimensionless magnitude of the variable of interest (a value between 0 and 1), i.e. precipitation intensity or duration with x being the value associated with this magnitude. Using the data interpolated from five weather stations near the Richer watershed, the following coefficients were used to fit the duration curve: θ=1.0; k=1.0; k_x=7.25; Δ_x=1.5; k_{fx}=173.130905; Δ_{fx}=-0.027435; fx_{max}=34.0; x_{max}=1.0. The following coefficients were used to represent the upper range of *fx* values (equal to 0.008100) for

precipitation intensity: θ=1.6; k=1.08; k_x=12.1527; Δ_x=0.1; k_{fx}=0.445795; Δ_{fx}=0.0075. The following coefficients were used to represent the lower range of *fx* values for precipitation intensity: θ=4.0; k=1.0; k_x=4.131; Δ_x=0.4; k_{fx}=0.083641; Δ_{fx}=0.00003. However, in both cases fx_{max}=0.193232 and x_{max}=735.68. The gamma curves resulting from these coefficients are shown in Figure A.3. Note that these dimensionless curves may apply to other watersheds if they are subject to similar climate conditions.

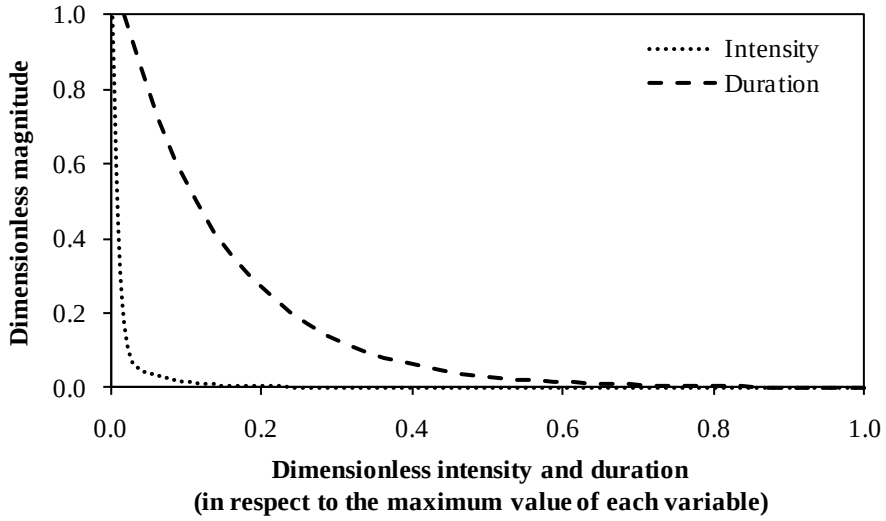

Figure A.3. Gamma curves illustrating the relationship between dimensionless magnitude and dimensionless precipitation intensity or duration using the historical data available at five weather stations located near the Richer Stream, Saint-Marc-sur-Richelieu, Québec: Trudeau Airport (Montréal), Natural Gault Reserve (St. Hilaire), Ste. Madelaine, St. Antoine and St. Amable.

Precipitation occurs only if C_{rand} (a randomly generated value between 0 and 1) is greater than 1 - k_{prec} (the yearly proportion of days with precipitation). If such is the case, the dimensionless magnitude of duration is given by:

$$fx_{duration} = \frac{C_{rand} - (1 - k_{prec})}{k_{prec}} \qquad \textit{(Equation A.16)}$$

The duration of precipitation $x_{duration}$ is found by solving Equations A.6 and A.7 for *x*. The magnitude of precipitation intensity $fx_{intensity}$ is given by:

$$fx_{intensity} = C_{rand} \cdot fx_{intensity,max} \qquad \textit{(Equation A.17)}$$

where $fx_{intensity,max}$ is the maximum precipitation intensity. Precipitation intensity $x_{intensity}$ is found by solving Equations A.14 and A.15 for x. The right set of coefficients must be selected in order to perform the calculation using the right gamma curve. Precipitation depth is found by multiplying $x_{intensity}$ and $x_{duration}$. The time at which precipitation H_{start} starts is given by:

$$H_{start} = C_{rand} \cdot (1 - x_{duration}) \qquad \textit{(Equation A.18)}$$

where $x_{duration}$ is in days, i.e. a value between 0 and 1. The end time H_{end} is found by summing H_{start} and $x_{duration}$.

The type of precipitation (rain and snow are considered in the model) is determined using from the current temperature value. Rain or snow applies to temperatures above or below 0°C, respectively. Fresh snow is assumed to have a density of 10% that of liquid water.

Snow compaction

The logic and equations related to snow melt are based on the work of Bertle (1966) that examined the effect of snow compaction processes on runoff with or without the addition of water. According to these laboratory experiments a snowpack will produce a runoff only if its density increases up to a threshold value of dpt=40%. The density can increase after the addition of water from rainfall or snowmelt. The first step consists in determining the threshold amount of water that will initiate runoff if added to a snowpack. The threshold depth PDt (in % of initial value) is given by:

$$PDt = \frac{147.4 \cdot ds_{init}}{ds_{init} + 0.474 \cdot dpt} \qquad \textit{(Equation A.19)}$$

where ds_{init} is the initial snowpack density (%). The threshold accumulated water content *PWt* (in% of initial value) is then given by:

$$PWt = \frac{PDt - 147.4}{-0.474} \qquad \textit{(Equation A.20)}$$

The threshold amount of added water is:

$$Wt_{added} = \frac{PWt}{100} \cdot W_{init} - W_{init} \qquad \textit{(Equation A.21)}$$

where W_{init} is the water equivalent depth of the snowpack, given by:

$$W_{init} = D_{init} \cdot ds_{init} \qquad \textit{(Equation A.22)}$$

where D_{init} is the initial snowpack depth.

If the amount of water added to the snowpack (W_{added}) is more important than the threshold value (Wt_{added}), water will drain from the snowpack and density of the snowpack will be equal to *dpt*. The amount lost (W_{drain}) is given by:

$$W_{drain} = W_{added} - Wt_{added} \qquad \textit{(Equation A.23)}$$

and the new snowpack depth D_{new} by:

$$D_{new} = \frac{PDt}{100} \cdot D_{init} \qquad \textit{(Equation A.24)}$$

If the amount of added water is lower than the threshold value, no water will drain from the snowpack. However, snowpack properties will change. The new accumulated water content (% of initial value) is:

$$PW = \frac{W_{init} + W_{added}}{W_{added}} \cdot 100 \qquad \textit{(Equation A.25)}$$

The new snowpack depth is:

$$D_{new} = \frac{D_{init} \cdot \left(147.4 - 0.474 \cdot PW\right)}{100} \qquad \textit{(Equation A.26)}$$

and the new snowpack density is:

$$ds_{new} = \frac{W_{init} + W_{added}}{D_{new}} \cdot 100 \qquad \textit{(Equation A.27)}$$

Evaporation and sublimation

The evaporation rate is given by:

$$ET = SVP \cdot \sqrt{\frac{M_w}{2 \cdot \pi \cdot R \cdot T}} \qquad \textit{(Equation A.28)}$$

where *ET* is the evaporation rate [kg/(m²·s)], *SVP* is the saturated vapour pressure [Pa] at temperature *T* [K], M_W is the molecular weight of water [0.018 (kg/mol)], and *R* is the universal gas constant [8.314 J/(mol·K)] (Estermann, 1955; Bohren and Albrecht, 1998, p. 187f.; Andreas, 2007). In the case of the evaporation rate, the Goff equation (1957) can be used to calculate vapour pressure over water:

$$\begin{aligned} &Log(SVP_w) = \\ &10.79574 \cdot (1 - 273.16/T) - 5.02800 \cdot Log(T/273.16) \\ &+ 1.50475 \cdot 10^{-4} \cdot \left(1 - 10^{(-8.2969(T/273.16-1))} - 1\right) \\ &+ 0.42873 \cdot 10^{-3} \cdot \left(10^{(4.76955(1-273.16/T))} - 1\right) + 0.78614 \end{aligned} \qquad \textit{(Equation A.29)}$$

where *T* is the temperature [K] and SVP_w is the saturated vapour pressure over water [hPa]. In the case of the sublimation rate, the Goff-Gratch equation (Smithsonian, 1984) can be used to calculate vapour pressure over ice:

$$\begin{aligned} &Log(SVP_i) = -9.09718 \cdot (273.16/T - 1) - 3.56654 \cdot Log(273.16/T) \\ &+ 0.876793 \cdot (1 - T/273.16) + Log(6.1071) \end{aligned} \qquad \textit{(Equation A.30)}$$

where *T* is the temperature [K] and SVP_i is the saturated vapour pressure over ice [hPa].

Evapotranspiration

The Penman-Monteith equation (Monteith & Unsworth, 1990) is used to calculate the evapotranspiration rate:

$$ET = \frac{S_{vpf} - (R_n - \Delta Hsoil) + \frac{(L_d * VPD * C_{va})}{r_a}}{S_{vpf} + \gamma * (1 + \frac{r_c}{r_a})} \qquad \textit{(Equation A.31)}$$

where ET is the evapotranspiration rate [cm/(m²·day)], S_{vpf} is the slope of vapour pressure function [kPa/˚C], R_n is the net solar radiation [MJ/(day·m²)], $\Delta H_{soil} = R_n \cdot 0.1$ is the soil heat flux [(MJ·day)/m²], L_d is the day length [hr], *VPD* is the vapour pressure deficit [kPa], C_{va} is the volumetric capacity of the air [0.0012 MJ/(m³·˚C)], γ is the psychometric constant [kPa/˚C], r_c is the reference canopy resistance to vapour transfer [day/m], and r_a is the aerodynamics resistance to vapour transfer [day/m]. The psychometric constant is given by:

$$\gamma = \frac{C_p \cdot P}{0.622 \cdot \lambda} \qquad \textit{(Equation A.32)}$$

where C_p is the specific heat of air [MJ/(kg·˚C)], *P* is the atmospheric pressure [kPa], and λ is the latent heat of vaporisation [2.26 MJ/kg]. The slope of the vapour pressure function [kPa/˚C] is given by:

$$S_{vpf} = \frac{SVP_{Tavg} \cdot 4098}{(T_{avg} + 237.3)^2} \qquad \textit{(Equation A.33)}$$

where $SVP_{T_{avg}}$ is the saturated vapour pressure at T_{avg}, the average daily temperature [˚C]. The saturated vapour pressure is calculated using Equation A.29 or A.30.

Net solar radiation

The following procedure calculated the net solar radiation using basic weather parameters such as temperature, latitude, Julian day, and vapour pressure at dew point. All

equations in this section (except those specified) are derived from a sample procedure used by the Sevier River Water Users Association (2008) to compute net radiation (2008). The net solar radiation [MJ/(day·m²)] is given by:

$$R_n = 0.77 \cdot R_s - R_{nl} \qquad \textit{(Equation A.34)}$$

where R_s is the measured shortwave radiation [MJ/(day·m²)] and R_{nl} is the net incoming longwave radiation [MJ/(day·m²)]. In the absence of field data, shortwave radiation may be derived from temperature data:

$$R_s = KT \cdot R_a \cdot \sqrt{T_{\max} - T_{\min}} \qquad \textit{(Equation A.35)}$$

where R_a is the extra-terrestrial radiation [MJ/(day·m²)], $T_{\max}$ is the maximum daily temperature [˚C], and $T_{\min}$ is the minimum daily temperature [˚C] (Hargreaves, G.H. & Samani Z.A., 1982). The extra-terrestrial radiation can be estimated using:

$$R_a = \frac{24 \cdot 60}{\pi} \cdot G_{sc} \cdot d_r \cdot \left[\omega_{sha} \cdot \sin\varphi \cdot \sin\delta + \cos\varphi \cdot \cos\delta \cdot \sin\omega_{sha}\right] \qquad \textit{(Equation A.36)}$$

where G_{sc} is the solar constant [0.082 MJ/(day·m²)], d_r is the inverse relative distance Earth-Sun [dimensionless], ω_{sha} is the sunset hour angle [rad], φ is the latitude [rad], δ is the solar declination [rad]. The inverse relative distance Earth-Sun and the solar declination can be calculated from

$$d_r = 1 + 0.033 \cdot \cos\left(\frac{J}{365} \cdot 2 \cdot \pi\right) \qquad \textit{(Equation A.37)}$$

$$\delta = 0.409 \cdot \sin\left(\frac{J}{365} \cdot 2 \cdot \pi - 1.39\right) \qquad \textit{(Equation A.38)}$$

where *J* is the Julian day. The sunset hour angle is given by:

$$\omega_{sha} = \arccos\left(-\tan\varphi \cdot \tan\delta\right) \qquad \textit{(Equation A.39)}$$

The net incoming longwave radiation is given by:

$$R_{nl} = \sigma \cdot \left[\frac{T_{\max} + T_{\min}}{2} \right] \cdot \left(0.34 - 0.14 \cdot \sqrt{e_a}\right) \cdot \left(1.35 \cdot \frac{R_s}{R_{s0}} - 0.35\right) \qquad \textit{(Equation A.40)}$$

where σ is the Stefan-Boltzman constant [$4.903 \cdot 10^{-9}\ MJ/(m^2 \cdot K^4)$], $T_{\max}$ is the daily maximum temperature [K], $T_{\min}$ is the daily minimum temperature [K], e_a is the vapour pressure at dew point [kPa], and R_{s0} is the clear sky-day shortwave radiation [MJ/(day·m²)] . The clear sky-day shortwave radiation is given by:

$$R_{s0} = \left(0.75 + 2 \cdot 10^{-5} \cdot z\right) \cdot R_a \qquad \textit{(Equation A.41)}$$

where *z* is the site elevation [m] and R_a is the extra-terrestrial radiation [MJ/(day·m²)]. The vapour pressure at dew point [kPa] is given by equation A.3 or A.4.

$$VP_{T_{dew}} = \frac{e^{T_{\min}} \cdot \left(RH_{\max}/100\right) + e^{T_{\max}} \cdot \left(RH_{\min}/100\right)}{2} \qquad \textit{(Equation A.42)}$$

where $T_{\min}$ is the minimum daily temperature [K], $T_{\max}$ is the maximum daily temperature [K], $RH_{\min}$ is the minimum daily relative humidity (%), and $RH_{\max}$ is the maximum daily relative humidity (%).

Snow melt

The relationship between the air temperature and snow melt is given by:

$$M = 0.45 \cdot T_{avg} \qquad \textit{(Equation A.43)}$$

where *M* is the amount of snow melt [mm/day] and T_{avg} is the average daily temperature [˚C] (Haith, 1985). The assumptions were made that snow compaction does not occur and that 1 cm of snow is equivalent to 1 mm of water.

Flow discharge

The model predicts the maximum daily flow discharge based upon daily precipitation depths received in the ten previous days. A rainfall score (*S*) is attributed to the amount of rain received by giving greater importance to recent days:

$$S = \sum_{jd=0}^{jd-10} \left(R_{jd} \cdot W_{jd} \right) \qquad \textit{(Equation A.44)}$$

where R_{jd} is the rainfall depth for the Julian day *jd* and W_{jd} is the weight attributed to this day. The following weights were used to calibrate the model for the Richer Stream (starting with the current day): 1.00, 1.00, 1.00, 0.90, 0.48, 0.00, 0.00, 0.00, 0.00, 0.00 and 0.00. This means that most of the weight is attributed to the rainfall depth received during the current day and the three previous days. The peak discharge reached in the Richer Stream in a day (m^3/s) is then given by:

$$Q_{peak} = Q_b + \frac{Q_\Delta + c}{d} \qquad \textit{(Equation A.45)}$$

$$Q_\Delta = a \cdot e^{b \cdot S} \qquad \textit{(Equation A.46)}$$

where a=0.0070, b=0.1100, c=-0.0031, d=0.8872, Q_b is flow discharge before the increase and Q_Δ is the increase in discharge due to rainfall. The value of each coefficient was obtained by minimizing the coefficient of determination in the curve of historical Q_{peak} as a function of *S*. A total of 26 events were used, which produced a r^2 value of 0.98 (Figure A.4a). This procedure is able to accurately predict peak discharge values with a minimal amount of data (Figure A.4b).

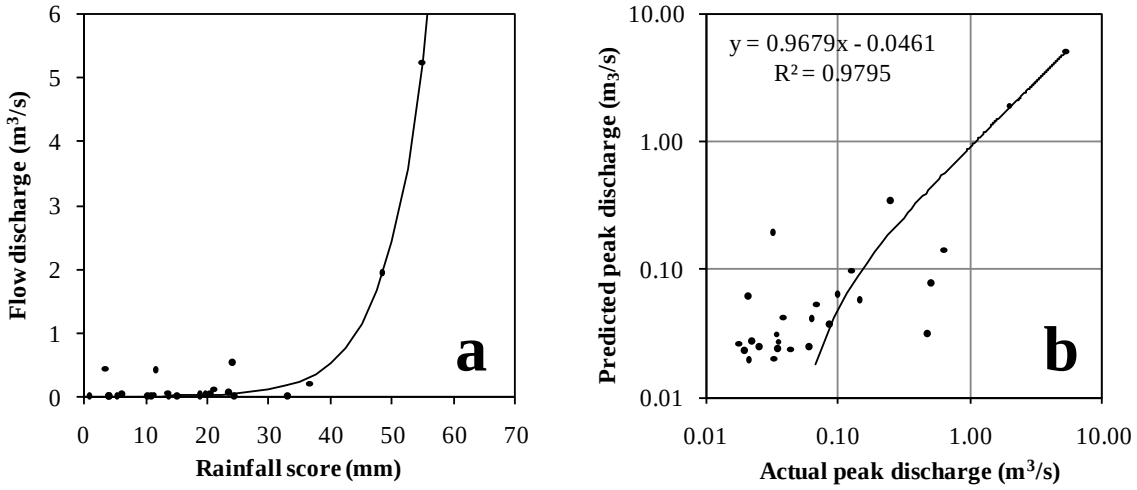

Figure A.4. (a) Relationship between flow discharge and rainfall score. (b) Predicted versus actual peak discharge for 26 events.

The rate of decrease of flow discharge was determined from 25 event hydrographs. A two-part regression equation fits well the data. The equations are given by:

$$Q = 10 \cdot e^{-135 t_{high}^{0.9117}} \qquad Q \geq 0.1 \text{ m}^3\text{/s}, \; r^2 = 0.999 \qquad \textit{(Equation A.47a)}$$

$$Q = 0.1 - 0.1 \cdot e^{-0.79 t_{low}^{-0.5421}} \qquad Q < 0.1 \text{ m}^3\text{/s}, \; r^2 = 0.994 \qquad \textit{(Equation A.47b)}$$

where t_{high} is the time required (in hours) for the discharge to fall from 10.0 m^3/s to a specific discharge above 0.1 m^3/s and t_{low} is the time required for a discharge below 0.1 m^3/s to fall to a lower specific discharge.

To simplify the hydrograph, it is assumed that the maximum discharge in a day occurs at the beginning of the day (0:00) whereas the minimum discharge happens at the end of the day (24:00). Predicted flow discharges are closer to reality from April to July 2009 and from October to December 2009. Although the predicted flow discharges are lower than the historical values in August and September 2009, encountered values were relatively small (below 0.3 m^3/s). The effect of snowmelt is badly predicted in February and March 2009, possibly due to surface runoff over a frozen soil. The predicted values

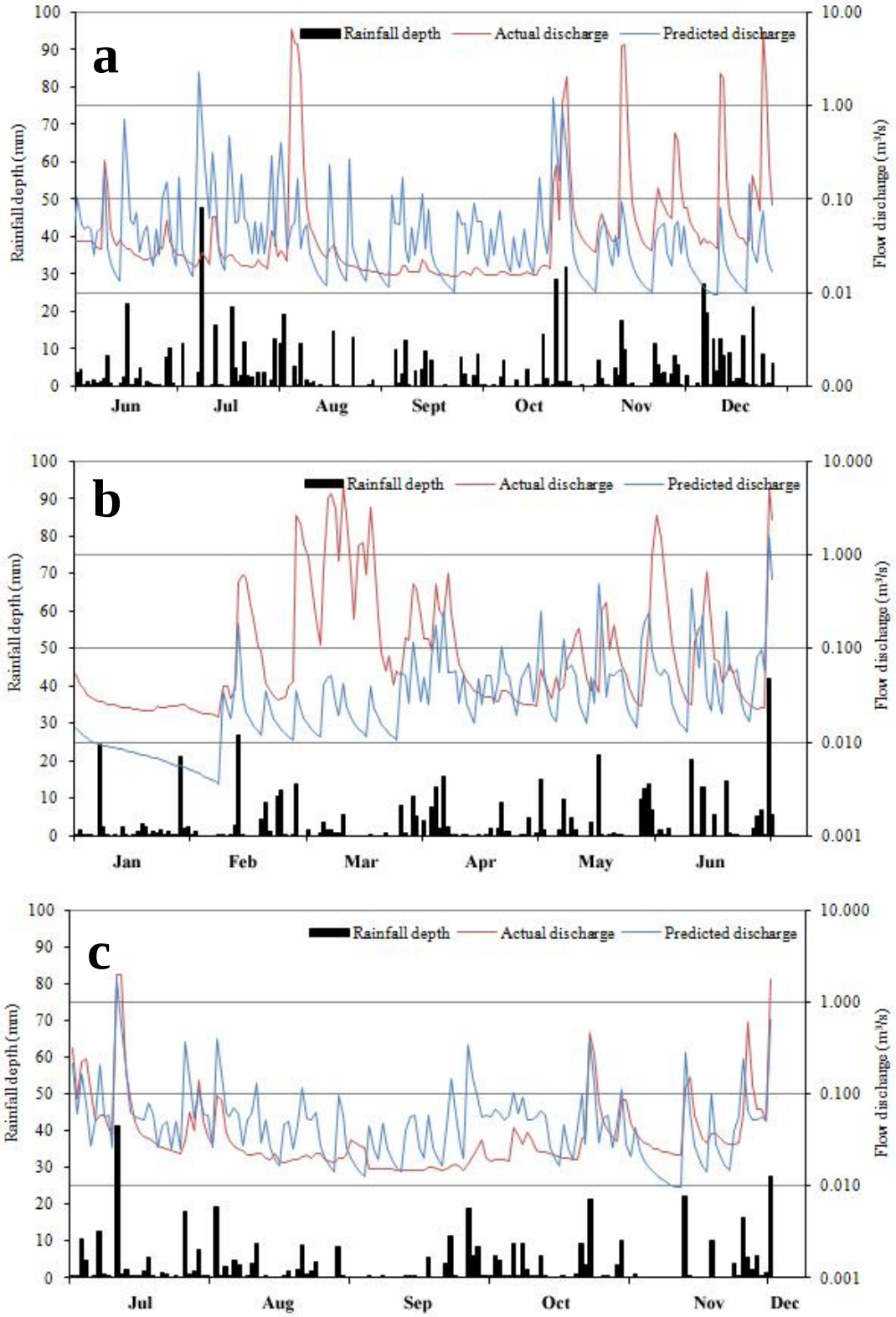

Figure A.5. Historical flow discharge, predicted flow discharge and precipitation depth in (a) 2008 and in (b-c) 2009 on the Richer watershed.

are far from historical values, with the exception of the successfully predicted peak discharge encountered in October. This situation may be explained by the availability of precipitation data closer to the Richer watershed in 2009. This also suggests that local precipitation events significantly influence stream hydrology.

The predicted flow discharge is only valid at the location of the gauging station that recorded flow depth. In order to estimate flow discharge for upstream or downstream channel sections, it is necessary to establish a relationship between the distance D_i from the head of the river to the section i and the area A_i responsible for the flow observed at section i. In the case of the Richer Stream, the equation is given by:

$$A_i = 0.0016 \cdot D_i + 7.4831 \qquad r^2=0.99 \qquad \textit{(Equation A.48)}$$

where A_i is in km^2 and D_i is m. The discharge at section j is given by:

$$Q_j = Q_i \cdot \frac{A_j}{A_i} \qquad \textit{(Equation A.49)}$$

Hydraulic conditions

The formula of flow discharge Q is given by:

$$Q = V \cdot A \qquad \textit{(Equation A.50)}$$

where V is flow velocity and A is the cross-sectional area that the flow occupies. Flow velocity [m/s] is calculated with the Manning equation:

$$V = \frac{R^{2/3} \cdot S_0^{1/2}}{n} \qquad \textit{(Equation A.51)}$$

where R is the hydraulic radius [m], S_0 is the flow surface slope (estimated with bed slope) [1] and n is Manning roughness coefficient [1]. The hydraulic radius is given by:

$$R = \frac{A}{P} \qquad \textit{(Equation A.52)}$$

where A is the cross-sectional area occupied by the flow and P is the wetted perimeter. Using trigonometry, the cross-sectional area A and wetted perimeter P of a trapezoidal channel are given by:

$$A = B_{bed} \cdot Y - \frac{Y^2}{2 \cdot \tan\theta_{left}} - \frac{Y^2}{2 \cdot \tan\theta_{right}} \qquad \textit{(Equation A.53)}$$

$$P = 2 \cdot B_{bed} + Y \cdot \left(\frac{1}{\sin\theta_{left}} + \frac{1}{\sin\theta_{right}} + \frac{1}{\cos\theta_{left}} + \frac{1}{\cos\theta_{right}} \right) \qquad \textit{(Equation A.54)}$$

where B_{bed} is the channel bed width, Y is the flow depth and θ_{left} and θ_{right} are the bank angles in degrees. The Manning roughness coefficient of the Richer channel (a relatively straight channel with a clay bed whose banks are covered with grass species) is a function of the channel depth:

$$n = Y_{n_{\max}} \cdot Y^{\alpha} \cdot e^{((1-a)\alpha)} \cdot \beta + n_{\min} \qquad \textit{(Equation A.55)}$$

where $a=Y/\ Y_{n,max}$ is the relative flow depth compared to the channel depth in a particular section. For the Richer Stream, $Y_{n,max}$ =0.19. If Y is lower than $Y_{n,max}$, α=1.1 and β=0.75. Otherwise, α=5.2 and β=0.672.

The unit stream power Ω [W/m^2] is calculated using the following formula:

$$\Omega = \frac{Q \cdot S \cdot g \cdot \rho_t}{B_{surface}} \qquad \textit{(Equation A.56)}$$

where Q is flow discharge [m^3/s], S is the bed slope [1], g is the acceleration due to gravity [m/s2], ρ is flow mass density at temperature t and $B_{surface}$ is surface flow width [m]. Bed shear stress τ_0 [N/m^2] is given by:

$$\tau_0 = \rho \cdot g \cdot R \cdot S_0 \qquad \textit{(Equation A.57)}$$

where R is the hydraulic radius [m] and S_0 is the flow surface slope.

A.4. The sediment transport module

In this module, sediment transport was divided into two categories: overland and instream transport. The instream sediment transport can be divided in deposition and entrainment. The summation of those three processes gives the net change in channel volume.

Channel cross-sectional area

The difference between deposition and entrainment rates modifies the channel cross-sectional area, thus the amount of water that can flow in the channel. In the current model, the channel was assumed to erode and aggrade uniformly while the banks keeping a stable angle to simplify calculations. This assumption is inexact since erosion dominates in the upper part of the banks and deposition dominates in the lower part. The new dimensions were then calculated based upon the change in the channel cross-sectional area, and assuming that the total channel width would remain stable over time.

Overland transport

Potential overland transport of sediment was estimated using the universal soil loss equation (Wischmeier & Smith, 1965). The main equation is given by

$$SRO_{potential} = R \cdot K \cdot L_s \cdot C \cdot P \qquad \textit{(Equation A.58)}$$

where $SRO_{potential}$ is the rate of sediment runoff [t/ha], R is the rainfall erosivity factor [N/hr], K is the soil erodibility factor [(t/ha)/(N/hr)], L_s is the slope length-gradient factor, C is the crop / vegetation / management factor and P is the support practice factor. Due to the lack of field data about runoff, the basic rainfall erosivity factor was used although Hann et al. (1994) suggested that using it could lead to errors. A value of 90 was attributed

to this factor (same as Ottawa, Ontario) due to the absence this information for Québec cities (Stone, 2007). The slope length-gradient factor is given by:

$$L_s = \left(0.045 \cdot X_i\right)^b \cdot \left(65.41 \cdot \sin^2 \theta_i + 4.565 \cdot \sin \theta_i + 0.065\right) \quad \textit{(Equation A.59)}$$

where X_i is the horizontal projected length of runoff [m] and θ_i is the slope angle of the drainage basin [rad]. Assuming p_{sk} to be the slope angle in degrees, the coefficient *b* is equal to 0.2 if $p_{sk} < 1$, 0.3 if $1 < p_{sk} < 3$, 0.4 if $3 < p_{sk} < 5$, and 0.5 if $p_{sk} \geq 5$. The amount of sediment actually delivered to the stream by the overland flow is estimated using:

$$SRO_{actual} = SRO_{potential} \cdot SDR \quad \textit{(Equation A.60)}$$

$$SDR = 0.4724A^{-0.125} \quad \textit{(Equation A.61)}$$

where *SDR* is the sediment delivery ratio from Vanoni (1975) equation, and *A* is the drainage area [mi²] (Lim et al., 2005).

Instream sediment entrainment rate

The entrainment rate can be calculated using

$$q_{se} = 0.008\sqrt{sgd}\left[0.14\frac{\rho}{\rho_s}\left(14\sqrt{\tau_*} - \frac{0.9}{\sqrt{\tau_*}}\right) - \frac{\omega_w}{\sqrt{sgd}}\right] \quad \textit{(Equation A.62)}$$

where q_{se} is the deposition rate [m³/s], *s* is the sediment specific gravity defined by $\left(\rho_s - \rho\right)/\rho$, ρ_s is the sediment mass density [km/m³], ρ is the water mass density [km/m³], *g* is the acceleration due to gravity [m/s²], *d* is the sediment mean diameter [m], $\tau_* = \mu^2/\left(s \cdot g \cdot d\right)$ is a dimensionless bed shear stress, and ω_s is the fall velocity [m/s] (Itakura & Kishi, 1980). Stoke's law describes the fall velocity as:

$$\omega_s = \frac{(\rho_s - \rho) \cdot g \cdot d^2}{18 \cdot \mu} \qquad \textit{(Equation A.63)}$$

where $\mu = \sqrt{\tau_0 / \rho}$ is the shear velocity [m/s] and τ_0 is the bed shear stress.

Instream sediment deposition rate

The deposition rate can be calculated using

$$q_{sd} = \omega_s \cdot C_a \qquad \textit{(Equation A.64)}$$

where q_{sd} is the deposition rate [m³/s], ω_s is the sediment fall velocity [m/s] and C_a is volumetric concentration of sediment near channel bed (Itakura & Kishi, 1980). The former can be calculated using Stoke's law while the later can be defined as:

$$C_a = C \cdot \frac{P_\varepsilon}{(1 - e^{-P_\varepsilon})} \qquad \textit{(Equation A.65)}$$

where C is the concentration of suspended sediment at 0.05 depth from channel bed and P_ε is the Peclet's number defined as:

$$P_\varepsilon = \frac{\omega_s \cdot Y}{\varepsilon} \qquad \textit{(Equation A.66)}$$

where ω_s is the sediment fall velocity, Y is the flow depth [m], and ε is the vortex viscosity factor that is defined by:

$$\varepsilon = \frac{k \cdot \mu_* \cdot Y}{6} \qquad \textit{(Equation A.67)}$$

where k is the Von Karman constant (0.4), μ_* is the shear velocity [m/s], and Y is the flow depth [m].

Instream bedload transport

Bedload transport is calculated using Shen and Hung (1972) since this formula can be used for flume and small natural rivers with silt and clay beds, but was more specifically designed for the Niobrara and Middle Loup Rivers. These two rivers drain a sandy agricultural area of Nebraska (Shen & Wang, 1979). The Middle Loup River is a tributary of the Loups River whereas the Niobraraer is a tributary of the Missouri River. The bedload is then the difference between total load and suspended load. Shen and Hung bedload formula is given by:

$$\log C_{ppm} = 109{,}503.872 \cdot Sh^3 - 326{,}309.589 \cdot Sh^2 + 324{,}214.747 \cdot Sh - 107{,}404.459 \qquad \textit{(Equation A.68)}$$

where

$$Sh = \left[\frac{V \cdot S^{0.57159}}{\omega^{0.31988}} \right]^{0.0075018} \qquad \textit{(Equation A.69)}$$

where V is flow velocity [ft/s], S is the energy slope and ω is the fall velocity [ft/s] (Julien, 1995).

A.5. Testable approaches

A.5.1. Re-meandering

The hydro-morphological model allows modifying the sinuosity of individual channel sections. The new bed slope is given by:

$$S_{0,new} = S_{0,init} \cdot \left(\frac{s_{new}}{s_{init}} \right) \qquad \textit{(Equation A.70)}$$

where $S_{0,init}$ and $S_{0,new}$ are the bed slopes before and after re-meandering, and s_{init} and s_{new} are the sinuosity values before and after re-meandering. To take account of the existence of meanders prior to re-meandering, the concept of regional sinuosity was incorporated in the analysis to attribute value of sinuosity to a straight section if it is included in a meander belt or in a sinuous section. Therefore, the variable s_{init} can also refer to the regional sinuosity. Changing the sinuosity affects the required amplitude of river corridor. The new meanders are assumed to for a elliptical planform whose equation is given by:

$$L_c \approx \frac{\pi}{2} \cdot \left[3 \cdot (a+b) - \sqrt{(3 \cdot a + b)(a + 3b)} \right] \qquad \textit{(Equation A.71)}$$

where L_c is the channel length (half the perimeter of an ellipse) and, a and b are the semi-minor and –major axes. The amplitude of the river corridor can be determined with:

$$A = 2 \cdot (b + c) + B_{full} \qquad \textit{(Equation A.72)}$$

where A is the width of the river corridor, b is the length of the semi-minor axis, c is the width of the buffer between the high water line and the riparian lands, and B_{full} is the width of the river at bankfull stage (maximum width achieved in 1.5 year).

Changing the sinuosity also affects channel roughness (thus flow velocities), more specifically the coefficient m in the following equation:

$$n = m \cdot \sum_{i=0}^{4} n_i \qquad \textit{(Equation A.73)}$$

n_i are coefficients for some channel characteristics affecting roughness

m is the meandering coefficient = 1.0 (s = 1) or 1.3 ($s \geq 1.5$)

Flow hydraulic properties can then be solved by taking account of the new bed slope and roughness values.

Although channel dimensions, shape and cross-sectional area could be modified with a new planform design, the model assumes that the value of each of these parameters remains identical to that of the channel configuration without re-meandering. It is assumed that the volume of water held in a specific section will be held in a more voluminous section (after re-meandering). Therefore, flow depth, velocity and discharge are reduced in a meandering section. The new discharge is given by:

$$Q_{new} = Q_{init} \cdot \left(\frac{V_{new}}{V_{init}} \right) \qquad \textit{(Equation A.74)}$$

where Q_{init} and Q_{new} are the flow discharges before and after re-meandering, and V_{init} and V_{new} are the maximum volumes of water that can be held in a specific channel section before and after re-meandering.

A.5.2. Backwater ponds

The hydro-morphological model allows the use of one or several backwater ponds per channel section. Here, a pond is defined as a hydrological retention basin that is attached to the river. The water flowing in the river is free to move in and out of each pond. The maximum volume of water (V_{max}) that can be held in all the ponds connected to a specific channel section is given by:

$$V_{\max} = A \cdot Y \qquad \textit{(Equation A.75)}$$

where A is the pond area and Y is the depth of the channel in the current section.

The volume of water accumulating in ponds during the rising limb of a hydrograph contributes to reducing the peak discharge of this event. The accumulated water will evacuate as stream flow drops to the base level. The falling limb will therefore have a gentler slope than without the ponds. Based on the analysis of the Richer hydrology, the rising time (t_{rising}) is on average 12 hours. A good estimation of the volume evacuated by the stream during the rising limb (V_{rising}) is given by:

$$V_{rising} = t_{rising} \cdot \frac{Q_{base} + Q_{peak}}{2} \qquad \textit{(Equation A.76)}$$

where Q_{base} and Q_{peak} are the base and peak discharges, respectively. The volume of water held in the ponds during the event must be subtracted from the area under the hygrograph's curve before the peak and added to the area under the curve after the peak. The retained volume by a specific pond ($V_{retained}$) is given by:

$$V_{retained} = \Delta Y \cdot A \qquad \textit{(Equation A.77)}$$

where ΔY is the change in flow depth and A is the pond area. The new peak discharge can be calculated by solving Equation A.76 for Q_{peak} and giving V_{rising} a value of V_{rising} - $V_{retained}$. The new flow depth must be calculated and Equation A.77 must be solved for ΔY recursively to ensure that it matches pond depth.

Without considering retained water and assuming no further precipitation or snowmelt, the discharge should fall at the end of the day to a value (Q_{end}) that can be evaluated with Equation A.47. The volume of water evacuated by the stream over the day ($V_{falling}$) is given by:

$$V_{falling} = \int_{t=0}^{24} Q_t dt \qquad \textit{(Equation A.78)}$$

where Q_t is the flow discharge at any time interval t. The volume that should evacuate from the basin ($V_{evacuated}$), considering the hydraulic conditions at peak time and those at the end of the day, is given by:

$$V_{evacuated} = \left(Y_{peak} - Y_{end}\right) \cdot A \qquad \textit{(Equation A.79)}$$

where Y_{peak} and Y_{end} are the maximum and final flow depths (of the falling limb) and A is the pond area. However, the river is unable to evacuate both $V_{falling}$ and $V_{evacuated}$. Instead, the more realistically volume of water evacuated from the pond ($V'_{evacuated}$) is given by:

$$V'_{evacuated} = \frac{V_{evacuated}}{V_{evacuated} + V_{falling}} \cdot V_{falling} \qquad \textit{(Equation A.80)}$$

The new flow depth at the end of the day (Y_{end}) can be calculated from Equation A.79 by setting $V_{evacuated} = V'_{evacuated}$. Since flow depth must be equal in the stream (compared to pond depth), flow discharge is predicted from Y_{end}.

The installation of one pond affects flow discharge in downstream channel sections. Peak flow discharge $Q_{i,pond}$ in a section i affected by upstream ponds is given by:

$$Q_{i,pond} = \frac{Q_{i,nopond} - Q_{i-1,nopond}}{Q_{i-1,nopond}} \cdot Q_{i-1,pond} \qquad \textit{(Equation A.81)}$$

where $Q_{i,no\ pond}$ and $Q_{i-1,no\ pond}$ are the peak discharges of the current and previous channel sections supposing that there are no upstream ponds, and $Q_{i,pond}$ and $Q_{i-1,pond}$ are the peak discharges of the current and previous sections of the stream considering that there is at least one pond located upstream of the current section. Unknown discharge values can be calculated using Equations A.48 and A.49.

A.5.3. Addition of riparian vegetation

Since a 3 m riparian buffer strip is sufficiently large to trap agrochemicals (Boutin et al., 2003), the hydro-morphological model assumes that such a vegetation strip can also prevent a significant proportion of the overland transported sediments on an agricultural stream from leaching in an adjacent stream. The model also assumes that the proportion of trapped sediments is a function of the buffer strip width and that this proportion increases linearly with width from 0 to 100%. However, the overland transport rate is also a function of other factors including gradient, shape of drained land, drainage area and slope length seasonality which can have an impact on soil compaction, crusting and vegetation cover (Mathier & Roy, 1993). Certain management strategies such as the construction of levees and the adoption of alternative land maintenance practices (e.g. semi-direct practice that consists in voluntarily stopping ploughing) may also be considered.

A.5.4.Climate change scenarios

The hydro-morphological model allows applying a climate change to a historical or randomly generated dataset of weather conditions. The predicted monthly changes in the amount of precipitation [%] and in the average temperature [°C] are simply applied to the daily value. Monthly precipitation and temperature deltas are available at no charge from many online sites. The model allows the addition and selection of various climate change scenarios.

A.6. References

Andreas, E. L. (2007). New estimates for the sublimation rate for ice on the moon. *Icarus, 186*(1), 24-30.

Bertle, F.A. (1966). Effect of snow compaction on runoff from rain on snow, Bureau of Reclamation, Engineering Monograph. No. 35, Washington.

Bohren, C.F., Albrecht, B.A. (1998). Atmospheric Thermodynamics. Oxford University Press, New York.

Boutin, C., Jobin, B., & Bélanger, L. (2003). Importance of riparian habitats to flora conservation in farming landscapes of southern Québec, Canada. *Agriculture, Ecosystems and Environment, 94*, 73-87.

Caissie, D., El-Jabi, N., & Satish, M. G. (2001). Modelling of maximum daily water temperatures in a small stream using air temperatures. *Journal of Hydrology, 251*, 14-28.

Estermann, I. (1955). Gases at low densities. In: Rossini, F.D. (Ed.), Thermodynamics and Physics of Matter. Princeton Univ. Press, Princeton, NJ, pp. 736–776.

Julien, P. Y. (1995). *Erosion and sedimentation.* Cambridge: Cambridge University Press.

Haith, D. A. (1985). An Event-Based Procedure for Estimating Monthly Sediment Yields. *Transactions of the American Society of Agricultural Engineers, 28*(6), 1916-1920.

Hann, C.T., Barfield, B.J., & Hayes, J.C. (1994). Design hydrology and sedimentology for small catchments. Academic Press, New York.

Hargreaves, G.H. & Samani, Z.A. (1985). Reference crop evapotranspiration from temperature. *Transaction of ASAE, 1*(2), 96-99.

Itakura, T. & Kishi, T.(1980). Open channel flow with suspended sediments. *Journal of hydraulics Div., ASCE, 106*(8), 132501343.

Lim, K. J., Sagong, M., Engel, B. A., Tang, Z. X., Choi, J. D., & Kim, K. S. (2005). GIS-based sediment assessment tool. Catena, 64(1), 61-80.

Mathier, L. & Roy, A. G. (1993). Temporal and spatial variations of runoff and rainwash erosion on an agricultural field. *Hydrological processes*, *7*, 1-18.

Monteith J.L. & Unsworth M.H. (1990). Principles of environmental physics. New York: Edward Arnold, 291 pp.

Sevier River Water Users Association (SRWUA) (2008). Net radiation: Richfield Weather Station. Retrieved April 12, 2008, from Sevier River Water Users Association

Web site: http://www.sevierriver.org/et/raws/radiation.php

Shen, H. W. & Wang, W. C. (1979). Missouri River sediment transport relationships (MRD Sediment Series no. 17). Omaha, Nebraska: U.S. Army Engineer Division, Missouri River Corps of Engineers.

Smithsonian Met. Tables, 5th ed., pp. 350, 1984.

Stone, R. P. (2007). Universal Soil Loss Equation (USLE). Retrieved April 12, 2008, from the Ministry of Agriculture, Food and Rural Affairs of Ontario

Web site: http://www.omafra.gov.on.ca/english/engineer/facts/00-001.htm

Vanoni, V.A., 1975. Sedimentation Engineering, Manual and Report No. 54. American Society of Civil Engineers, New York, N.Y.

Wischmeier, W.H., & Smith, D.D. (1965). Predicting rainfall-erosion losses from cropland east of the Rocky Mountains. U.S. Department of Agriculture, Agricultural Research Service, Agriculture Handbook 282.